

UNIVERSITY OF THESSALY
DEPARTMENT OF MECHANICAL ENGINEERING



DIPLOMA THESIS

Recent Advances in Hydrogen Production & Storage

Authors:

Dali Kyriaki & Pampoukidou Natalia

Supervisor:

Prof. Dr. P. Tsiakaras

Volos, 2022

ΠΑΝΕΠΙΣΤΗΜΙΟ ΘΕΣΣΑΛΙΑΣ
ΤΜΗΜΑ ΜΗΧΑΝΟΛΟΓΩΝ ΜΗΧΑΝΙΚΩΝ



ΔΙΠΛΩΜΑΤΙΚΗ ΕΡΓΑΣΙΑ

Πρόσφατες Εξελίξεις σε Υλικά για την Παραγωγή & Αποθήκευση του Υδρογόνου

Συγγραφείς:

Δάλη Κυριακή & Παμπουκίδου Ναταλία

Επιβλέπων:

Καθ. Δρ. Π. Τσιακάρας

Βόλος, 2022

© 2022, Κυριακή Δάλη, Ναταλία Παμπουκίδου

Η έγκριση της διπλωματικής εργασίας από το Τμήμα Μηχανολόγων Μηχανικών της Πολυτεχνικής Σχολής του Πανεπιστημίου Θεσσαλίας δεν υποδηλώνει αποδοχή των απόψεων του συγγραφέα (Ν. 5343/32 αρ. 202 παρ. 2).

Εγκρίθηκε από τα Μέλη της Τριμελούς Εξεταστικής Επιτροπής:

1st Examiner: Dr Tsiakaras Panagiotis
(Supervisor) Professor
Department of Mechanical Engineering
School of Engineering
University of Thessaly

2nd Examiner: Dr Charalampous Georgios
Assistant professor
Department of Mechanical Engineering
School of Engineering
University of Thessaly

3rd Examiner: Dr Angeliki Brouzgou
Assistant professor
Department of Energy systems
Faculty of Technology
University of Thessaly

Acknowledgements

First of all, we would like to express our gratitude to Prof. Panagiotis Tsiakaras for his guidance, support, and insightful comments throughout the course of this thesis.

We would also like to thank the members of the committee Assistant Prof. Georgios Charalampous and Assistant Prof. Angeliki Brouzgou for dedicating time to read and evaluate our thesis.

Lastly, we would like to express our deepest appreciation to our family and friends who have supported and encouraged us during the course of our academic years.

INDEX

ABSTRACT	12
ΠΕΡΙΛΗΨΗ	14
CHAPTER I - INTRODUCTION	16
CHAPTER II - THEORY	18
2.1 Fundamentals of Hydrogen	18
2.2 Properties of Hydrogen	19
2.2.1 Physical Properties	19
2.2.2 Chemical properties	20
2.2.2.1 Flammability range	20
2.2.2.2 Auto-ignition temperature	21
2.2.2.3 Burning speed & Flame characteristics.....	21
2.2.2.4 Air/fuel ratio	21
2.3 Hydrogen in Fuel Cells.....	22
2.3.1 Parts and mechanism of FC:	22
2.3.2 Applications of Fuel Cells	24
2.3.2.1 Power	24
2.3.2.2 Cogeneration	24
2.3.2.3 Portable power systems.....	25
2.3.2.4 Transportation	25
2.3.2.4.1 Heavy-duty on road Vehicles	28
2.3.2.4.2 Rail	29
2.3.2.4.3 Ships.....	29
2.3.2.4.4 Aviation	30
2.4 Environmental Impact of Hydrogen Fuel	30
2.4.1 Background	30
2.4.2 "Grey", "Blue", & "Green" Production	31
2.4.3 Environmental Impact Factors & Greenization Factors	32
2.4.4 Leakage of Hydrogen	34
2.5 Hydrogen Economy.....	34
2.5.1 Energy Transition	35
2.5.2 Consumption/Demand	37

2.5.3 Technical Challenges	38
2.5.4 Future Trends	39
2.5.4.1 Vehicle Power Systems	39
2.5.4.2 "Blue" & "Green" Hydrogen	39
2.5.4.3 Nanotechnology for Production, Storage & Transformation.....	40
2.5.4.4 Porous Materials-Based Physical Sorption.....	40
2.5.4.5 Metal/Chemical Hydrides-Based Chemical Sorption.....	40
2.5.4.6 Ionic Liquids for Hydrogen Storage Applications	40
CHAPTER III - HYDROGEN PRODUCTION	41
3.1 Background.....	41
3.2 Production from Fossil Fuels	43
3.2.1 Production from Hydrocarbons	43
3.2.1.1 Steam Methane Reforming (SMR).....	43
3.2.1.1.1 Process Description	43
3.2.1.1.2 Catalysts.....	44
3.2.1.2 Partial Oxidation (POX)	45
3.2.1.2.1 Partial Oxidation (Non-catalytic) of Heavy Residual Oil	45
3.2.1.2.2 Catalytic Partial Oxidation	46
3.2.1.3 Autothermal Reforming (ATR).....	46
3.2.1.4 Combined Reforming	48
3.2.1.5 Plasma Reforming	48
3.2.2 Production from Coal	49
3.2.2.1 Coal Gasification	49
3.2.3 Capture and Storage of CO ₂	50
3.3 Production from Renewable Sources	52
3.3.1 Hydrogen Production from Nuclear Energy	52
3.3.2 PV Supported Hydrogen Production	52
3.4 Production from Water Splitting	53
3.4.1 Water Electrolysis.....	54
3.4.1.1 Electrolytes	55
3.4.1.2 Catalysts	56
3.4.1.3 Oxygen evolution reaction (OER)	58
3.4.1.4 Hydrogen evolution reaction (HER)	59

3.4.2 Photoelectrochemical Water Splitting (Photolysis)	61
3.4.3 Photocatalytic Water Splitting	62
3.4.3.1 Photosynthesis.....	62
3.4.3.2 Mechanism	63
3.4.3.3 Photocatalyst Materials	64
3.4.4 Hydrogen Production from Wind Energy	64
3.4.5 High-Temperature Decomposition	65
3.4.6 Thermolysis and Thermochemical Water Splitting	66
3.5 Biomass to Hydrogen	67
3.5.1 Thermochemical Biomass Gasification.....	68
3.5.2 Hydrogen from Pyrolysis-Derived Bio-Oil.....	69
3.6 Biological Production of Hydrogen	70
3.6.1 Photobiological Production (Biophotolysis)	71
3.6.2 Dark Fermentation	72
3.6.3 Photo-Fermentation.....	73
3.6.4 Microbial Electrolysis.....	73
3.6.5 Factors Affecting Biohydrogen.....	73
3.6.6 Final Comparison.....	74
CHAPTER IV - HYDROGEN STORAGE	76
4.1 Background.....	76
4.2 Gaseous-State Storage System.....	77
4.3 Liquid-State Storage System	78
4.3.1 Liquid Organic Hydrogen Carriers (LOHCs)	79
4.3.2 Ammonia NH ₃	80
4.4 Solid-State Storage System	81
4.4.1 Metal Hydrides.....	83
4.4.1.1 Overview	83
4.4.1.2 Types of Metal Hydrides	86
4.4.1.3 Mg-Based Hydrides	87
4.4.1.4 Recent Developments in Improving Hydrogen Storage in Metal Hydrides	88
4.4.1.4.1 Alloying with Other Elements	88
4.4.1.4.2 Catalysis	89

4.4.1.4.3 Nanostructuring.....	90
4.4.1.4.4 Nanoconfinement.....	91
4.4.1.4.5 Altering reaction pathway	91
4.4.1.5 Applications	91
4.4.1.6 Challenges	94
4.4.2 Complex/Chemical Hydrides.....	95
4.4.2.1 Overview	95
4.4.2.2 Types of Complex/Chemical Hydrides	96
4.4.2.2.1 Alanates (LiAlH ₄ , NaAlH ₄ , and Mg(AlH ₄) ₂).....	96
4.4.2.2.2 Borohydrides (LiBH ₄ /NaBH ₄ /Mg(BH ₄) ₂)	99
4.4.2.2.3 Alane (AlH ₃)	100
4.4.2.2.4 Amides (LiNH ₂ /NaNH ₂ /Mg(NH ₂) ₂)	101
4.4.2.2.5 Ammoniates of Borohydrides	101
4.4.3 Nanoporous Carbon Materials.....	102
4.4.3.1 Overview	102
4.4.3.2 Recent Advances of Nanoporous Carbon Materials.....	103
4.4.3.3 Carbon Materials for Hydrogen Storage	105
4.4.3.3.1 Graphite	105
4.4.3.3.2 Graphene	106
4.4.3.3.3 Carbon Nanotubes (CNTs)	107
4.4.3.3.4 Fullerene	109
4.4.3.3.5 Carbon and Graphite Nanofibers (CNFs & GNFs).....	110
4.4.3.3.6 Activated Carbons (ACs)	111
4.4.3.3.7 Zeolite-Template Carbons.....	112
4.4.3.3.8 Carbide-Derived Carbons.....	112
4.4.3.3.9 Metal-Organic Frameworks/-Derived Carbons (MOFs/MDCs).....	113
4.4.3.4 Comparison of Hydrogen Storage Capacity of Different Carbon Materials ..	114
4.4.3.5 Challenges	115
4.4.4 Electrochemical Hydrogen Storage	116
CHAPTER V - CONCLUDING REMARKS	119
BIBLIOGRAPHY	123

LIST OF FIGURES

Figure 1: Gravimetric & volumetric energy density of combustible materials and batteries [4].	20
Figure 2: Variation of Hydrogen Flammability Limits with Temperature [5].	21
Figure 3: Basic schematic of a Fuel Cell [11].	22
Figure 4: Micro-combined heat and power systems (micro-CHP) [16].	24
Figure 5: Breakdown of energy usage in the transport sector globally in 2015. The outer ring gives the share of individual modes. “Other” is primarily passenger rail and air freight. The middle and inner rings aggregate these uses by mode and function. Data from EIA.35 Total consumption was 110 million TJ in 2015 worldwide, equivalent to 37 kW h per person per day in OECD countries and 7 kW h in non-OECD countries [17].	25
Figure 6: Block Diagram of a Hydrogen Car (Image: BMW) [24].	27
Figure 7: GHG emissions by sector worldwide [28].	31
Figure 8: Hydrogen Content Factor (HCF), Greenization Factor (GF), and Environmental Impact Factor (EIF) of hydrogen and other fossil fuels [38].	33
Figure 9: Sources of hydrogen production (Based on the data from the Global Hydrogen Review 2021, International Energy Agency, 2021).	37
Figure 10: Block Diagram of SMR plant [63].	44
Figure 11: Catalytic Partial Oxidation principle.	46
Figure 12: Schematic diagram of ATR unit [71].	47
Figure 13: Schematic of combined reforming [72].	48
Figure 14: Overview of CO ₂ capture processes and systems [75].	51
Figure 15: The basic principle for Carbon Capture and Storage (CCS) [76].	51
Figure 16: Hydrogen cycle.	53
Figure 17: Energy demand for water and steam electrolysis.	54
Figure 18: Schematic illustration of the catalyst’s role in lowering the activation energy barrier [85].	57
Figure 19: Tafel plot for an anodic process (oxidation) [87].	58
Figure 20: Processes involved in overall photocatalytic water splitting on a heterogeneous photocatalyst [108].	63
Figure 21: Design of an isolated stand-alone hybrid wind-hydrogen system for a zero-energy house [120].	65

Figure 22: Sulphur-Iodine cycle simplified scheme [123].	66
Figure 23: Main gasifier types [141].	69
Figure 24: Schematic illustration of biological production of Hydrogen [150].	71
Figure 25: Volumetric versus mass densities achieved by various hydrogen-storage technologies (Modified from [157]).	78
Figure 26: A simplified model of a metal hydride hydrogen storage [45].	84
Figure 27: Conceptual model of MgH ₂ cluster (a) plain, (b) nanocrystalline, and (c) nanocatalyst-doped materials [160].	87
Figure 28: Hydrogen storage in reversible light metal hydrides (Reproduced from [169]).	89
Figure 29: Schematic of a two-stage metal hydride reservoir [161].	92
Figure 30: Metal hydride hydrogen-fuel-cell-powered system [161].	93
Figure 31: Hydrogen content in various storage options (Adapted from [178]).	94
Figure 32: Hydrogen storage density in physisorbed materials, metal/complex, and chemical hydride [160].	95
Figure 33: The crystal structures of (a) LiAlD ₄ , where Li cations are surrounded by five isolated [AlD ₄] - tetrahedra. Copyright 2002 Elsevier; (b) NaAlD ₄ , in which Na atoms are surrounded by eight [AlH ₄] - tetrahedra in a distorted square antiprismatic geometry. Copyright 2003 Elsevier; (c) Mg(AlH ₄) ₂ , showing six-coordinated Mg and four-coordinated Al in a distorted MgH ₆ octahedral geometry. Views along (A) the a-axis and (B) the c-axis. Copyright 2005 Elsevier [159].	97
Figure 34: (a) Low- and high-temperature structures of LiBH ₄ determined from XRD. Blue, green, and red spheres represent boron, lithium, and hydrogen, respectively. Copyright 2007 Elsevier. Crystal structure of cubic (b) α-NaBH ₄ . Copyright 2010 ACS Publications, (c) γ-Mg(BH ₄) ₂ [159].	100
Figure 35: H ₂ absorption capacities at 77 and 296-308K as a function of surface area of carbon materials [182].	103
Figure 36: Molecular structure of graphite [156].	105
Figure 37: SEM micrographs of graphite after exfoliation [156].	106
Figure 38: Molecular structure of grapheme [156].	106
Figure 39: Typical TEM (a,b) and SEM (c) images showing the morphologies of the MWNTs (CNT) [199].	107

Figure 40: Calculated amount of adsorbed hydrogen in weight percent on CNTs, assuming condensation of hydrogen: (a) Monolayer adsorbed at the surface of nanotubes as a function of the number of shells (NS) (markers and line, axis: left and bottom) (b) hydrogen condensed in the cavity of nanotubes as a function of the diameter (dashed lines, axis: left and top) for various number of shells, NS=1 (SWNT), NS=2, NS=5, NS=10 [194]. 108

Figure 41: Molecular structures of fullerenes: (a) C₆₀ and (b) C₇₀ (Modified from [210]). ... 109

Figure 42: SEM of graphitic nanofiber prepared by decomposition of C₂H₄:H₂ = 1:4 gas flow over NiCu alloy powder [213]. 110

Figure 43: Molecular structure of activated carbon [215]. 111

Figure 44: The minimized unit cell of MOF5 viewed from two different directions. In the left image the open pore structure is visible. White spheres, hydrogen; light gray, carbon; dark gray, oxygen; black, zinc. The hydrogen-adsorption sites are indicated by arrows [224]. 113

Figure 45 Hydrogen storage capacity of different carbon materials [191]. 115

Figure 46: Schematic of three-electrode CP system [228]. 118

LIST OF TABLES

Table 1: Heat of combustion of various fuels. 18

Table 2: Properties of Hydrogen 19

Table 3: Characteristics of different types of fuel cells. 23

Table 4: National goals for the use of hydrogen filling stations, thousand units [23]. 26

Table 5: Examples of stated national goals to reduce emissions and increase absorption of greenhouse gases [23]. 36

Table 6: Technology comparison of natural gas-based hydrogen production. 47

Table 7: Contents and Heating Values of Different Types of Coal. 49

Table 8: Typical specifications of the water electrolysis technologies methods. 55

Table 9: Comparison between different biological production methods. 75

Table 10: Overview of some selected parts of the U.S. DOE technical system goals for on-board H-storage for light-duty fuel cell vehicles [45]. 77

Table 11: Energy Content of Various Types of Metal Hydrides [161]. 86

Table 12: Density, H₂ densities & standard heat of formation of complex hydrides. 98

Table 13: Hydrogen release and uptake properties of some metal N-H systems. 101

ABSTRACT

Hydrogen is a very promising energy carrier which can help transitioning from fossil fuels to sustainable energy sources with zero harmful by-products. Since John Bockris proposed the term "hydrogen economy" in the 1970s, hydrogen energy has been regarded as one of the cleanest and most promising energy utilization ways. However, in order to achieve a global hydrogen economy, there are a lot of challenges needed to be overcome. In this review, we analyze the methods of hydrogen production (**CHAPTER III**), and the emerging materials for hydrogen storage (**CHAPTER IV**). Prior to that, we take a look at the physical properties of hydrogen, such as its molecular weight, density and energy content per unit mass, and chemical characteristics, like flammability range, auto-ignition temperature, burning speed, and air-fuel ratio in a combustion engine (**CHAPTER II**). The most significant advantages of hydrogen come from the high-efficiency energy conversion technologies that hydrogen enables, such as H₂ internal combustion engines and fuel cells. Chapter **2.3** explains the parts, mechanisms, as well as the applications of the hydrogen fuel cells, that are making these benefits possible. Chapter **2.4**, examines the environmental impact of hydrogen as a fuel and chapter **2.5** introduces the concept of "hydrogen economy".

The hydrogen production technologies from both fossil and non-fossil fuels are presented in **CHAPTER III** starting with steam reforming, partial oxidation, auto-thermal, pyrolysis, and plasma technology. The gasification of biomass and coal follows, and their potential contribution to our future energy needs is discussed. Additionally, water electrolysis technology is reviewed along with several critical electrochemical parameters concerning the OER and HER catalytic reactions (chapter **3.4.1**). Water electrolysis can be combined with one form of renewable energy to get eco-friendly technology such as nuclear, wind, or solar. These methods are also discussed in this paper. Currently, the greater percentage of hydrogen fuel is produced from the steam reforming, gasification, and partial oxidation technologies using fossil fuels. These technologies have numerous challenges to deal with such as the total energy consumption and carbon emissions to the environment that are still too high. The final chapter (chapter **3.6**) of hydrogen production outlines various routes of biological H₂ production, substrates, and utilization of various biomasses as feedstocks for bio-hydrogen production. In the conclusion of the chapter a comparison table including all the above methods is presented.

New materials for safe hydrogen storage must be developed due to the fact that hydrogen, in its gas state, is extremely flammable, so in case of a misuse while transferred there is a high possibility of explosion. **CHAPTER IV** presents the latest advances in materials and mechanisms that will potentially make hydrogen storage viable. While all techniques of hydrogen storage are examined, materials-based hydrogen storage systems (chapter **4.4**) receive special attention. Chapter **4.4.1** reviews the types of metal hydrides as well as the recent techniques developed to improve their hydrogen storage ability. Metal hydrides have remarkable characteristics for hydrogen storage but are too heavy. Thus, in Chapters **4.4.1.3** and **4.4.2** light weight Mg-based and complex/chemical hydrides with high gravimetric capacity are examined. Then, in chapter **4.4.3** the hydrogen storage capacities, the pore characteristics, and the preparation methods of nanoporous carbons, including activated carbons, carbide-derived and zeolite-templated carbons are analysed. The interest is focused mainly on recently developed metal–organic frameworks, which demonstrate promising properties for hydrogen storage applications. Finally, in chapter **4.4.4** the concept of electrochemical hydrogen storage and the method of chronopotentiometry are introduced.

ΠΕΡΙΛΗΨΗ

Το υδρογόνο είναι ένας πολλά υποσχόμενος φορέας ενέργειας που μπορεί να βοηθήσει στην ενεργειακή μετάβαση από τα ορυκτά καύσιμα σε βιώσιμες πηγές ενέργειας με μηδενικά επιβλαβή υποπροϊόντα. Από τότε που ο John Bockris πρότεινε τον όρο «οικονομία υδρογόνου» τη δεκαετία του 1970, η ενέργεια του υδρογόνου θεωρείται ως ένα από τα πιο καθαρά και υποσχόμενα πρότυπα ενεργειακής χρήσης. Ωστόσο, για να επιτευχθεί μια παγκόσμια οικονομία υδρογόνου, υπάρχουν πολλές προκλήσεις που πρέπει να ξεπεραστούν. Σε αυτήν την εργασία, αναλύουμε τις μεθόδους παραγωγής υδρογόνου (**CHAPTER III**) και τα αναδυόμενα υλικά για την αποθήκευση υδρογόνου (**CHAPTER IV**). Στην αρχή, ρίχνουμε μια ματιά στις φυσικές ιδιότητες του υδρογόνου, όπως το μοριακό του βάρος, την πυκνότητα του και το ενεργειακό του περιεχόμενο ανά μονάδα μάζας, όπως και τα χημικά χαρακτηριστικά, όπως το εύρος ευφλεκτότητας, τη θερμοκρασία αυτόματης ανάφλεξης, τη ταχύτητα καύσης και την αναλογία αέρα-καυσίμου σε έναν κινητήρα εσωτερικής καύσης (**CHAPTER II**). Τα πιο σημαντικά πλεονεκτήματα του υδρογόνου προέρχονται από τη χρήση του σε υψηλής απόδοσης τεχνολογίες μετατροπής ενέργειας, όπως οι κινητήρες εσωτερικής καύσης υδρογόνου και οι κυψέλες καυσίμου. Το κεφάλαιο **2.3** εξηγεί τα μέρη, τους μηχανισμούς, καθώς και τις εφαρμογές των κυψελών καυσίμου υδρογόνου, που καθιστούν δυνατά αυτά τα οφέλη. Το κεφάλαιο **2.4**, εξετάζει τις περιβαλλοντικές επιπτώσεις του υδρογόνου ως καύσιμο και το κεφάλαιο **2.5** εισάγει την έννοια της «οικονομίας υδρογόνου».

Οι τεχνολογίες παραγωγής υδρογόνου τόσο από ορυκτά όσο και από μη ορυκτά καύσιμα παρουσιάζονται στο **CHAPTER III** ξεκινώντας με την αναμόρφωση με ατμό, τη μερική οξείδωση, την αυτόθερμη αναμόρφωση, την πυρόλυση και την τεχνολογία πλάσματος. Ακολουθεί η αεριοποίηση της βιομάζας και του άνθρακα και συζητείται η πιθανή συμβολή τους στις μελλοντικές μας ενεργειακές ανάγκες. Επιπρόσθετα, αναθεωρήθηκε η τεχνολογία ηλεκτρόλυσης νερού και αρκετές κρίσιμες ηλεκτροχημικές παράμετροι που αφορούν τις καταλυτικές αντιδράσεις OER και HER (κεφάλαιο **3.4.1**). Η ηλεκτρόλυση νερού μπορεί να συνδυαστεί με ανανεώσιμες πηγές ενέργειας, όπως πυρηνική, αιολική ή ηλιακή ενέργεια, για να αποκτήσει ακόμα πιο «πράσινο» χαρακτήρα. Αυτές οι μέθοδοι συζητούνται επίσης σε αυτήν την εργασία. Επί του παρόντος, οι πιο κοινές μέθοδοι παραγωγής υδρογόνου αποτελούνται από τις τεχνολογίες αναμόρφωσης ατμού, αεριοποίησης και μερικής

οξειδωσης ορυκτών καυσίμων. Αυτές οι τεχνολογίες έχουν διάφορες προκλήσεις, όπως η μεγάλη συνολική κατανάλωση ενέργειας ενώ οι εκπομπές άνθρακα στο περιβάλλον εξακολουθούν να είναι πολύ υψηλές. Το τελευταίο κεφάλαιο (κεφάλαιο **3.6**) της παραγωγής υδρογόνου περιγράφει διάφορες οδούς βιολογικής παραγωγής υδρογόνου και χρήσης διαφόρων βιομάζας ως πρώτη ύλη για την παραγωγή βιοϋδρογόνου. Στο τέλος του κεφαλαίου παρουσιάζεται ένας πίνακας που συγκρίνει όλες τις παραπάνω μεθόδους.

Πρέπει να αναπτυχθούν νέα υλικά για την ασφαλή αποθήκευση του υδρογόνου, καθώς το υδρογόνο, στην αέρια κατάσταση του, είναι εξαιρετικά εύφλεκτο, επομένως σε περίπτωση κακής χρήσης του κατά τη μεταφορά, υπάρχει μεγάλη πιθανότητα έκρηξης. Το **CHAPTER IV** παρουσιάζει τις πιο πρόσφατες εξελίξεις σε υλικά και μηχανισμούς που θα καταστήσουν μελλοντικά βιώσιμη την αποθήκευση υδρογόνου. Ενώ εξετάζονται όλες οι τεχνικές αποθήκευσης υδρογόνου, τα συστήματα αποθήκευσης υδρογόνου με βάση τα υλικά (κεφάλαιο **4.4**) λαμβάνουν ιδιαίτερη προσοχή. Το Κεφάλαιο **4.4.1** εξετάζει τους τύπους υδριδίων μετάλλων καθώς και τις πρόσφατες τεχνικές που έχουν αναπτυχθεί για τη βελτίωση των ιδιοτήτων τους για αποθήκευση υδρογόνου. Τα υδρίδια μετάλλων έχουν αξιοσημείωτα χαρακτηριστικά για την αποθήκευση υδρογόνου αλλά παραμένουν πολύ βαριά. Έτσι, στα κεφάλαια **4.4.1.3** και **4.4.2** εξετάζουμε ελαφριά υδρίδια με βάση το μαγνήσιο και σύνθετα/χημικά υδρίδια με υψηλή βαρυμετρική ικανότητα. Στη συνέχεια, στο κεφάλαιο **4.4.3** αναλύουμε τις χωρητικότητες αποθήκευσης υδρογόνου, τα χαρακτηριστικά των πόρων και τις μεθόδους παρασκευής νανοπορωδών ανθράκων, συμπεριλαμβανομένων των ενεργών ανθράκων, των ανθράκων που προέρχονται από καρβίδιο και των ανθράκων που προέρχονται από ζεόλιθο. Εστιάζουμε κυρίως στα πρόσφατα αναπτυγμένα μεταλλικά-οργανικά πλαίσια, τα οποία επιδεικνύουν πολλά υποσχόμενες ιδιότητες για εφαρμογές αποθήκευσης υδρογόνου. Τέλος, στο κεφάλαιο **4.4.4** εισάγουμε την έννοια της ηλεκτροχημικής αποθήκευσης υδρογόνου και τη μέθοδο της χρονοποτενσιομετρίας.

CHAPTER I - INTRODUCTION

In recent decades, the use of fossil fuels, especially gas and oil, has increased tremendously. In 2018, 79.5 % of the energy economy relied on non-renewable and environmentally harmful energy sources such as coal, petroleum oil, and natural gas. This poses many down effects on our energy systems, some of which are the depletion of the finite resources and the polluting carbon dioxide emissions from the by-products. This problem sets a strong demand for better energy sources, that will be abundant, ideally renewable, and that will produce harmless by-products to the environment.

A possible solution to this energy crisis could be the use of hydrogen, which can be produced by plenty of sources, like water, organic materials and biomass. Hydrogen is a colorless, odorless, tasteless and non-toxic molecule, which provides a combustion resource that generates no air pollutants or greenhouse gases, with pure water as the only by-product. Additionally, hydrogen could work greatly as an energy carrier due to the fact that it stores the highest density by weight. It could also increase the efficiency of the energy conversion process for both internal combustion engines and proton exchange membrane fuel cells. Some of hydrogen uses include power generation, cogeneration of heat and energy for industrial or residential use/purposes and transportation including heavy duty on road vehicles, rail, aviation, and ships.

The fact that a country's socioeconomic development is heavily reliant on its transportation system cannot be overstated. Unfortunately, the transportation sector not only consumes a significant amount of fossil fuels, but its increasing consumption is also contributing to the escalation of global climate damage. The transportation sector's greenhouse gas (GHG) emissions are considered severe, and road vehicles are the single largest source of major atmospheric pollutants such as CO₂. Hydrogen as a fuel has already found applications in experimental cars, and all of the major car companies are competing to build a commercial car and market hydrogen fuel automobiles in the near future. Hydrogen is already a dominant fuel for space programs across the world. It powers aerospace transports used to construct the International Space Station, as well as to provide electricity and portable water to its inhabitants.

Unlike oil and natural gas, which are naturally stored on Earth, hydrogen energy must be produced from other resources before it can be used. To that end, developing efficient methods for hydrogen production is a critical step in the hydrogen economy. To obtain hydrogen fuel, three main synthetic pathways are used: steam methane reforming, coal gasification, and water electrolysis. The reaction of steam with methane or coal at high temperatures during the process of steam methane reforming and coal gasification results in the simultaneous generation of hydrogen and CO₂. These two methods account for more than 95 % of global hydrogen fuel production, but unfortunately, the process consumes a lot of fossil fuels and pollutes the environment.

In contrast, hydrogen production from water splitting, which is the reverse reaction of hydrogen combustion, uses water as the only feedstock and allows for a close hydrogen

cycle with zero carbon emissions, making it the most green and sustainable method. However, the high cost of water electrolysis to produce hydrogen limits its widespread use, resulting in only a minor fraction of total hydrogen production (about 4 %). As a result, producing cheap hydrogen from water electrolysis that gradually replaces hydrogen production from fossil fuels is a significant challenge. Renewable powers are intermittent energy sources, and the existing electricity grid infrastructure is not well designed to absorb the excess power from them. Water electrolysis for hydrogen production could provide a route to transform the excess powers into chemical fuels, enabling the increased utilization of renewable sources.

A major key to a fully developed hydrogen economy is the development of safe, light, compact, and cost-efficient hydrogen storage. The typical liquid-state and gaseous-state storage system, in the form of pressurized hydrogen gas, cause cost and safety issues to on-board applications; hence, they do not meet the long-term goals of a hydrogen economy. Recently, solid-state hydrogen storage has been proposed as a long-term option. Depending on the materials, this storage method is based on either chemical sorption as in metal/chemical hydrides or physical sorption as in porous materials.

Metal hydride storage systems have shown great potential for storing large amounts of hydrogen in a safe, compact, and reversible manner, making them an increasingly appealing option for hydrogen applications. However, the techno-economic viability is yet to be realized since no metal hydride, at the moment, meets all of the necessary standards for a practical hydrogen economy, due to slow kinetics, small hydrogen storage capacity, and unacceptable hydrogen absorption/desorption temperatures. On the other hand, physisorption in porous materials allows for hydrogen storage under low-stringency conditions. Physically adsorbed molecules of hydrogen are weakly attached to a surface; therefore, easily released. Porous carbons appear to be the most efficient hydrogen storage candidate, with the added benefits of being relatively inexpensive to produce and easy prepare.

The development of a mature hydrogen economy is dependent on breakthroughs in the discovery of new materials and on the fundamental understanding of the nanoscale phenomena that govern hydrogen interactions with materials. However, the ultimate evolution of a hydrogen economy is determined by factors other than technical feasibility. As with all new technologies, comparisons of hydrogen with a developing mix of alternatives for performance, cost, efficiency, convenience, reliability, availability, and safety, will determine its future course. The outcomes of these comparisons are changing as the costs of fossil fuels and environmental mitigation of their use rise, and as engineering and scientific advances change the mix of competing alternatives. Although a mature hydrogen economy necessitates technical and economic solutions for production, storage, and use, there is value in implementing any of these without addressing the others. As a result, while a full-fledged hydrogen economy encompassing production, storage, and use may be the ultimate goal, partial implementation of hydrogen as a storable energy carrier for use in stationary and personal fuel cell applications is a desirable outcome by itself.

CHAPTER II - THEORY

2.1 Fundamentals of Hydrogen

Hydrogen holds all the desirable qualities of a future ideal fuel in all aspects including social, economic, and environmental and is therefore seen as a key component of future energy systems. This is owing to the following characteristics. Firstly, to its abundance. It is the ninth most abundant element in earth's crust (1400 mg/kg) and second most abundant element in sea after oxygen. It also accounts for 91% of our solar system by weight. Secondly, to its lowest molecular weight with highest energy content of any fuel. It has an incredible energy storage capacity, and it's been proven from experiments and calculations that 1 kg of hydrogen contains 120 MJ of energy, which surpasses double of most conventional fuels. **Table 1** shows the energy contents of alternative fuels in comparison with hydrogen. Another important trait of hydrogen is its non-toxicity and sustainability, as its exhaust product when consumed in a fuel cell is only water, which not only makes it pleasant for the environment but beneficial as well.

Table 1: Heat of combustion of various fuels.

Fuel	Energy (kcal/g)
Hydrogen	34
Petroleum	10.3-8.4
Graphite	7.8
Castoroil	9.4
Wood	4.2

Hydrogen can be stored as a fuel and used in transportation or in power generation systems with the help of fuel cells, but it can also be used in internal combustion engines or turbines. It can be used in cars, in houses, for portable power, and in a variety of other applications. Hydrogen can be produced from many domestic resources, including natural gas, nuclear power, biomass, and renewable power like solar and wind. The use of hydrogen will bring many benefits to the environment and the economy some of which will probably be: (i) maximization of renewable energy sources, (ii) decrease of air pollution by generating minimal carbon, greenhouse gases and oxide emissions, (iii) the drop of oil imports, (iv) economic prosperity. These are the reasons why hydrogen is being considered as a solution to the current energy challenges and global warming that threaten to destroy the environmental safety and the energy security worldwide.

The main aspects of the hydrogen economy to consider are production, storage, conversion, transportation, and application. Unlike other fuels, hydrogen is hard to store and transport [1]. Because hydrogen is very flammable and can easily be oxidized in pipelines and containers, thus special precautions must be taken when storing it [2]. Hydrogen production

using renewable energy sources, and storage in ionic form (electrochemical hydrogen storage) are both safe methods to handle. Due to the difficulties connected to hydrogen energy, hybrid systems combining renewable energy with fuel cells are being considered as a viable option to meet future global energy needs [3].

2.2 Properties of Hydrogen

2.2.1 Physical Properties

Hydrogen's atomic structure, consisting of a single proton and a single electron, makes it the lightest and simplest of all chemical elements. It is a colorless, odorless, tasteless gas that has, after helium, the second lowest boiling point, -252.9°C (-423.2°F), and the second lowest freezing point, -259.3°C (-434.7°F), of all elements. Other important properties are listed in **Table 2** below.

Table 2: Properties of Hydrogen

Property	Value
Molecular weight	2.01594
Density of gas at 0°C and 1 atm.	0.08987 kg/m ³
Density of solid at -259°C	858 kg/m ³
Density of liquid at -253°C	708 kg/m ³
Melting temperature	-259°C
Boiling temperature at 1 atm.	-253°C
Critical temperature	-240°C
Critical pressure	12.8 atm.
Critical density	31.2 kg/m ³
Heat of fusion at -259°C	58 kJ/kg
Heat of vaporization at -253°C	447 kJ/kg
Thermal conductivity at 25°C	0.019 kJ/ms $^{\circ}\text{C}$
Viscosity at 25°C	0.00892 centipoise
Heat capacity (Cp) of gas at 25°C	14.3 kJ/kg $^{\circ}\text{C}$
Heat capacity (Cp) of liquid at -256°C	8.1 kJ/kg $^{\circ}\text{C}$
Heat capacity (Cp) of solid at -259.8°C	2.63 kJ/kg $^{\circ}\text{C}$

Hydrogen has the highest energy content per unit mass of any other fuel. On a weight basis, hydrogen has an energy content of 140.4 MJ/kg as seen on **Figure 1**, which is nearly three times that of gasoline (48.6 MJ/kg). However, on a volume basis the situation is reversed: liquid hydrogen stands lower on the scale with a value of 8,491 MJ/L vs. 31,150 MJ/L for gasoline. The physical nature of the fuel affects the energy density of hydrogen, whether it is in liquid or gaseous phase. Additionally, altering the pressure can increase or decrease the volumetric energy density.

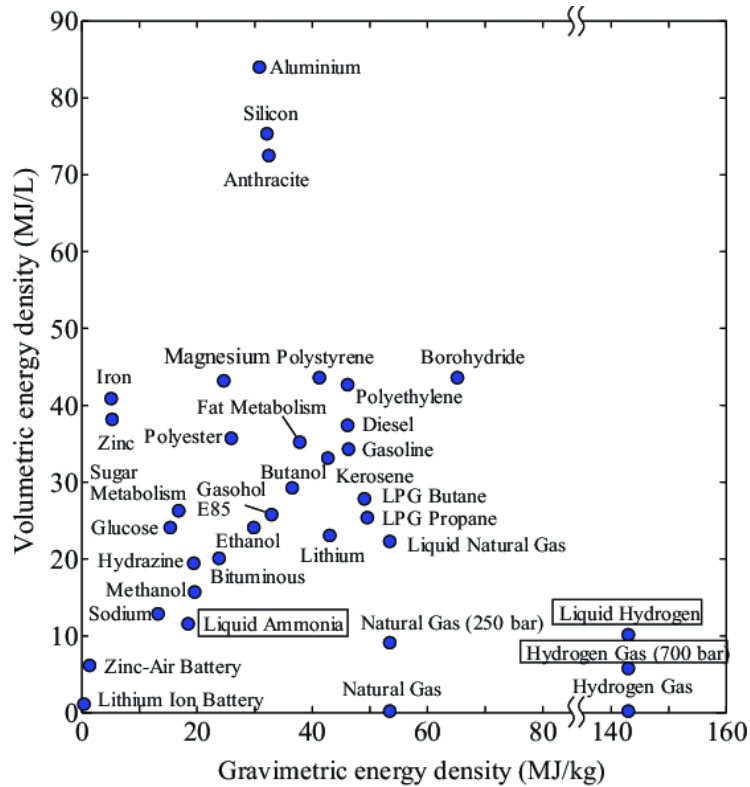


Figure 1: Gravimetric & volumetric energy density of combustible materials and batteries [4].

At ordinary temperatures, hydrogen is comparatively nonreactive unless it is activated in some way. On the contrary, hydrogen atom is chemically very reactive, which is why it is not found chemically free in nature. In fact, very high temperatures are required to dissociate molecular hydrogen into atomic hydrogen. Even at 5000 K, about 5% of the hydrogen remains un-dissociated. In nature, hydrogen is mostly bound to oxygen or carbon atoms. As a result, hydrogen must be regarded as an energy carrier—a method of storing and transmitting energy derived from a primary energy source.

Although hydrogen is non-toxic, it can act as a simple asphyxiant by displacing the oxygen in the air. Hydrogen diffuses much faster through air than other gaseous fuels, with a diffusion coefficient in air of 0.61×10^{-4} , the rapid dispersion rate of hydrogen is its greatest safety feature.

2.2.2 Chemical properties

2.2.2.1 Flammability range

At standard atmospheric temperature, hydrogen is flammable over a very wide range of concentrations in air (4-75%) which is much broader than gasoline range, 1-7.6% and it is also explosive over a wide range of concentrations (15-59%). The flammability limits increase with temperature as illustrated in **Figure 2**.

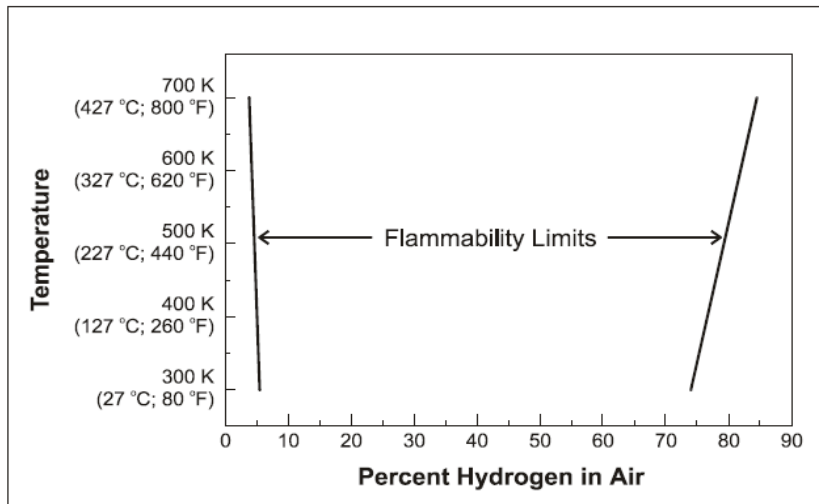


Figure 2: Variation of Hydrogen Flammability Limits with Temperature [5].

2.2.2.2 Auto-ignition temperature

The auto-ignition temperature is the minimum temperature required to initiate self-sustained combustion in a combustible fuel mixture in the absence of an external ignition. Each type of fuel has a different ignition temperature. For hydrogen, the autoignition temperature is relatively high at 1085°F (585°C). This makes it difficult to ignite a hydrogen/air mixture solely through heat without some additional ignition source. Although hydrogen has a higher auto-ignition temperature than methane, propane or gasoline, its ignition energy (1.9×10^{-8} Btu or 0.02 mJ) is about an order of magnitude lower and therefore more easily ignitable. Even an invisible spark or static electricity discharge from a human body (in dry conditions) may have enough energy to cause ignition. Nevertheless, it is critical to understand that the ignition energy for all these fuels is very low, so conditions that will ignite one fuel will generally ignite any of the others [6].

2.2.2.3 Burning speed & Flame characteristics

The burning speed of hydrogen at 8.7-10.7 ft/s (2.65-3.25 m/s) is nearly an order of magnitude higher than that of methane or gasoline (at stoichiometric conditions). As a result, hydrogen fires burn quickly and tend to be relatively short-lived. Hydrogen burns more vigorously than gasoline, but for a shorter period. Pools of liquid hydrogen burn very rapidly at 0.098-0.197 ft/min (3-6 cm/min) compared to 0.0098-0.00656 ft/min (0.3-1.2 cm/min) for liquid methane, and 0.00656-0.0295 ft/min (0.2-0.9 cm/min) for gasoline pools [7].

Hydrogen flames are pale blue and almost invisible in daylight due to the absence of soot. Visibility is increased by the presence of moisture or impurities (such as sulfur) in the air. Hydrogen flames are readily visible in the dark or low-light conditions.

2.2.2.4 Air/fuel ratio

The stoichiometric air/fuel (A/F) mass ratio for the complete combustion of hydrogen in air is approximately 34:1, which is much higher than 15:1 A/F required for gasoline. Because

hydrogen is a gaseous fuel at ambient conditions, it occupies more of the combustion chamber than a liquid fuel. As a result, less of the combustion chamber can be occupied by air [8].

2.3 Hydrogen in Fuel Cells

Hydrogen is an energy carrier that can be used to store, move, and deliver energy produced from other sources. It is a clean fuel that, when consumed in a fuel cell, produces only water. The FC is one of the several energy conversion technologies that can be fueled by hydrogen. Aside from being pollution-free, FCs are quiet and can achieve efficiencies that are two to three times greater than the standard internal combustion engines (ICE). Key hydrogen end-use technologies are making significant progress towards commercialization. The FC applications include generating electricity for the utility grid or micro-grids or heating buildings, for transport vehicles, buses, and materials handling equipment and also in portable applications such as laptops or cell phones. Using pure hydrogen as fuel, the sole output to the environment is water, thus avoiding the effects of releasing particulates, toxic substances or gases contributing to the greenhouse effect.

2.3.1 Parts and mechanism of FC:

Fuel cells basically involve a reversal of electrolysis. A fuel cell always contains two electrodes. Depending on the type of fuel cell, pure hydrogen (H_2) or a fuel containing hydrocarbons is fed through the anode while pure oxygen (O_2) or air as an oxidation material is fed through the cathode. An electrolyte separates the anode and cathode. A catalyst at the anode oxidizes the fuel molecules that separate into protons and electrons, which take different paths to reach the cathode. Electrons flow over a large circuit and produce electric energy while the remaining positively charged ions diffuse through the electrolyte. The waste product is water. **Figure 3** shows the basic working diagram of a fuel cell. The fuel cell does not shut down or require charging, it produces electricity and heat with a constant supply of H_2 [6, 9, 10].

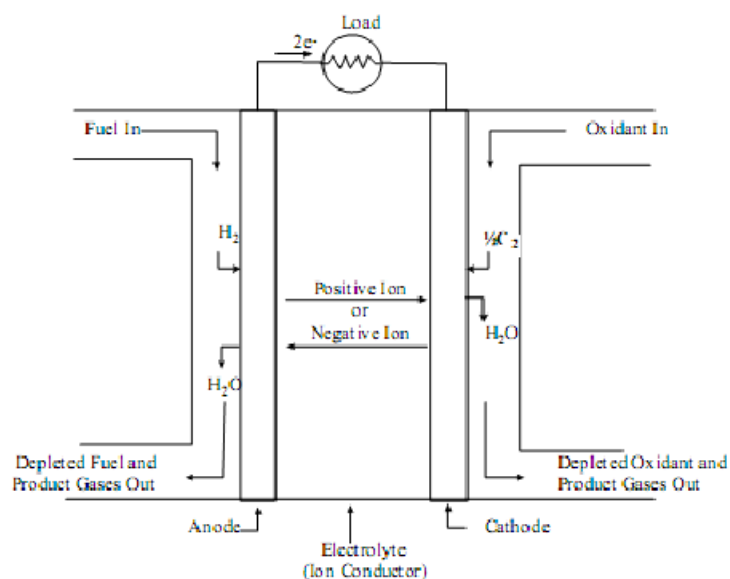


Figure 3: Basic schematic of a Fuel Cell [11].

Below are the main categories of FCs of scientific interest over the past years:

1. polymer electrolyte FCs (PEFCs; also called proton exchange membrane FCs (PEMFCs))
2. solid oxide FCs (SOFC)
3. alkaline FCs (AFC)
4. phosphoric acid FCs (PAFC)
5. molten carbonate FCs (MCFC).

Table 3: Characteristics of different types of fuel cells.

	<i>Temperature</i>	<i>Electrolyte</i>	<i>Fuel</i>	<i>Catalyst</i>	<i>Efficiency</i>	<i>Output</i>
<i>AFC</i>	90-100 °C	Potassium Hydroxide	H ₂	Nickel	60-70 %	10-100 kW
<i>PEMFC</i>	50-80 °C	Membrane Polymer	H ₂	Platinum	50-60 %	5-250 kW
<i>PAFC</i>	150-220 °C	Phosphoric acid	H ₂	Platinum	40 %	400-1000 kW
<i>MCFC</i>	650 °C	Molten carbonate	H ₂ , CO, CH ₄	Nickel	40-60 %	10 kW-2MW
<i>SOFC</i>	800-1000 °C	Yttria stabilized zirconia	H ₂ , CO, CH ₄	Perovskites	50-60 %	1 kW-2MW

The electrolyte is the main characteristic that distinguishes the different types of fuel cells because it determines the operating temperature, which varies widely between types as seen in **Table 3** above. Various types of electrolytes are conductive to various ions, so the fuel in each type of fuel cell varies. Electrolytes can be in liquid or solid form and operate at high or low temperatures. Electrolytes operating at low temperatures require the help of catalysts made up of precious or non-precious metals, those aim to accelerate the relevant chemical reactions. A basic catalyst for each type of fuel cell is also seen on the table. The fuel cell efficiency is defined as a ratio between the electricity output (kW) and hydrogen consumed, which is calculated according to Faraday's Law. These values are also stated in the table above accordingly [12-14].

More recently, direct alcohol fuel cells (DAFCs) have gained attention and scientific interest due to their simplicity and their high-power density. However, as DAFCs have evolved, several issues concerning their performance optimization have arisen, and research for solutions is already underway. These issues, which are to blame for the short lifetime and poor cell performance, can be summarized as follows: (a) low alcohol electro-oxidation kinetics, (b) alcohol crossover, and (c) electrode delamination [15].

2.3.2 Applications of Fuel Cells

2.3.2.1 Power

A stationary fuel cell can be used in commercial, residential, or industrial applications and for backup power generation. Fuel cells are also very useful as power sources in remote locations, such as weather stations, communication centers, and military applications, because they have no moving parts that require lubrication and maintenance when not in use.

At the moment, the use of hydrogen in power generation is negligible. It accounts for less than 0.2 % of total electricity supply, owing primarily to the use of high-hydrogen-content mixed gases from the steel industry, petrochemical plants, and refineries, as well as byproduct pure hydrogen from the chlorine-alkali industry. Hydrogen can be used as fuel in reciprocating gas engines and gas turbines. Over the last ten years, the global installed capacity of stationary fuel cells has increased rapidly, reaching 2.2 GW in 2020. Today's reciprocating gas engines can handle gases containing up to 70% hydrogen (on a volumetric basis), and various manufacturers have demonstrated engines containing 100% hydrogen, which should be commercially available in the coming years. At present, only 150 MW use hydrogen as fuel.

2.3.2.2 Cogeneration

Cogeneration fuel cell systems including micro combined heat and power (MicroCHP) systems are used to generate energy and heat for factories and homes. A schematic of the residential use is illustrated in **Figure 4**.

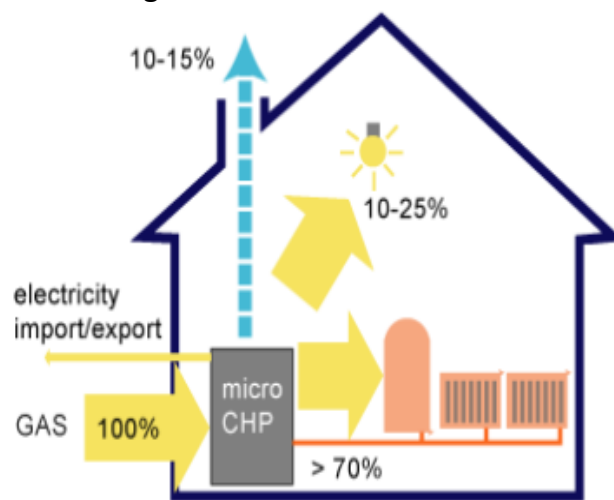


Figure 4: Micro-combined heat and power systems (micro-CHP) [16].

The system ensures continuous electrical energy while also generating hot air and water residues. The cogeneration system has an efficiency of up to 85%. A phosphoric acid fuel cell also employs a combined heat and power system, with an electrical efficiency of up to 90%. Solid oxide and molten carbonate fuel cells using combined heat and power systems can reach an efficiency of 60%.

2.3.2.3 Portable power systems

A portable fuel cell produces less than 5 kW of power and is relatively light in weight, weighing between 7 and 9 kg. The portable fuel cell market is quite large, accounting for roughly 40% of the total market size of \$10 billion. The first is the micro-fuel cell market, which is a small electronic device with a power range of 1-50 W. The second market is 1-5 kW power generators for applications such as military outposts and remote oil fields. Because of its higher energy density, it can be a very effective and environmentally friendly alternative to lithium-ion batteries. The only disadvantage of the micro-fuel cell system is the addition of system elements (the cell, the necessary fuel, and peripheral attachments), which results in an increase in weight, nearly 530 Wh/kg, whereas lithium batteries weigh around 44 Wh/kg.

2.3.2.4 Transportation

Maybe the current best-known use of hydrogen is from the transportation sector. Hydrogen as a fuel has already found applications in experimental cars and all the major car companies are in competition to build a commercial car and start marketing hydrogen fuel automobiles, at a higher cost compared to gasoline cars but with an expectancy to decrease with time. In addition to cost, longevity, frequency of repair, and performance in cold weather are other areas in which fuel cells are not yet competitive with gasoline engines for their widespread use. The applicability of hydrogen in fuel cells depends on the mode of transport, which reflects the diverse character of the transportation industry that includes air, land, and sea transportation, as well as passenger and shipping (**Figure 5**). Light-duty vehicles account for about half of global transportation energy demand, and the number of passenger vehicles is predicted to double from one billion to 2.5 billion by 2050 (Energy Information Administration, 2017).

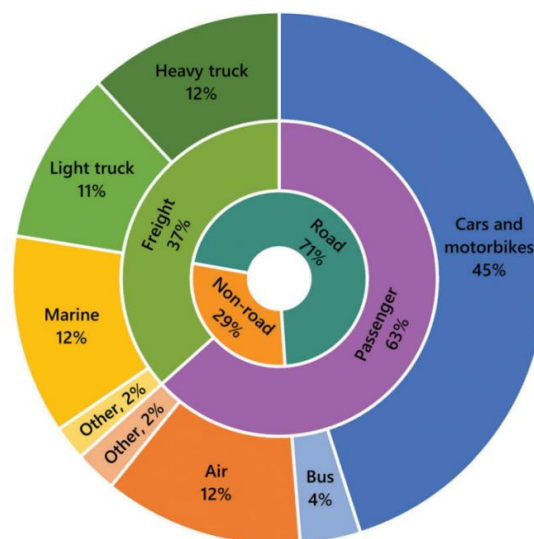


Figure 5: Breakdown of energy usage in the transport sector globally in 2015. The outer ring gives the share of individual modes. “Other” is primarily passenger rail and air freight. The middle and inner rings aggregate these uses by mode and function. Data from EIA.³⁵ Total consumption was 110 million TJ in 2015 worldwide, equivalent to 37 kW h per person per day in OECD countries and 7 kW h in non-OECD countries [17].

Hydrogen is one of the three main low-carbon transport options, along with electric vehicles (EVs) and biofuels. Hydrogen avoids the slow recharging and limited range associated with EVs, and the air quality and land-use effects of biofuels [18]. Hydrogen vehicles could improve air quality, helping tackle climate change. This is of urgent priority since Europe faces over 500.000 premature deaths every year due to NO_x emissions and particulates [19]. Also, €24 billion with external costs around €330–940 billion are the costs induced by air pollution in Europe annually, because of healthcare, crop yield loss, illness-induced loss of production, and damage to buildings. This has led big cities to announce bans on diesel-powered vehicles leading up to 2025 [20], while France and the UK focus more on pure combustion cars and trucks regulations by 2040 [21, 22].

Several countries have proclaimed their purpose to develop fleets of hydrogen vehicles up to 1 million by 2030. These strategies approach the total of 4.6 million (**Table 4**). This is still a tiny number given the existing fleet of Internal Combustion Engine vehicles, which are over 1 billion, but it is comparable to the amount of electric vehicles, which was around 5 million, in 2018 [23].

Table 4: National goals for the use of hydrogen filling stations, thousand units [23].

	2020	2022	2023	2025	2028	2030
US	13	40				
California						1 000
Japan	40			200		800
France		5			20 – 50	
China	5			50		1 000
The Netherlands	2					
Korea			81			1 800

Internal combustion engines ('ICEs') that can be converted to run on pure hydrogen ('HICEs') could see early implementation because they are far less expensive than fuel cells. However, because hydrogen combustion is much less efficient than fuel cells and produces NO_x, it is unlikely to play a major part in transportation in the long run. Dual-fuel automobiles can run on both hydrogen and natural gas or diesel, while in bi-fuel powertrains the driver can switch between the fuels. This allows current infrastructure to be used, however, it is not emission free and may eventually be replaced by lower-carbon alternatives.

Drivers of electric vehicles are often concerned about the range and time needed for recharging. Battery-powered vehicles take approximately 45 minutes to recharge themselves whereas hydrogen vehicles are refuelled in less than 10 minutes. Moreover, hydrogen vehicles are much lighter in weight, in comparison to battery vehicles, which is a beneficiary element for heavy vehicles like trucks and buses. Not only limited to on-road vehicles hydrogen fuel cells also find applications in marine ships. An IC engine uses less than 20% of the fuel, while the fuel cell uses 60% of the fuel, making the efficiency of the fuel cell better compared to the IC engines. When used as vehicle fuel, the low density of hydrogen necessitates that a large volume of hydrogen must be fed to provide an adequate driving range. A typical set-up of a Hydrogen Electric Car is

presented in **Figure 6**. Hydrogen is stored in the Hydrogen Tank which fuels the Fuel Cell, the electricity generated is stored in a Battery and is used to power the Electric Engine. The engine propels the movement of the wheels to eventually drive the car.

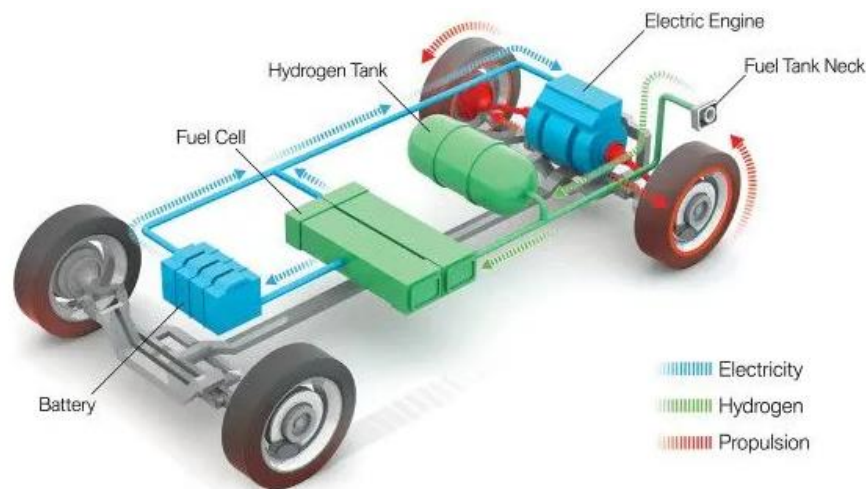


Figure 6: Block Diagram of a Hydrogen Car (Image: BMW) [24].

Fuel cell electric vehicles (FCEVs) predominantly use PEM fuel cells that offer high efficiency, high power density and cold-start capabilities. A 60 kW fuel cell is typical for European cars, which is substantially larger than residential use fuel cells. Competing markets include conventional internal combustion engines (ICEs), battery electric vehicles (BEVs) and plug-in hybrid vehicles (PHEVs), which allow most journeys to be completed using a battery, and switch to the engine or fuel cell for longer journeys.

Fuel cells require catalyst metals such as nickel and platinum which are extremely energy intensive to produce. Just as with other low carbon technologies (solar PVs and nuclear), the energy required to manufacture the fuel cell and the resulting carbon emissions are important as these offset the savings made during operation. But the battery is also composed of very hazardous materials like cobalt, lead, and lithium which are non-friendly to the environment as well as to human health. The most commercially used PEMFC mainly comprises of polymers and graphite which are environmentally friendly and easily available, apart from platinum [6].

A comparison of HFCVs in which the hydrogen was produced by (i) steam reforming of natural gas, (ii) wind electrolysis and (iii) coal gasification by Jacobson, Colella, & Golden [25]:

Wind hydrogen fuel-cell vehicles HFCVs may save 2300 to 4000 lives/year and \$32 billion to \$180 billion/year in the United States relative to hybrids, and wind or natural gas HFCVs may save 3700 to 6400 lives/year and reduce asthma by 1 million to 3 million cases/year relative to current fossil-fuel on-road vehicles FFOVs. The three HFCV cases all reduced health costs (because most improvements in air quality resulted from eliminating FFOV exhaust), wind and natural gas HFCVs reduced such costs the most and reduced ozone by up to 20 ppb. Wind HFCVs reduced climate costs the greatest, making them the most beneficial environmental technology. Natural gas HFCVs increased CH₄ but reduced CO₂ and so these

are ranked second. Hybrids reduced climate costs but had increased health costs relative to coal HFCVs, suggesting a rough tie for third. Both HFCVs and Hybrids outranked FFOVs in health and climate costs.

For automotive applications PEM fuel cells appear to be most suitable, because of the low temperature range of their working conditions, allowing their system to start up faster than those technologies using high temperatures fuel cells. Moreover, the solid state of their electrolyte (providing no leakages and low corrosion) and their high power density make them fit for transport applications. Automotive grade PEMFC designs using available technology to convert hydrogen to electricity at typical efficiencies around 50-60%, when the balance of plant components and the power to run them are included. Balance of plant components include air humidifiers, water pumps, air compressors, cooling fans, filters, reservoirs, and water separators. Although Pt is the best-known catalyst for this reaction, it cannot meet the demands of a mature hydrogen economy because of its high cost and limited CO-tolerance (<10 ppm). For large-scale stationary applications, solid-oxide fuel cells operating continuously in the range of 800–1000°C are the favoured technology for their economies of scale [12, 14].

Two-wheeled vehicles like motorbikes are dominant for passenger transport in many regions. Their low fuel consumption allows them to be refuelled using hydrogen canisters from vending machines. FCEV motorbikes could also contribute toward better city air quality and noise pollution targets. Lastly, fuel cells could be used in agricultural equipment such as tractors and recreational applications such as golf carts. This remains one of the few profitable sectors today [9, 10].

The two major challenges today for fuel cells in the automotive industry are cost and durability. Current fuel cell systems are estimated to cost five times as much as automotive internal combustion engines (about \$25-35/kW), even when cost savings for high-volume manufacturing are applied. Major contributors to the cost are platinum electrocatalyst, membrane, and bipolar plates. Automotive fuel cell systems will also need to be as durable and reliable as current automotive engines (5,000 h lifespan or 150,000 mi. drive range) under heavy load cycling. Variations in cell potential and relative humidity levels accelerate the degradation of both the catalyst and the membrane. Also, fuel cells need to be able to function over the full range of vehicle operating conditions (-40 to +40°C) [13, 26].

2.3.2.4.1 Heavy-duty on road Vehicles

Whilst FCEVs face strong competition from ICE and BEV passenger cars, they may be the best (and possibly the only) realistic zero-carbon option for high-utilisation, heavy-duty road transport vehicles such as buses and trucks. Back-to-base operations require fewer refuelling stations, making them more extensively used, and lowering initial refuelling costs. Three key differences for heavy-duty transport are low manufacturing volumes (meaning the cost gap with ICE becomes smaller), and the need for greater longevity and energy density. The US DOE expects 25000-hour operating lifetime for fuel cell buses, versus just 8000 for passenger cars. Fuel cell buses consume 10 times more hydrogen per kilometre

than passenger cars – amplifying range limitations. Thus, they are likely to remain unsuitable outside of urban environments [17].

Fuel cell buses, in particular, have attracted significant attention and are fairly mature, with a Technology Readiness Level (TRL) of 7. On-board tanks typically hold around 40 kg of hydrogen stored in the bus roof, and reduced space restrictions mean this can be stored at 350 bar, lowering tank and compression costs. Fuel cell buses may have a higher total cost of ownership (TCO) than diesel by 2030 but could be even cheaper if deployed at scale.

Trucks have a high potential for fuel cell adoption due to their high energy requirements and a lack of other low-emission alternatives. Light goods vehicles with short low-speed journeys could be equipped with batteries and range-extender vehicles; however, long-haul heavy vehicles with high utilisation of about 50000-hour stack lifetime will almost certainly require hydrogen. Auxiliary Power Units (APUs) for heavy-duty vehicles are also being developed using fuel cells. To avoid engine idling, these could power refrigeration units and other loads on stationary HGVs (e.g., cabin heating, cooling, lighting, and electrical devices). FCEV trucks have seen lower implementation than buses due to the HGV market being highly cost sensitive with limited government support or intervention, and transport companies being hesitant to change. Interest could grow as diesel trucks begin to be blocked from major city centres.

2.3.2.4.2 Rail

Since the early 2000s, hydrogen and fuel cell technologies have been demonstrated in rail applications such as mining locomotives, switchers, and trams. In 2018, Alstom launched the first commercial service of a hydrogen fuel cell passenger train on a 100-kilometer route in Germany. Since then, two Alstom trains in Germany have traveled more than 180 000 kilometers, and more countries have begun testing and adopting fuel cell trains. Although hydrogen powertrains are 50% more expensive than diesel, their economic viability is dependent on lower-cost fuel. Hydrogen trains could be used on routes that are difficult or expensive to electrify due to route length or urban space constraints. A fuel-cell-powered train has roof-mounted hydrogen tanks and a 500-mile range.

2.3.2.4.3 Ships

Marine applications hold great promise for hydrogen deployment, with fuel cells being tested for propulsion in a few projects, including ferries. Hydrogen is expected to gain traction sometime after 2030 due to the growth of emissions-controlled zones (such as the Baltic Sea and urban ports) and hydrogen's higher efficiency than LNG. Most vessels have long lifetimes and are built in small numbers that are highly tailored to specific applications; this may impede the introduction of new propulsion systems. With ferries consuming up to 2000 kg of hydrogen per day, cryogenic storage is required, and fuel costs are more crucial than upfront capital, with hydrogen costing significantly less than \$7 per kg required.

2.3.2.4.4 *Aviation*

Aviation is one of the most difficult sectors to decarbonize, with little progress made in reducing emissions from aircraft propulsion. The industry group ATAG sees hydrogen fuel cells as having a role in flights of up to 1 600 km, and hydrogen combustion in short and potentially medium-haul flights. If the technology is successfully developed, hydrogen fuel cells could be used in 75% of commercial flights. However, the climate benefits of hydrogen for aviation are questionable because it produces more than double the water vapour emissions of kerosene; water vapour at high altitudes, although short lived in the atmosphere, causes radiative forcing, and thus contributes to net warming. Except for small or low-flying aircraft, significant hydrogen deployment is thought unlikely before 2050. Another setback is the need for equipment to mitigate NO_x emissions.

Fuel cells have been tested for use in aircraft auxiliary power units as well as taxiing aircraft to and from airport terminals. There is an increasing motivation to improve air quality around airports and fuel cells could play an important role by powering ground vehicles and buses, followed by the need for a lower number of refuelling stations with high utilisation. Unmanned aerial vehicles (UAVs) are also gaining popularity for civilian and military applications. Fuel cell UAVs are quieter, more efficient, and have lower vibration and infrared signatures than fossil fuel-powered UAVs. They are also lighter than battery systems and have a greater range. Fuel cell UAVs are currently significantly more expensive than battery UAVs; however, the cost disparity will close as manufacturing volume increases [3].

2.4 Environmental Impact of Hydrogen Fuel

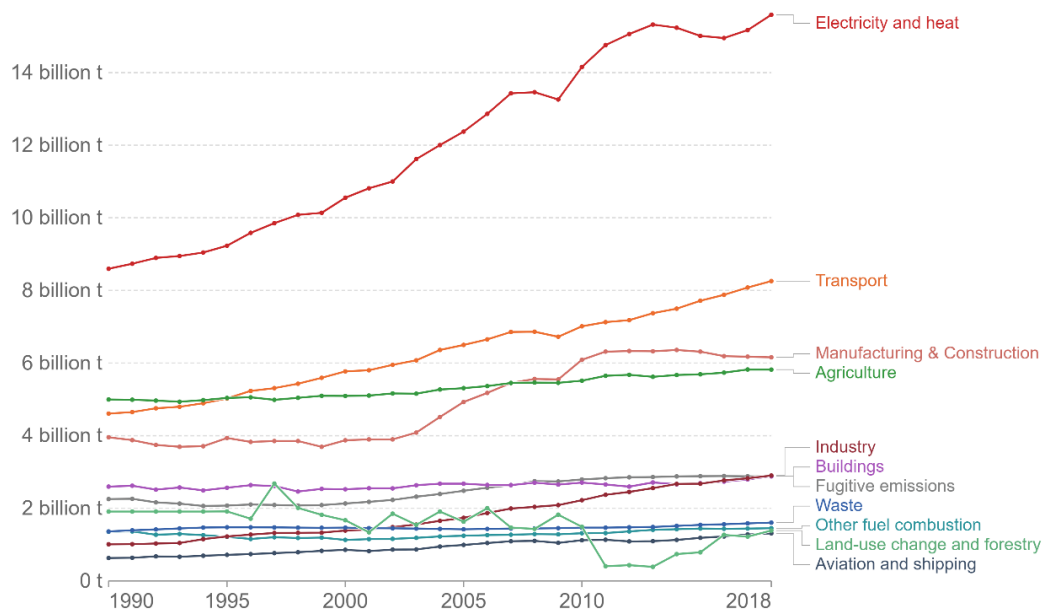
2.4.1 Background

On the one hand there is a challenge to acquire new sustainable energy sources. On the other hand, continuous extraction and combustion of fossil fuels that is followed by serious environmental consequences is necessary to meet the growing energy demands caused by population, urbanization, and industrialization in both developing and developed countries.

In **Figure 7** we see that electricity and heat production are the largest contributors to global emissions worldwide exceeding 14 billion tons of carbon dioxide-equivalents (CO₂e) in 2018, followed by the transport, manufacturing and construction and agriculture sectors weighing between 5-9 billion tons of carbon dioxide-equivalents (CO₂e). In Europe the distribution by sector aligns with the figure, but this is not the same everywhere. If we look at the United States, for example, transport is a much larger contributor. Whereas in Brazil most emissions come from agriculture and land use change. The global breakdown for CO₂ is similar to that of total greenhouse gases, electricity and heat production dominates, followed by transport, then manufacturing and construction [27]. It is clear that high fossil fuel usage and consumption in the power and transport sector increase emission of pollutants, causing serious negative externalities and environmental degradation.

Greenhouse gas emissions by sector, World

Greenhouse gas emissions are measured in tonnes of carbon dioxide-equivalents (CO₂e).



Source: CAIT Climate Data Explorer via Climate Watch

OurWorldInData.org/co2-and-other-greenhouse-gas-emissions • CC BY

Figure 7: GHG emissions by sector worldwide [28].

The greenhouse gas (GHG) emissions from the transport sector are severe, and road vehicles are the single largest source for the major atmospheric pollutants. Such pollution is not only bad for the environment, but it could also prove dangerous for human health and well-being. The rate of fossil fuel consumption is higher than the rate of the fossil fuel production of nature. One of the complications will be the scarcity of automobile fuel in the world which will create problems in the transport sector. It is evident that we need a clean energy system in the near future [6, 29-33].

2.4.2 "Grey", "Blue", & "Green" Production

The power of **hydrogen** and its important effect on cleaning the environment when used as fuel for transport, heat and other energy applications is easily understood. The overall hydrogen gas quality, while "green" when used as a fuel, is influenced by the production method. Thermochemical production processes for the production of hydrogen may lead to the presence of contaminants such as methane (CH₄), nitrogen (N₂), carbon monoxide (CO) and carbon dioxide (CO₂); other trace constituents, argon (Ar), ammonia (NH₃), formic acid (HCOOH), formaldehyde (HCHO), total hydrocarbons (THC) excluding CH₄, sulphur-containing compounds, and halogens depend on the type of feedstock utilized and the level of pre-treatment and purification. Possible contaminants from electrolytic routes to produce hydrogen are oxygen (O₂), N₂, CO₂ and water (H₂O).

Steam methane reforming from natural gas (SMR) or coal gasification are the most common methods for producing hydrogen nowadays. In terms of the cost of hydrogen produced (1-2 US \$/kg, depending on coal and gas costs), this low-cost technology, that is well-established on the industrial sector, is likely that will be providing the majority of hydrogen for the next

30–50 years, until cheaper sustainable solutions are found[34]. The carbon footprint of manufacturing processes, however, becomes an equally significant factor in the period of the Energy Transition. Carbon dioxide emissions from SMR are 10 kg CO₂/kg H₂. As a result, this hydrogen is known as "grey." By this indicator, it is either similar or 2.5 times worse than conventional natural gas, depending on the source (gas or coal). Clearly, it is more optimal to use natural gas rather than "grey" hydrogen in terms of decarbonisation, hence it cannot take place in the future hydrogen economy.

An alternative is to produce "grey" hydrogen while combining Carbon Capture and Storage technology (CCS). The hydrogen captured in this way is known as "blue". Unlike SMR, CCS is still in the early stages of commercialization. Global CCS Institute claimed that only 18 big CO₂ capture plants were operational worldwide, in 2018, with another 5 under construction and 20 in phases of development [23].

The second option to "grey" is "green" hydrogen, which is produced by electrolysis using low-carbon energy, primarily from renewable sources. Hydrogen produced by electrolysis is not always called "green". The carbon footprint of the electricity used in the operation determines that. For example, most known units in Germany use electricity from the grid rather than renewables, so hydrogen produced is classified as "grey" due to its relatively large carbon footprint. Connecting an electrolyzer entirely to renewables can alleviate this problem, but the load factor of the electrolyzer is reduced nearly in half in this case. The decarbonization of the electricity industry, which is expected to reach 100% by 2050 in Germany, is another approach to make the electrolysis process "greener."

Only "green" hydrogen may be used in sectors other than electricity generation, hence it is a cornerstone of the whole concept of hydrogen economy, with research centers centered around it in most hydrogen programs [23].

2.4.3 Environmental Impact Factors & Greenization Factors

Hydrogen gas was sampled from three different production sources (SMR, alkaline and PEM water electrolyzer) for the sake of understanding the level and variety of contaminants in real samples of hydrogen. Comparison of the hydrogen contaminant amount fraction against the threshold set by ISO 14687 Grade D (for hydrogen vehicles) affirms that the quality of hydrogen produced from the three routes investigated is below the threshold or at the threshold for all constituents [35].

Another way to compare the Environmental Impact Factor of carbon and hydrogen is:

$$EIF \text{ of carbon} = \frac{\text{Carbon (CO}_2\text{) emission by fossil fuel consumption}}{\text{Natural carbon (CO}_2\text{) circulation}} \quad (1)$$

$$EIF \text{ of hydrogen} = \frac{\text{H}_2\text{O emission through hydrogen energy system}}{\text{Natural water vaporization}} \quad (2)$$

Based on a hydrogen energy system, the average EIF of hydrogen is 0.0001. The EIF of carbon is more than 100 times larger than that of hydrogen [35].

The greenization factor was originally introduced by Dincer and Zamfirescu [36] as:

$$GF = \frac{EI_{bc} - EI_{gc}}{EI_{gc}} \quad (3)$$

Where EI is the environmental impact. Bc stands base (reference) case for which the greenization process is applied to and gc stands for greenized case [35].

Dincer [37] defined as greenization as a new discipline to help achieve better efficiency, better cost effectiveness, better environment, and hence better sustainability in two ways:

1. as a process of converting traditional/conventional systems with higher environmental damage, less efficiency, more cost, etc. into more efficient, more cost effective, and more environmentally friendly ones as greenized systems, and
2. as a process of developing new energy solutions under SSS (System, Source, Service) criteria which are greener than the traditional/conventional ones.

The greenization factor ranges from 0 to 1. Energy systems with greenization factor of 1 reflect a fully greenized system with no or minimum negative environmental impact, when greenization factor of 0 indicates the reference system [36].

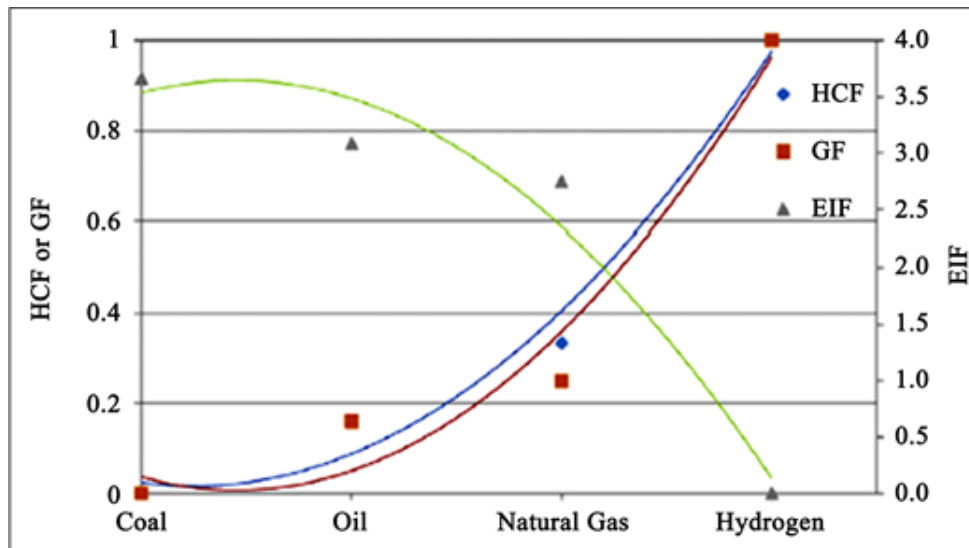


Figure 8: Hydrogen Content Factor (HCF), Greenization Factor (GF), and Environmental Impact Factor (EIF) of hydrogen and other fossil fuels [38].

Figure 8 presents the greenization factor (GF), the environmental impact factor (EIF) and the hydrogen content factor (HCF) of four different energy fuels (coal, oil, natural gas, and hydrogen) [37].

2.4.4 Leakage of Hydrogen

Recently, there have been some concerns over possible problems related to hydrogen gas leakage, as the molecular hydrogen leaks from most containment vessels. It is hypothesized that if significant amounts of H₂ escape to stratosphere, H* free radicals can be formed due to ultraviolet radiation, which in turn can enhance the ozone depletion. However, the effect of these leakage problems may not be significant as the amount of hydrogen that leaks presently is much lower (by a factor of 10-100) than the hypothesized 10-20%.

Leaks of liquid hydrogen evaporate very quickly since the boiling point of liquid hydrogen is extremely low. Hydrogen leaks are dangerous because they can cause fires where they mix with air. But the small molecular size that raises the risk of a leak also results in very high buoyancy and diffusivity; therefore, leaked hydrogen rises and becomes diluted quickly, especially outdoors. This results in a very localized region of flammability that disperses quickly. The buoyancy declines as the hydrogen dilutes with distance from the leakage site, and the tendency for the hydrogen to continue rising decreases. Very cold hydrogen, resulting from a liquid hydrogen leak, becomes buoyant soon after it evaporates. In contrast, leaking gasoline, or diesel evaporates slowly resulting in a widespread and lingering fire hazard. A stream of hydrogen from a leak is almost invisible in daylight. Compounds such as mercaptans and thiophanes that are used to scent natural gas cannot be added to hydrogen for fuel cell use as they contain sulfur that would poison the fuel cells [3, 39-44].

2.5 Hydrogen Economy

The “Hydrogen Economy” or “Hydrogen Energy System” is a hypothetical concept for a system in which hydrogen is the primary energy carrier. During a presentation at the General Motors (GM) Technical Center in 1970, John Bockris was the first to introduce the term. The major goal of a hydrogen economy is for hydrogen to be produced primarily from readily available energy sources, with the goal being to replace the fossil fuels used in industry, transportation, and residential sectors. Hydrogen economy is being proposed to be a and long-term solution to the following interconnected problems of the world:

- (i) depletion of natural resources,
- (ii) global environmental issues,
- (iii) food shortage - malnourishment in the 3rd world countries,
- (iv) health problems, and
- (v) expanding growth of the Earth’s population.

The issues regarding the fossil fuel economy are severe and overwhelming, but the growth of the hydrogen economy will have tremendous benefits to the environment, economy, energy security, and consumers. However, rapid conversion from a fossil fuel to hydrogen has been challenged by severe technological, scientific, and social obstacles. The extremely low density of hydrogen makes storage a crucial issue in the transition. Although refineries and chemical industries commonly employ hydrogen, the expenses of generation, storage,

and delivery are too costly and unsatisfactory for most energy applications. Even so, the enormous benefits of the hydrogen economy are so exciting that governments all over the world are investing heavily in improving the potentials of the energy system [45].

In 2003, The High-Level Group for Hydrogen and Fuel Cell Technologies of the European Commission proposed that the European Union should have achieved a hydrogen-based economy by 2050, and anticipated that by 2040, 35% of newly produced vehicles will be fuelled by zero carbon hydrogen. The Energy Efficiency and Renewable Energy, Fossil Energy, Nuclear Energy, and Science Offices of the US Department of Energy, suggested that the conversion to hydrogen-powered fuel cell automobiles should take place around 2020 [45]. Yet, today, hydrogen is used for less than 2% of Europe's current energy consumption and mostly to make chemical products like fertilizers and plastics. Moreover, 96% of this hydrogen is produced by natural gas, emitting 70 to 100 million tons CO₂ annually in the process. Hydrogen, however, can be produced using renewable energy. The good news is that in 2020, the European Commission adopted a new hydrogen policy. It includes a variety of actions, ranging from research and innovation to manufacturing and infrastructure, as well as the international dimension. In line with the European Green Deal, the plan will explore how production and usage of renewable hydrogen might help decarbonize the economy while being cost-effective (also helping the economic recovery after COVID-19) [46].

Thus, the new European Commission's goal, presented in July 2020, is to upscale the supply and demand of renewable hydrogen. The strategic objective is to install 40 GW of renewable hydrogen electrolyser capacity in EU, which will be producing about 5 Mt of renewable hydrogen. This will be based upon an estimated demand of renewable hydrogen in the EU of up to 10 Mt per year by 2030 [47].

2.5.1 Energy Transition

"The Energy Transition" is a global transformation process taking place in the international energy sector. It is related primarily to decarbonization and low carbon production [48]. Declarations of several countries, made in 2015 during the Paris Agreement, oblige to limit greenhouse gas emissions by 25–40% by 2030. Germany and the United Kingdom have announced their intention to cut emissions by 80-100% by 2050 [23] (as shown in **Table 5**).

The most active countries in the EU are Germany and the United Kingdom. However, in 2017, an all-European initiative called FCH JU (Fuel Cells and Hydrogen Joint Undertaking) was launched. By May 2018, it was already membered by 89 regions and cities from 22 European nations. Participants in this European effort express their desire to include hydrogen technology into their energy strategy as part of the "Energy Transition," which includes the implementation of projects worth around €1.8 billion over the next five years [23].

In the summer of 2014, the Japanese program "Strategic Roadmap for Hydrogen and Fuel Cells" was introduced. The program targets to widen the climate or technological agenda in order to begin the development of a "hydrogen-based society" [49]. The roadmap includes

precise key indicators for various technical chains at once, including hydrogen generation, storage, transit, and usage, with 2020, 2025, 2030, and 2050 milestones. The target for hydrogen utilization in Japan is to expand from 200 tons to 10 million tons per year by 2050. In 2017 the state funding for the program was 310 million Euros, and the overall amount is expected to be several billion Euros by 2040 [49].

Table 5: Examples of stated national goals to reduce emissions and increase absorption of greenhouse gases [23].

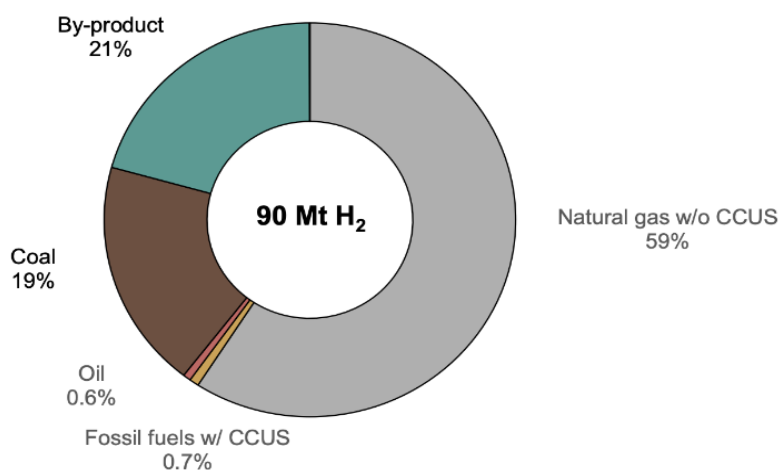
Countries	Declared contribution towards mitigating climate change
US	by 2025 to reduce greenhouse gas emissions by 26 - 28% from 2005 levels
Canada	2030 - by 30% from 2005 levels
Germany	2030 - by 40-55% from 1990, 2050 – by 80-95%
France	2030 - by 40% from 1990 levels
Norway	2030 - by 40% from 1990 levels
Brazil	2025 - by 37% from 2005 levels
Mexico	2030 - by 22—36% from the baseline
China	By 2030 – to reduce greenhouse gas emissions by 1 US Dollar of GDP, carbon intensity by 65% , reaching the peak of absolute value of emissions no later than 2030
Australia	2030 - by 26 - 28% compared to 2005

The United States has been operating a hydrogen program, under various names, since the 1970s. The initiative acquired a second impetus in the twenty-first century, when the US DOE Hydrogen and Fuel Cells Program obtained annual funding of \$120 million and almost double that amount in 2004-201. The Hydrogen Council, at corporate level, is the most well-established organization in the field of hydrogen technology. By the end of 2018, the organization, which was created in Davos in 2017, had grown to 53 firms from 11 countries, with a combined workforce of 3.8 million employees and yearly earnings of €1.8 trillion. The Hydrogen Council, in its program study, indicated that its members were eager to invest at least €1.9 billion per year in Research & Development (R&D) and market development from 2018 to 2022. The organization's long-term vision is to develop a market for hydrogen technologies worth \$2.5 trillion, create 30 million jobs, and expand hydrogen's role as an energy carrier to 18% of global final energy consumption, by 2050.

According to the International Energy Agency, only three forms of fossil fuels occupied comparable shares of over 12-19% of global final energy consumption in 2017: gas (22 %), coal (27%), and oil (32%)[50]. This indicates that by 2050, hydrogen's contribution in the global energy sector might be comparable to that of each of these resources, and it will be far more important than the roles of nuclear power plants, hydropower, and bio-energy combined [23].

2.5.2 Consumption/Demand

With the transition to environmentally sustainable energy systems and the potential of hydrogen to become one of the two (along with electricity) major energy carriers of the future, demand for hydrogen could rise dramatically in the coming decades. **Figure 9** depicts the current world's distribution of resources for hydrogen production. Fossil fuel-based hydrogen accounts for 78% of the world's hydrogen production whereas a small portion of hydrogen (about 0.03%) is produced by water electrolysis. An important observation is that the production of hydrogen from light hydrocarbons requires a minimal amount of energy compared to water electrolysis.



IEA. All rights reserved.

Note: CCUS = carbon capture, utilisation and storage.

Figure 9: Sources of hydrogen production (Based on the data from the Global Hydrogen Review 2021, International Energy Agency, 2021).

Global hydrogen demand was approximately 90 Mt H₂ in 2020, having grown in double since the turn of the millennium. Almost all of this demand comes from refining and industrial uses. Annually, refineries consume close to 40 Mt H₂ as feedstock and reagents or as a source of energy. Demand is somewhat higher (more than 50 Mt H₂) in the industry sector, mainly for feedstock. Chemical production accounts for around 45 Mt H₂ of demand, with roughly three-quarters directed to ammonia production and one-quarter to methanol. The remaining 5 Mt H₂ is consumed in the direct reduced iron (DRI) process for steelmaking. This distribution has remained almost unchanged since 2000, apart from a slight increase in demand for DRI production. The adoption of hydrogen for new applications has been slow, with uptake limited to the last decade, when fuel cell electric vehicle (FCEV) deployment started, and pilot projects began to inject hydrogen into gas grids and use it to generate electricity. Positive results from these experiences prompted the development of some hydrogen technologies to the point of commercialization [6-8].

2.5.3 Technical Challenges

Global energy demand is predicted to triple by 2050, so oil and gas supply will be insufficient to meet this need. Hydrogen and fuel cells have turned out to be an essential alternative for many countries' future energy systems in the industrial, residential, and transportation sectors. However, hydrogen production, storage, cost, reliability, and use must be improved, in order to be included in future energy systems. The following are some of the technical issues that the hydrogen economy faces:

- Development of a sustainable route, free of CO₂, for mass production of hydrogen at a competitive cost.
- The volumetric energy density of liquid hydrogen very low, and hydrogen liquefying necessitates significant amounts of energy [51].
- Hydrogen is difficult to store as an energy carrier and to use as a fuel. The handling of unstable and possibly explosive hydrogen gas (b.p.: -253°C) requires special conditions, such as high pressure, special materials to avoid diffusion and leakage, and massive safety precautions [52].
- Development of practical mobile and stationary hydrogen storage systems.
- Development of efficient and safe infrastructures for hydrogen transport and distribution.

Regardless, many governments and major industries seem to be gradually committing themselves to improve the hydrogen economy.

During the switch era, modern maintenance/gasification methods, carbon dioxide absorption, and the development of novel, efficient, and cost-effective electrochemical processes are necessary. Fuel cells can replace latest power systems, such as batteries in cars and central/distributed power generation. The technology that fuel-cells can offer is quite appealing. This is because the efficiency of hydrocarbon fuels can currently be improved on the market. This will be achievable since hydrogen will be plentiful in the future. The main issues of fuel cells that need to be resolved are cost reduction and increase in durability of materials and components [3].

Many technological innovations are required to transition from a carbon-based energy economy to one that is more sustainable, not just in energy production but also in energy storage, transportation, transformation, and final usage. We encounter enormous engineering and scientific challenges at each one of these stages. In many circumstances, the materials available today are incapable of providing the requisite efficiency at a reasonable cost. Innovative materials with unique qualities are already helping to address some of these obstacles, thanks to the extraordinary control over the structure, size, and organization of matter that nanotechnologists around the world are gaining [53].

2.5.4 Future Trends

Because of its huge energy content and zero emissions, hydrogen has been hailed as the future fuel by the world's top economies. However, the standards for sustainable, safe, and efficient production, storage, and use have yet to be met. The US DOE in 2020 has set a hydrogen energy target in terms of storage density, which needs to be met, in order to totally replace fossil fuels on-board vehicles. Also, the cost of hydrogen production, storage, and use in fuel cells is currently quite high. Another necessity in hydrogen power systems, is to increase the round-the-trip efficiency (in-to-out electricity). Many experts throughout the world are working to find the best answers to these problems, but it will take much too long before all vehicles on the road run on hydrogen [3].

2.5.4.1 Vehicle Power Systems

Regarding the future automobile powering technology, electric vehicles (EVs) use lithium-based batteries as an energy storage, which limits the range of distance to cover in a single charge. Additionally, lithium batteries are expensive to recycle so they end up in landfills when their life is through, which results in an accumulation of harmful lithium on the planet. One solution to the problem could be to produce hydrogen from renewable sources of energy, store it in ionic-form porous materials, and then use it in fuel cells to generate power [3].

Future research will focus on hybrid systems that combine the benefits of hydrogen fuel cell technology with one or more traditional renewable energy sources. A future vehicle powering system could include a solar rooftop, a stack of fuel cells to power electricity-driven motors, and a hydrogen storage-based battery. Unlike conventional fuels, this system would release no hazardous emissions and have a far greater range than currently available EVs. Another example is a vehicle featuring vertical wind turbines on side panels to connect the vehicle's wind draft, a fuel cell to power electricity-driven motors, and a hydrogen storage-based battery. Without a doubt, these future technologies can save financial investment, worth millions of dollars, needed to construct electricity and/or hydrogen charging stations [3].

2.5.4.2 "Blue" & "Green" Hydrogen

It is worth noting that "green" and "blue" hydrogen are gaining popularity. According to the International Energy Agency, electrolyser investments are increasing, with total installed capacity of units set to nearly triple in the next 2-3 years, reaching 150 MW. In isolated coastal areas, efficient hybrid structures based on electrolysers, wind, and solar power plants are viable. These would be capable of producing "green" hydrogen at a cost acceptable for export. The cost of hydrogen will be reduced in the market because electrolysers develop more quickly, and renewable energy prices fall. Measures to increase demand for electrolysers are considered as far more significant than demonstration projects and investment in R&D. As a result, "green" and "blue" hydrogen can complement each other. Between 2040 and 2050 (when their prices are expected to equalize globally), "blue" hydrogen could serve as an effective "bridge" for the development of other technical aspects [23]. According to most researchers, the basic technologies around which the

hydrogen manufacturing sector will develop are electrolysis and steam methane reforming. Plasma reforming, ionic membrane reforming, sorption-enhanced steam methane reforming, methane decomposition (pyrolysis) with the release of solid carbon, micro-channel reactors, and high temperature gas cooled nuclear reactors are among other methods. Commercialization of these technologies is still in its early phases [54].

2.5.4.3 Nanotechnology for Production, Storage & Transformation

Novel multifunctional materials developed from the vast and multidisciplinary field currently known as nanotechnology are crucial for overcoming some of the technological limits of non-renewable energy options. PV solar cells are improving their efficiency while lowering their manufacturing and electricity production costs at an exceptional rate, thanks to improved nanomaterials. Better nanostructured materials for increased hydrogen adsorption capacity, more effective catalysts for water splitting, and simpler, cheaper fuel cells are all helping to improve hydrogen production, storage, and conversion into power in fuel cells [53].

2.5.4.4 Porous Materials-Based Physical Sorption

In porous materials-based systems, the potential for achieving reliable hydrogen storage capacity is growing. Porous carbonaceous materials and metal-organic frameworks (MOFs) have been recognized as suitable for hydrogen storage among the current porous materials. Some research has also emphasized on how carbon materials and porous hybrid composites of MOFs can improve hydrogen storage capacities, hydro-stability, and temperature stability. Most current research efforts are centred on improving the performance of physical sorption of porous materials at room temperature [55].

2.5.4.5 Metal/Chemical Hydrides-Based Chemical Sorption

The term "metal hydride" refers to both traditional hydrides like Mg_2NiH_4 and $LaNi_5H_6$, as well as complex hydrides like alanates, borohydrides, and amides. Light-weight hydrides like MgH_2 and $LiBH_4$ have sparked a lot of interest among metal hydrides because of their high gravimetric and volumetric densities for hydrogen storage. Slow hydrogen desorption/absorption kinetics, high thermal stability, unwanted side gases, and irreversible hydrogen storage are all drawbacks of metal/chemical hydrides. There are several solutions to these problems, with the ones aiming at lowering the operating temperature, improving uptake/release kinetics, and controlling the formation of undesirable gases during desorption getting special attention [56, 57].

2.5.4.6 Ionic Liquids for Hydrogen Storage Applications

Ionic liquids are appealing for hydrogen storage applications because of their unique physico-chemical characteristics. The most basic concept is to find a hydrogen-rich ionic liquid with a low molecular weight that can be used as a hydrogen storage material. In addition, the operating temperature, H_2 release rate, and H_2 purity are all important factors that have sparked considerable research into new ionic liquid molecules with superior hydrogen storage performance [58, 59].

CHAPTER III - HYDROGEN PRODUCTION

3.1 Background

The key driving forces for the progress of hydrogen production and utilization are based on the premise that the fuel cell is a proven technology and hydrogen is in abundant supply on Earth. Hydrogen, as a fuel and energy carrier, plays a significant role in worldwide energy supply mix, with the potential to reduce dependence on the current pollutant imported fuels, and to address issues such as energy supply security and climate change. The transition to hydrogen energy systems has already begun, and we are steadily approaching fully established hydrogen energy systems that will be incorporated into our daily lives. Hydrogen can be obtained from a variety of available, reliable, and abundant energy and material resources. Fossil fuels, biomass, renewables, and nuclear power are among these resources.

Despite these promising benefits, there remain several obstacles to overcome before reaching full potential of the hydrogen economy. Hydrogen, unlike fossil fuels, does not currently have a large-scale production, storage, delivery, or end-use infrastructure. Hence, the first challenge is to construct a solid, convenient, reliable, efficient, and clean infrastructure that will necessitate large investments. Although current hydrogen production, storage, and delivery methods are used by chemical and refining industries, it is considerably expensive for large end-use energy requirements. Also, current standards and policies do not emphasize the cost reduction associated with energy and environmental security that would be a great economic benefit of widespread hydrogen use as a fuel and energy carrier.

The goal of developing sustainable hydrogen production methods is to come up with a shared idea for present and future hydrogen energy systems. The aim is also to develop a mutual timeline for realizing the hydrogen economy vision. The following declaration summarizes the goal of hydrogen energy systems: hydrogen is a universally promising future clean source of energy. It is versatile, safe, reasonably priced, available locally, and may be used in every aspect of life and any part of the world.

The following are the most major driving forces and motivations for creating advanced hydrogen production systems:

- Hydrogen, as a fuel and energy carrier, plays a significant role in worldwide energy supply mix, with the potential to reduce dependence on imported fuels and pollutant emissions.
- The transition to hydrogen energy systems has already begun, and we are rapidly approaching fully established hydrogen energy systems that are incorporated into our daily lives.
- Hydrogen energy systems, along with all components, need inventive approaches.
- When it comes to bringing hydrogen into existing markets, there are some "chicken and egg" issues.

- To make hydrogen a preferred energy option, state, regional and local governments must develop and maintain a reliable and consistent energy policy.
- To create innovative ways to manufacture and use hydrogen energy, strong collaborations between academia, industry, governments, and the general public are required.
- A global vision of hydrogen energy is necessary, in order to strengthen research, development, outreach, demonstration, policies of hydrogen production, delivery, storage, and end-use.

Although water electrolysis is an obvious and convenient route to hydrogen it is prohibitively expensive for large-scale hydrogen manufacture due to the high cost of electricity and the relatively low efficiency of its production. Also, producing hydrogen from coal was initially commercially successful, but it required handling large amounts of solids as well as dealing with high levels of catalyst poisons together with unpleasant environmental emissions. Interest in using hydrocarbons as a source of hydrogen was sparked in parts of the world where cheap naphtha or natural gas became available in large quantities, and this approach proved more economical and easier to operate than the old coal-based processes.

Today hydrogen production technologies fall into four general categories:

- thermal processes
- electrolytic processes
- solar-driven processes
- biological processes.

Thermal processes use the energy present in various resources, such as natural gas, coal or biomass, to release hydrogen, which is part of their molecular structure. In other processes, heat, in combination with closed chemical cycles, produce hydrogen from feedstocks such as water, these are known as ‘thermochemical’ processes. Thermal processes for hydrogen production typically involve steam reforming, a high-temperature process in which steam reacts with a hydrocarbon fuel to produce hydrogen. Many hydrocarbon fuels can be reformed to produce hydrogen, such as natural gas, diesel, renewable liquid fuels, gasified coal, or gasified biomass.

Electrolytic processes use electricity to split water into hydrogen and oxygen. Hydrogen produced via electrolysis results in zero greenhouse gas emissions, depending on the source of the electricity used. The two electrolysis pathways of great interest for wide-scale hydrogen production, which result in near-zero greenhouse gas emissions, are electrolysis using renewable electricity sources and nuclear high-temperature electrolysis (HTE).

Photolytic or solar-driven processes use light energy to split water into hydrogen and oxygen. These include photobiological, photoelectrochemical, and solar thermochemical processes. Photobiological processes use the natural photosynthetic activity of bacteria and green algae to produce hydrogen. Photoelectrochemical processes use specialized semiconductors to separate water into hydrogen and oxygen. Solar thermochemical hydrogen production uses concentrated solar power to drive water splitting reactions mostly along with species such as metal oxides.

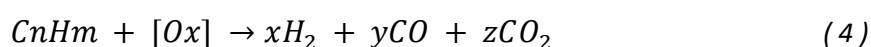
Biological processes use microbes such as bacteria and microalgae to produce hydrogen through biological reactions. In microbial biomass conversion, the microbes break down organic matter like biomass or wastewater to produce hydrogen, while in photobiological processes the microbes use sunlight as the source of energy [60, 61].

3.2 Production from Fossil Fuels

It is possible to use most fossil fuels to produce hydrogen in a variety of ways, each with its own set of complexities. The hydrogen production from natural gas and coal is discussed in this chapter. Carbon dioxide is emitted as a by-product during these procedures, and it should be captured to ensure a cleaner hydrogen production. The feasibility of fossil-fuel based hydrogen production is determined by the plant's scale of operation and whether it has centralized or distributed operation.

3.2.1 Production from Hydrocarbons

Most industrial hydrogen is manufactured by the following hydrocarbon-based oxidative processes: steam reforming of light hydrocarbons (e.g., natural gas and naphtha), partial oxidation (PO_x) of heavy oil fractions, and autothermal reforming (ATR) which is a combination of steam reforming and PO_x. The oxidative conversion of hydrocarbons to hydrogen can be represented by the following generic chemical equation:



, where C_nH_m is a hydrocarbon (n ≥ 1, m ≥ n) and O_x is an oxidant such as O₂, H₂O, or CO₂.

High operational temperatures of the oxidative conversion processes are needed due to the relative 'inertness' of methane and other saturated hydrocarbons that make up the hydrocarbon feedstock for hydrogen production.

Carbon dioxide is emitted as a by-product during these procedures, and it should be captured to ensure clean hydrogen production [8, 62].

3.2.1.1 Steam Methane Reforming (SMR)

Despite the fact that various new hydrocarbon-based hydrogen production technologies exist, none of them has yet to be commercialized. The SMR is by far the most important and widely used process for the industrial manufacture of hydrogen. The steam reforming process is known as the hydrocarbon's conversion with steam into hydrogen, carbon oxides, methane, and unconverted steam mixture. The typical feedstock ranges from natural gas and liquified petroleum gas (LPG) to liquid fuels including naphtha and in some cases kerosene.

3.2.1.1.1 *Process Description*

The main stages of an SMR plant include natural gas feedstock desulfurization, catalytic reforming, CO conversion (or water-gas shift [WGS]), and gas separation/H₂ purification (**Figure 10**).

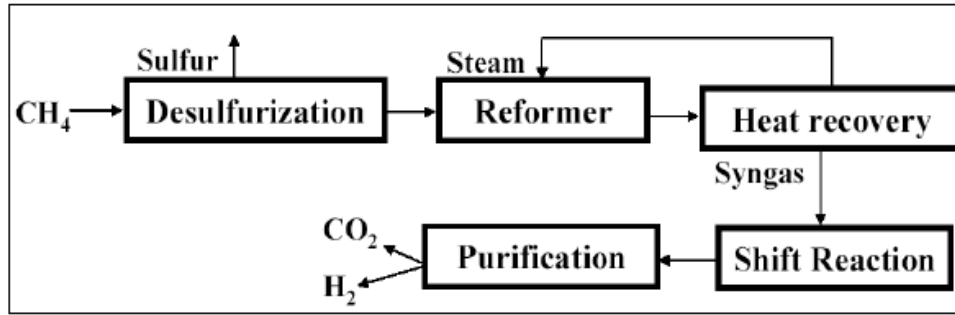
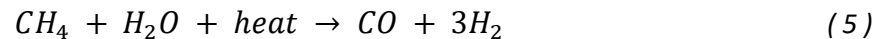


Figure 10: Block Diagram of SMR plant [63].

Because of the high sensitivity of the reforming and WGS catalysts to sulfur poisoning, a high degree of feedstock desulfurization is required, and it is accomplished in the desulfurization unit (DSU). After the DSU, the natural gas is fed to a catalytic reformer where it reacts with steam to produce synthesis gas (syngas). Depending on the content of higher (C2+) hydrocarbons in the natural gas, there may be an additional step, called pre-reforming, which is designed to remove them. The resulting mixture is preheated to 500°C and introduced to the catalytic reforming reactor. There methane and steam undergo an endothermic reaction, yielding hydrogen and carbon monoxide (Eq. (5)). The methane gas supplied to the reaction chamber acts as the heat source for this endothermic process. This reaction occurs at temperatures ranging from 700 to 850°C, and pressure ranging from 3 to 25 bar.



The output gas mixture containing H_2 , around 12% CO by volume, and steam (and usually about 4% of unconverted methane) leaves the reformer at about 800–900°C. It is cooled rapidly to about 350°C (thereby generating steam) and is fed to WGS reactors, where CO reacts with steam over a catalyst bed and is converted to H_2 and CO_2 .



The H_2 is separated from CO_2 and purified at the final stage of the process.

The hydrogen plant efficiency is defined as the total energy produced by the hydrogen plant divided by the total energy consumed by the plant, determined by the following formula:

$$\eta = \frac{E_{H_2} + E_{steam, 4.8 \text{ MPa}}}{E_{NG} + electricity + E_{steam, 2.6 \text{ MPa}}} \quad (7)$$

where η is the energy efficiency, E_{H_2} the energy in H_2 product, $E_{steam, 4.8 \text{ MPa}}$ the 4.8 MPa steam energy (exported), E_{NG} the NG energy, and $E_{steam, 2.6 \text{ MPa}}$ the 2.6 MPa steam (required). Energy efficiency of SMR is in the range of 65-85%.

3.2.1.1.2 Catalysts

Since the introduction of hydrocarbon steam reforming for industrial hydrogen production there has been continuous improvement of the catalysts used. High content nickel

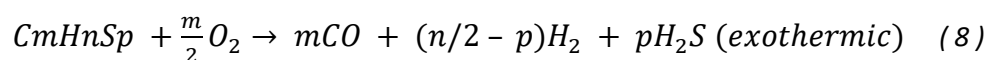
containing a variety of promoters has remained the most universally used catalyst due to its relatively low cost. Improvements have concentrated on extending catalyst life, improving activity, inhibiting carbon forming reactions, and by improving the physical properties to provide strength and low pressure-drop characteristics. The role of the promoter is to provide support for the catalytically active metal to achieve a stable and high surface area. It determines the dispersion of the catalytically active metal particles (the catalytic activity increases with the increase in dispersion of metal particles over the support surface). Furthermore, it affects the catalyst's reactivity, resistance to sintering, and coke deposition by choosing the nature of the chemical bonding between the metal and the support and may even participate in the catalytic action itself. Some commonly used supports for SMR catalysts are α - and γ -Al₂O₃, MgO, MgAl₂O₄, SiO₂, ZrO₂, and TiO₂ [14].

3.2.1.2 Partial Oxidation (POX)

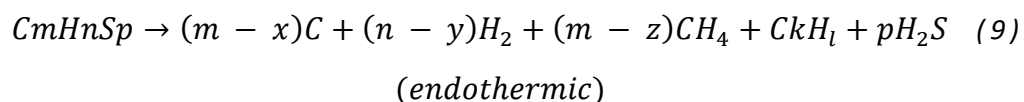
Another important commercial route to hydrogen production is the PO_x of hydrocarbons. In the PO_x process, fuel is partially combusted with pure oxygen in such a way that the fuel is converted into a mixture of H₂ and CO. Because a great amount of oxygen is added to a reagent stream, the overall process is exothermic, so the reactor does not require a heat source. The efficiency of the partial oxidation process of methane is recorded about 50%. In the PO_x method the hydrogen produced is sent to the water-gas shift (WGS) reactor and is then purified by using a suitable purification method. The POX process can be carried out catalytically or non-catalytically. The non-catalytic POX process operates at high temperatures (1100–1500°C), and it can utilize any possible carbonaceous feedstock including heavy residual oils (HROs) and coal. The catalytic process is carried out at a significantly lower range of temperatures (600–900°C) and, generally, uses light hydrocarbon fuels as a feedstock, for example, natural gas and naphtha [62, 64-67].

3.2.1.2.1 Partial Oxidation (Non-catalytic) of Heavy Residual Oil

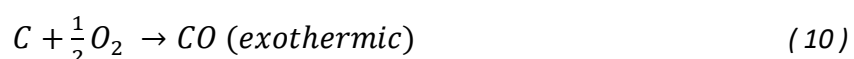
The major reaction during PO_x of sulfurous heavy oil fractions can be presented by the following generic chemical reaction:



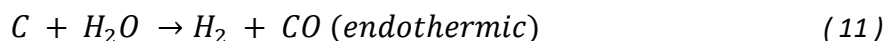
Other (both exothermic and endothermic) reactions occur in the PO_x reactor including the cracking reaction:



incomplete carbon (coke) combustion:



and coke gasification:



as well as the previously mentioned WGS and methane reforming reactions.

At the final purification step, the residual CO (some tenths of a percent) is catalytically converted to CH₄ in the presence of H₂ by methanation reaction (which is the reverse of the methane reforming reaction):



The resulting water is removed by adsorption and the final product is dry hydrogen with the purity of about 98.6 vol%. The thermal efficiency of this process is 69.5%. Major disadvantages of the PO_x process are the need for large quantities of pure oxygen (thus, requiring an expensive air separation plant), and the production of large quantities of CO₂ emissions [68, 69].

3.2.1.2.2 Catalytic Partial Oxidation

The production of synthesis gas based on heterogeneous catalytic reactions using O₂ (air) as an oxidant is referred to as catalytic PO_x (CPO). The common CPO of methane can be explained by the following equation:

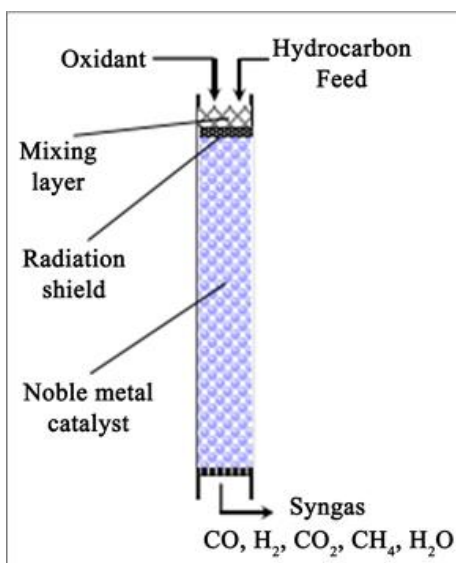
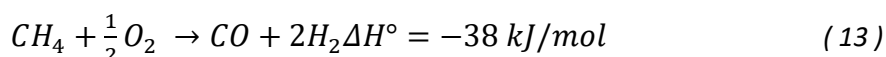


Figure 11: Catalytic Partial Oxidation principle.

Most commonly used catalysts for the CPO reaction include refractory supported Ni and noble metal-based (e.g., Rh, Pt, Pd, Ir, Ru, and Re) catalysts in the form of pellets, monoliths, and foams. The CPO of hydrocarbons is a very complicated process as indicated in **Figure 11**, and mechanistic investigations of this reaction are still challenging resulting in a difficulty to control in large-scale industrial operations.

3.2.1.3 Autothermal Reforming (ATR)

ATR is a combination of PO_x and steam reforming. The total reaction is exothermic, with an output temperature ranging from 95 to 1100°C. The pressure in the reactor can reach 100 bar.

The autothermal reformer consists of three zones: the combustion, thermal, and catalytic zone, these are indicated in **Figure 12**. The feed is introduced to the combustion zone and mixed intensively with steam and a sub stoichiometric amount of oxygen or air. In the thermal zone, above the catalyst bed, further conversion occurs by homogeneous gas-phase reactions. In the catalytic zone, a reforming catalyst (typically, alumina-supported Ni catalyst) carries out steam reforming of hydrocarbons at an operating pressure in the range of 1.8-6.7 MPa. Then, the product CO is converted to H₂ via the water-gas shift reaction. The output gas purification significantly raises operating costs and reduces overall system efficiency [70].

Simplistically, ATR of methane at a temperature T can be represented as follows:

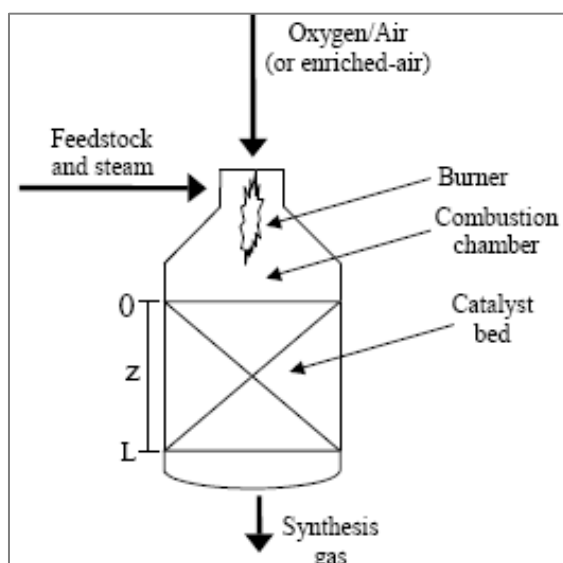
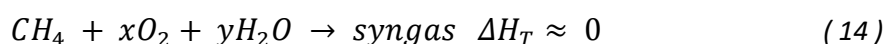


Figure 12: Schematic diagram of ATR unit [71].

Ni-based catalysts are the most used in methane autothermal reaction, mainly due to their low cost. Unfortunately, the severe reaction conditions can lead to the rapid deactivation of the catalyst, so the use of promoters or bimetallic catalytic systems can improve the performance of these catalysts.

Each process has certain advantages and disadvantages, which are summed up in **Table 6**.

Table 6: Technology comparison of natural gas-based hydrogen production.

Technology	Pros	Cons
SMR	High efficiency Emissions Costs for large units	Complex system Sensitive to natural gas qualities
POX or ATR	Smaller size Costs for small units Simple system	Lower efficiency H ₂ purification Emissions and flaring

3.2.1.4 Combined Reforming

If the goal of the process is to control the H₂/CO ratio in the synthesis gas, or to increase pressure while consuming less oxygen, the combination of steam reforming and ATR reactors is preferable. The first reactor is a relatively small steam reformer from which the reformat gas goes to a secondary ATR reactor (**Figure 13**).

Combined reforming (also called 'secondary reforming') is the dominating process for the manufacturing of synthesis gas for NH₃ production from natural gas and naphtha.

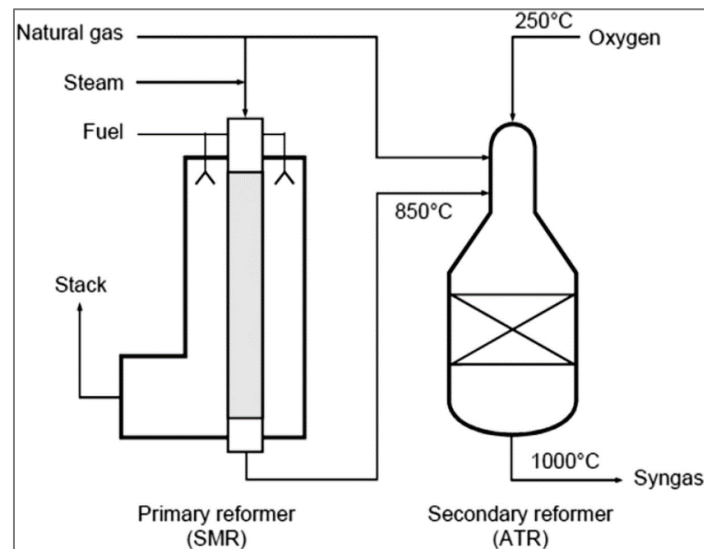
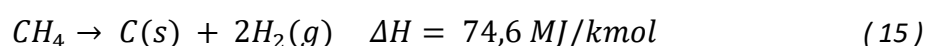


Figure 13: Schematic of combined reforming [72].

3.2.1.5 Plasma Reforming

Plasma technology is an important method to produce the hydrogen fuel using hydrocarbons or alcohols. Plasma, known as the fourth state of the material, is an ionized state of matter that comprises of electrons in an excited state along with other atomic substances. Plasma can potentially be utilized as the preferred medium in processes with high voltage electric current release since it contains electrically charged particles. The plasma technology can be classified into thermal and non-thermal plasma (non-equilibrium plasma) based on the energy level (temperature, plasma state, and electronic density).

Hydrogen production using ammonia decomposition is a novel method that can be established to produce pure hydrogen by using the plasma membrane reactor, it can produce 99.999% pure hydrogen gas at normal temperature and atmospheric pressure, without using a catalyst. In plasma arc decomposition, natural gas (typically methane) is split into hydrogen and carbon black (soot) due to chemical activity of the thermal plasma. Carbon black is in solid phase; therefore, it stays at the bottom of the reactor as hydrogen is generated and separately accumulated in gas phase. The plasma arc decomposition reaction of natural gas can be written as:



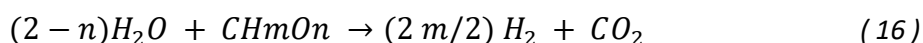
3.2.2 Production from Coal

Coal is the most abundant fossil fuel on Earth and is expected to continue to be a significant source of energy for the immediate next years. Coal is formed from plant materials through the coalification process, which occurs underground over long periods of time. Coal is a complex mixture of organic chemical substances made up of carbon, hydrogen, oxygen, and trace amounts of nitrogen and sulfur, as well as moisture and minerals. According to its degree of coalification, coal is classified into different ranks: lignite (brown coal), sub bituminous coal, bituminous coal, and anthracite, each having a different carbon and moisture content and heating value. The specific values are illustrated in the table below (**Table 7**).

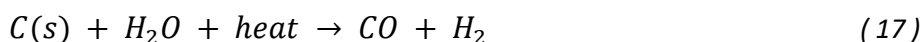
Table 7: Contents and Heating Values of Different Types of Coal.

Coal	Dry, Carbon content (%)	Moisture content before drying (%)	Dry, volatile content (%)	Heat Content (MJ/kg)
Peat	<60	75	63-69	15
Lignite	65-70	35-55	53-63	17-18
Sub-Bituminous Coal	70-76	18-38	42-53	18-23
Bituminous Coal	76-86	8-18	14-46	23-33
Anthracite	86-92	7-10	3-14	32-33

The following equation offers a large-scale method of producing hydrogen from water and coal (CH_mO_n):



Practically, high-temperature flow processes maximize carbon conversion to gas, avoiding the development of char, tars, and phenols. Carbon is converted to carbon monoxide and hydrogen as shown here:

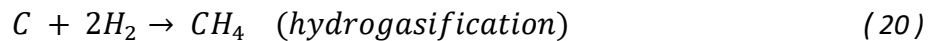
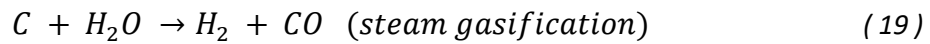
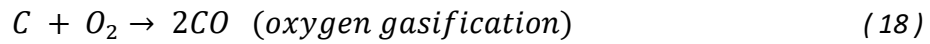


Because the reaction is endothermic, extra heat is required, which can be achieved with methane reforming. Although, producing hydrogen from coal is not as cost effective as producing hydrogen from previous hydrocarbons, it can be used where oil or natural gas are scarce, and coal is abundant. As a result, it is important to look for new and environmentally friendly ways to produce hydrogen from coal [73].

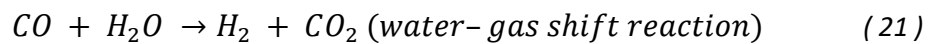
3.2.2.1 Coal Gasification

In coal gasification, at first coal is partially oxidized by using steam and O_2 in a high-temperature and high-pressure reactor. The products of this first step of the process are predominantly H_2 and CO along with some steam and CO_2 . This product gas mixture is called syngas.

Coal (solid carbon) is converted to syngas by the following gasification reactions:



After that, the syngas is sent to a unit to be processed in a shift reaction aiming to enhance the hydrogen amount in the syngas. The gas-phase water-gas shift reaction is important because it controls the equilibrium among CO, H₂, CO₂, and H₂O:



Later, the product gas is sent to a treatment unit to eliminate elemental sulfur or sulfuric acid in the product mixture.

Coal ash is a particular issue in coal gasification. The ash content of coal is approximately 10% or more. At high temperatures, ash undergoes a phase change, transitioning from solid to an intermediate soft stage and finally to liquid. Because softened ash has a high viscosity and adheres to the gasifier wall and gas outline, resulting in production difficulties, coal gasification is usually performed at a temperature below or above the temperature range at which ash softens [73, 74].

3.2.3 Capture and Storage of CO₂

All fossil fuel-based hydrogen production systems emit a lot of CO₂s. The amount of CO₂ emissions depends on each fossil fuel source and its hydrogen concentration. These emissions must be captured and stored, in order to develop a zero or minimum emissions hydrogen production system. This process is known as decarbonization and there are three techniques used to achieve it (**Figure 14**) [73]:

- Post-combustion: CO₂ emissions are eliminated from the combustion chamber's exhaust. This technique is mostly used in traditional steam turbines or in combined cycle gas turbine (CCGT) power plants. It is commonly employed by the "amine" process. The emissions stream consists of significant amounts of nitrogen and traces of nitrogen oxides, as well as steam, CO₂, and CO. Instead of being discharged directly to the atmosphere, they are passed through equipment which separates most of the CO₂. CO₂ can be captured using a liquid solvent or by other separation methods. The CO₂ is then fed to a storage reservoir and the remaining flue gas is discharged to the atmosphere.
- Pre-combustion: Pre-combustion capture involves reacting a fuel with oxygen or air and/or steam to mainly obtain a 'synthesis gas (syngas)' or 'fuel gas' composed of carbon monoxide and hydrogen. The carbon monoxide reacts with steam in a catalytic reactor, called a shift converter, to obtain CO₂ and more hydrogen. This CO₂ is then separated, usually by a physical or chemical absorption process, and the result is a hydrogen-rich fuel, which can be utilized in many applications.

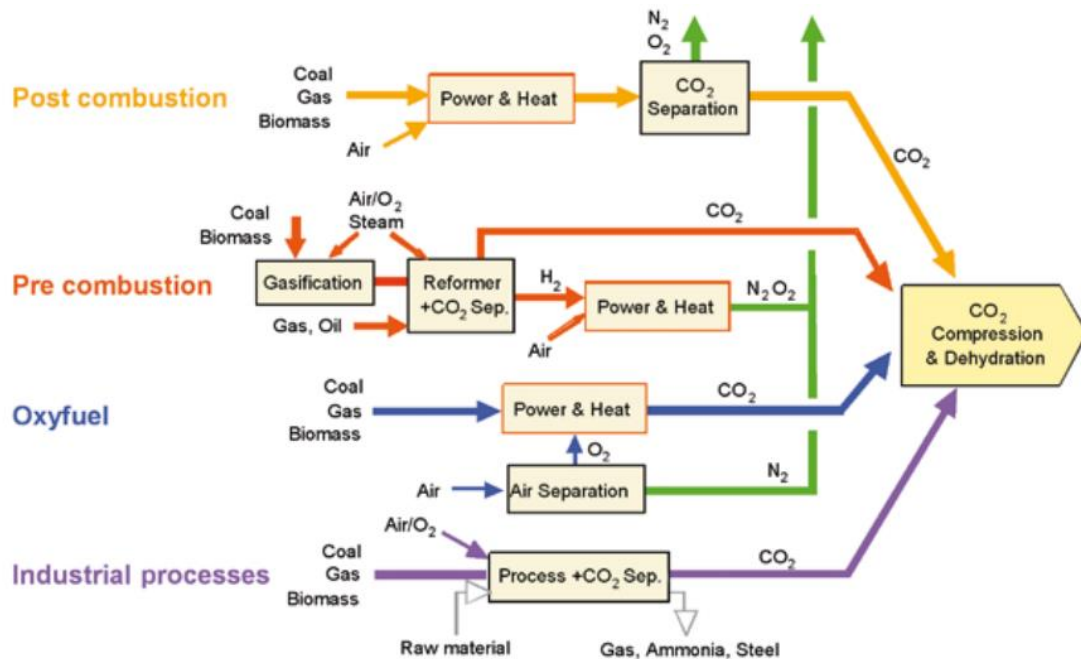


Figure 14: Overview of CO₂ capture processes and systems [75].

- Oxyfuel combustion: This method uses pure oxygen, instead of air, to react with fossil fuels. As a result, almost all the emissions are CO₂ and steam. Then, CO₂ can simply be captured by condensing the steam of the mixture.

Alongside renewable energy and nuclear power, Carbon Capture and Storage (CCS) is considered to be one of the key alternatives for reducing CO₂ emissions. The main concept of CCS includes capturing CO₂ by the plant, transporting it to a storage location, and permanently storing it in an isolated from the atmosphere place, as depicted in **Figure 15**. Potential technical storage methods are geological storage (in geological formations, such as oil and gas fields, un-mineable coal beds and deep saline formations, ocean storage (direct release into the ocean water column or onto the deep seafloor) and industrial fixation of CO₂ into inorganic carbonates [61, 76, 77].

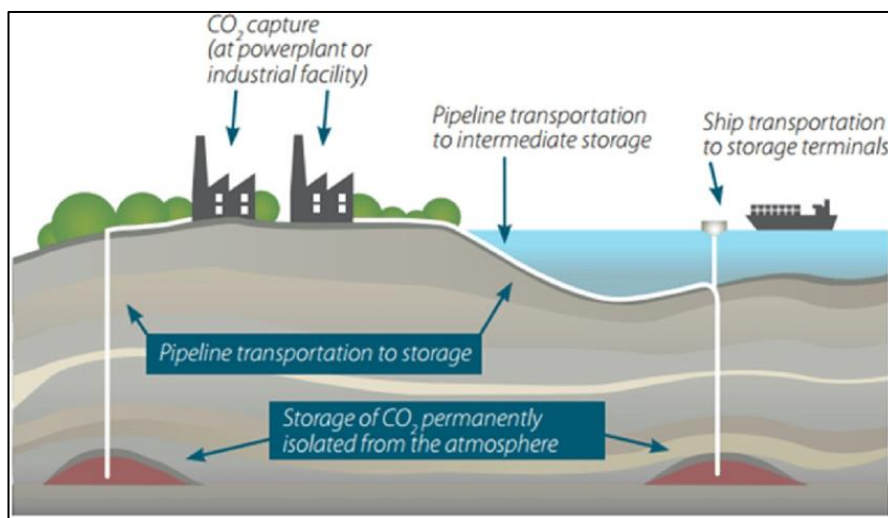


Figure 15: The basic principle for Carbon Capture and Storage (CCS) [76].

3.3 Production from Renewable Sources

3.3.1 Hydrogen Production from Nuclear Energy

Nuclear energy can be used in hydrogen production in three ways:

- Using the electricity from the nuclear plant for conventional liquid water electrolysis.
- Using both the high-temperature heat and electricity from the nuclear plant for high-temperature steam electrolysis or hybrid processes.
- Using the heat from the nuclear plant for thermochemical processes like the iodine-sulfur cycle or pyrolysis.

The viability of nuclear energy for H_2 production depends on the match between the characteristics of the H_2 systems and the nuclear energy in terms of the production scale, load factor, H_2 transmission and pipeline infrastructure.

Hydrogen production from water using nuclear energy offers one of the most appealing zero-emission energy strategies but steam reforming of natural Gas has the greatest potential for near-term development into a nuclear process heat system. The size of the conventional H_2 production facilities using steam reforming of natural gas has grown in recent years. The size of H_2 production units is now compatible with the scale of nuclear operations. In high-temperature gas-cooled nuclear reactors (HTGR), recycled helium is heated to temperatures up to 950°C, which is suitable for carrying out the SMR reaction.

At the present, only one nuclear reactor system, the gas-cooled (helium) reactor, has the high-temperature capabilities necessary to provide heat at sufficient temperatures to drive an H_2 production system. Alternatively, a reactor can be designed specifically for H_2 production. The advanced high-temperature reactor (AHTR) has been proposed to match H_2 production requirements [78].

A very high temperature reactor (VHTR) could be considered suitable to take on the nuclear energy's traditional role of generating electricity. It has many advantages over other types of nuclear reactor with the chief advantage being its unique capability of producing a high-temperature heat of about 950°C [61].

3.3.2 PV Supported Hydrogen Production

The state-of-the-art solar concentrators can provide solar flux concentrations in the following ranges, depending on the type of concentrator:

- Trough concentrators: 30-100 suns
- Tower systems: 500-5,000 suns
- Dish systems: 1,000-10,000 suns

For a solar concentration of 5000, the optimum temperature of the solar receiver is about 1270°C, giving a maximum theoretical efficiency of 75% (i.e., the portion of solar energy that

can be converted to the chemical energy of fuels). This temperature is adequate to conduct high-temperature endothermic SMR or CO₂ reforming of methane processes or water electrolysis. For PV supported electrolysis PV panels, converters between alternating current (AC) and direct current (DC) power, batteries, and hydrogen storage mediums are used in addition to the electrolyzer. PV supported electrolysis is currently a very expensive method for producing hydrogen in a sustainable manner. Aside from this method photon energy can be used to produce hydrogen by the photonic process. It can be divided further into two methods, the photocatalytic and the photo-electrolysis water splitting (photo-electrochemical water splitting), which will be further discussed in the next section.

3.4 Production from Water Splitting

In contrast to previous methods, hydrogen production from water splitting, being the reverse reaction of hydrogen combustion, uses water as the only feedstock and allows for a close hydrogen cycle with zero carbon emissions, making it the most green and sustainable method. However, high-cost limits the widespread use of water electrolysis, resulting in a minor fraction of the whole hydrogen production. Therefore, the challenge lies in making cheap hydrogen from water electrolysis that could eventually replace the hydrogen from fossil fuels.

The water-hydrogen cycle (**Figure 16**) is closed, unlike the fossil fuel energy chain that operates on a 'once-through' basis. Even though the hydrogen-water cycle is closed and sustainable, the energy chain can be open and depletable, if fossil energy is used to split water. Hydrogen production by electricity-driven water splitting can this way contribute to utilizing the large excess amount of electrical energy from the renewable energy resources and form clean fuel, hydrogen (H₂) [79].

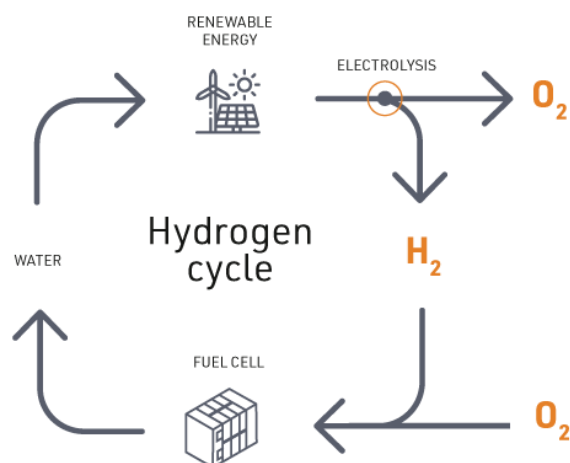
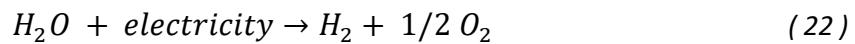


Figure 16: Hydrogen cycle.

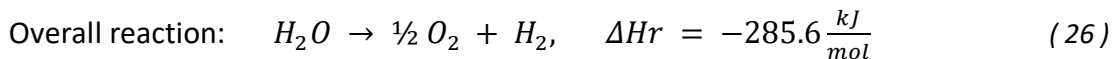
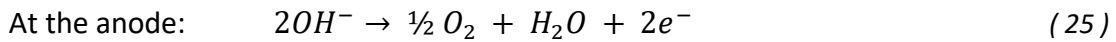
Hydrogen production can be achieved using many different processes that dissociate water molecules. Photo-electrolysis, high-temperature and low-temperature electrolysis, and photobiological hydrogen production are all covered in this section. The efficiency of the water-hydrogen cycle is key to determine its value. Inevitably today, more energy is needed to split water than is recovered on its recombination [76, 79].

3.4.1 Water Electrolysis

Water electrolysis is the process of splitting water into hydrogen and oxygen using electrical energy, as shown in Eq. (22). The water-splitting reaction includes two half reactions, and they are the anodic oxygen evolution reaction (OER) and the cathodic hydrogen evolution reaction (HER). The total energy required for water electrolysis increases slightly with temperature as shown in **Figure 17**, whereas the electrical energy required decreases. When high-temperature heat is available as waste heat from other processes, an HTE process may be preferable. This is very important, especially globally, because the majority of electricity is generated using fossil fuels with low efficiencies.



In a basic electrolysis cell, the following reactions take place:



Where ΔH_r is the enthalpy of the reaction.

The anode is the electrode connected to the positive terminal of a power supply and the cathode is the one connected to the negative terminal of a power supply. This is an endothermic reaction because water is more stable than its elements, so energy must be added to split it. A thermodynamic potential of 1.23 V is required to split water into H_2 and O_2 at 25°C and 1 atm. However, due to the kinetic barrier for the reaction, water electrolysis requires an even higher potential. One of the critical barriers that keep water splitting from being of practical use is the slow reaction kinetics of OER and HER due to high over potentials.

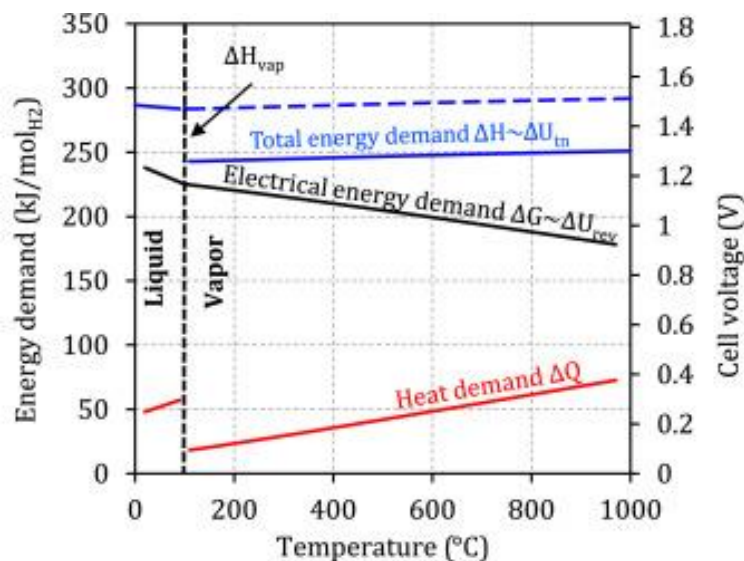


Figure 17: Energy demand for water and steam electrolysis.

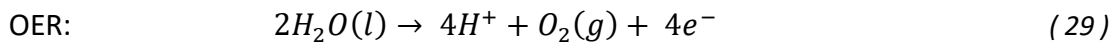
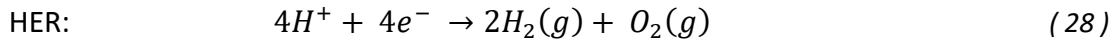
So, the overall applied potential (E_{ap}) for water electrolysis can be described as in the equation below where n_{HER} and n_{OER} are the overpotentials while n_{other} represents the total voltage drop resulting from other the system resistances.

$$E_{ap} = 1.23V + n_{HER} + n_{OER} + n_{other} \quad (27)$$

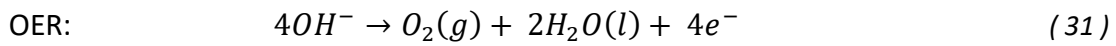
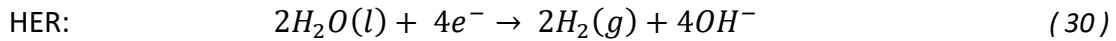
3.4.1.1 Electrolytes

Depending on the pH of the electrolyte the process goes as follows:

In acidic electrolyte:



In alkaline electrolyte:



In solid oxide electrolyte:

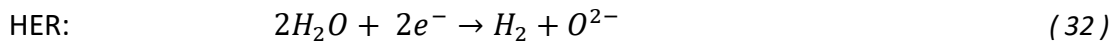


Table 8 lists the typical specifications of the water electrolysis technologies methods.

For the Polymer Electrolyte Membrane based electrolysis cell, the water splitting is performed under acidic condition and using PEM. The most used PEMs are the Nafion™ and Nafion™-based membranes because of their high thermostability, high ionic conductivity, excellent chemical stability, good mechanical strength, and robustness at a low temperature during high levels of relative humidity. But there are no large electrolyzers currently available because it is a relatively new technology.

Table 8: Typical specifications of the water electrolysis technologies methods.

Specification	Alkaline	PEM	SOE
<i>Technology maturity</i>	State of the art	Demonstration	R&D
<i>Cell temperature, °C</i>	60-80	50-80	900-1000
<i>Cell pressure, bar</i>	<30	<30	<30
<i>Current density, A/cm²</i>	0.2-0.4	0.6-2.0	0.3-1.0
<i>Voltage efficiency, %</i>	62-82	67-82	81-86
<i>Specific system energy consumption, kWh/Nm²</i>	4.5-7.0	4.5-7.5	2.5-3.5

Most commercial water electrolyzers today consist of an alkaline electrolyzer, a basic solution that can be obtained by adding potassium hydroxide (KOH) to water. However, the main drawback of alkaline water electrolysis is the limited current density because of the

increased Ohmic loss, and the decreased active electrode area caused by the formation of gas bubbles on the electrode surface, which is common in liquid electrolytes. In contrast, a PEM electrolyzer due to the elimination of liquid electrolyte can deliver a very high current density between 600-2000 mA cm⁻² while maintaining high voltage efficiency, obtaining hydrogen with a higher purity (greater than 99.99%) than alkaline electrolyzer.

Solid Oxide Electrolysis is the most electrically efficient but is still under development. Corrosion, seals, thermal cycling, and chrome migration are the major challenges faced by the SOE technology. SOEC systems that are operated at a high temperature generated from nuclear reactors can achieve efficiency up to 60%. The most practical electrolytes are typically dense ceramics capable of withstanding high temperatures, such as barium cerium yttrium zirconate (BZCY). The cathode is made of perovskites, such as lanthanum strontium manganite (LSM), which is usually supplied as a fine submicron powder. On the other hand, the anode is made of composites of nickel and zirconia-based (Ni-YSZ) ceramics or a barium yttrium zirconate nickel oxide composite (BZY15-NiO).

3.4.1.2 Catalysts

When considering a proper electrocatalyst for industrial applications the following criteria are mainly evaluated:

- efficiency and ability to deliver high current density at lower applied potentials
- durability and loss of performance
- cost
- sustainability, and toxicity,
- it must be based on earth-abundant elements rather than noble metals that might be depleted within the next century
- and recyclability.

The requirement of acidic media in PEM electrolyzers limits the OER electrocatalysts to noble metal and noble metal oxide catalysts, which are the state-of-the-art OER electrocatalysts in the acidic media. This requirement though leads to a high cost for the cell. Currently, efforts are focusing on Pt-based electrocatalysts, including alloys developed via novel synthesis methods, Pt combinations with metal oxides, core-shell structures, and surface-modified Pt/C catalysts to increase CO tolerance and stability [80]. In comparison with cells using acidic media, water splitting in alkaline media broadens the selection of the electrocatalysts to non-noble metals or metal oxides. However, the activity of HER in alkaline media is usually 2-3 orders of magnitude lower than the activity of HER in acidic media. Therefore, the design of optimal electrocatalysts suitable for the different media with low-cost, high catalytic activity, and good durability for electrolytic water splitting is challenging.

As for solid state electrolytes the catalytic and electrocatalytic behavior of the La_{0.6}Sr_{0.4}Co_{0.8}Fe_{0.2}O₃ (LSCF) perovskite deposited on yttria-stabilized zirconia (YSZ) was studied by Tsiakaras et al. [81], as well as the oxidative coupling of CH₄ on polycrystalline Ag films deposited on yttria stabilized zirconia (YSZ) at temperatures 720 to 850°C [82]. The study of

the electrical properties of nano-sized powders at a wide range of temperatures and oxygen partial pressures shows that $0.5\text{Ce}_{0.8}\text{Sm}_{0.2}\text{O}_{2-\delta}-0.5\text{BaCe}_{0.8}\text{Sm}_{0.2}\text{O}_{3-\delta}$ material has relatively good stability against CO_2 , an acceptable value of total conductivity and the lowest contribution of electron conductivity in both oxidizing and reducing atmospheres[83]. Some research has also been made on $\text{BaCe}_{1-x}\text{Gd}_x\text{O}_{3-\delta}$ (BCG) type ceramics when influenced by sintering additives like Cu [84].

There are many important parameters, including overpotential (η), specific activity, mass activity, turnover frequency (TOF), Tafel slope, Faradaic efficiency, and stability, which are frequently used to evaluate the performance of a catalyst.

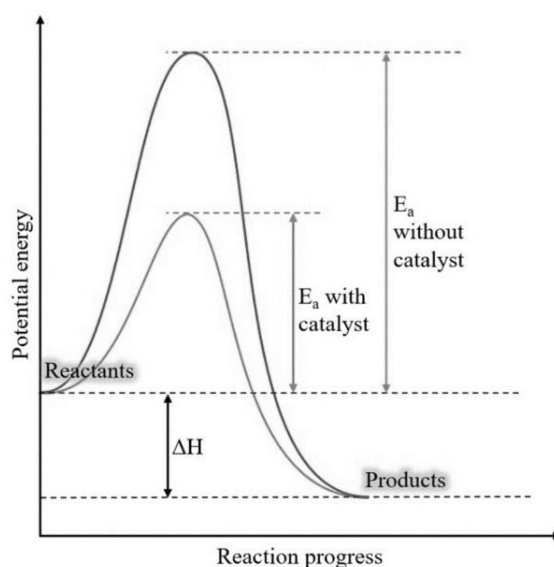


Figure 18: Schematic illustration of the catalyst's role in lowering the activation energy barrier [85].

An overpotential is required to assist the adsorption and desorption of OER intermediates and is described as the activation potential. Its value can be lowered by a good choice of catalyst with optimized binding energy, this process is shown in **Figure 18**. The overpotential (η) at a specific current density per geometric area is used as a primary indicator to evaluate the OER activity.

Transition-metal-based (oxy)hydroxides have proven so far to be the most active OER electrocatalysts. NiFe-based (oxy)hydroxides are reported to show the lowest OER overpotential in alkaline electrolytes.

The second common evaluation indicator is the Tafel slope, which reveals the dependency of the compensated overpotential on the current density. The Tafel slope is an important kinetic indicator and can be calculated from the Tafel equation, where η is the overpotential for OER, b is the Tafel slope, and j is the measured current:

$$\eta = a + b \log j \quad (34)$$

A smaller Tafel slope indicates that there is a significant current density increment as a function of the overpotential change, or in other words, faster electrocatalytic reaction kinetics (**Figure 19**). To further enhance their catalytic activity and increase the surface area, different methods,

such as nanostructure engineering, alloying engineering, surface modification engineering, and heterostructure engineering, can be performed. Heteroatom doping for example is considered an efficient strategy when tuning the electronic and structural modulation of catalysts to achieve improved performance towards renewable energy applications [86].

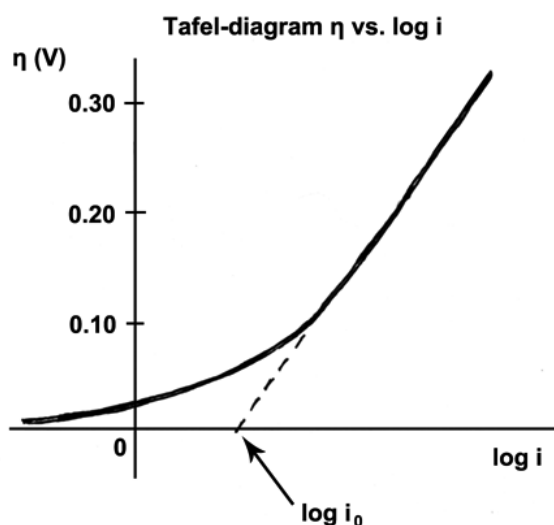


Figure 19: Tafel plot for an anodic process (oxidation) [87].

3.4.1.3 Oxygen evolution reaction (OER)

OER is known to be the major bottleneck in improving the overall efficiency of electrochemical water splitting. There are two main types of OER electrocatalysts, noble metal-based electrocatalysts, and non-noble metal based electrocatalysts. For the noble-metal based electrocatalysts, Ru and Ir-based catalysts are state-of-the-art.

Water splitting by PEM electrolysis is operated under acidic conditions. For OER, the Ir and Ru based electrocatalysts which have higher dissolution resistance in acidic condition are not suitable for practical large scale H_2 production due to their cost as well as limited supply and poor stability. For non-noble metal-based electrocatalysts, most of them, cannot survive under such conditions. Thus, there is a clear need for the development of stable and resilient non-noble metal OER electrocatalysts. Alternatively, earth-abundant metal-based catalysts have shown promising activity to avoid these shortcomings, due to the relatively low cost, good activity, and excellent stability towards OER, and thus received a great deal of interest for OER. These include first-row transition metals like Co-, Ni-, and Fe-based oxides whose activities depend on their crystal and electronic structures, and the oxidation state.

Co_3O_4 itself is an active and stable OER catalyst, with Co_3+Oh proposed as the most desirable configuration. Its spinel structure can host a variety of transition metals to tune the electronic structure and boost its activity.

In comparison to Co, Ni is much cheaper and less toxic. Fe can significantly increase NiO's OER activity. NiO is sensitive to an electrochemical aging process during electrolysis, resulting in the formation of nickel oxy/hydroxides. These species are catalytically active and can be activated further by incorporating Fe impurities from KOH electrolyte. The uptake of Fe species is the

reason for the high activity of Ni-Fe catalysts, with Fe⁴⁺ species likely as the active sites, making them the most common OER catalyst being employed in the industry-scale development.

Fe is very abundant and Fe-based catalysts have been employed in many industrial processes including the Haber-Bosch ammonia synthesis and the Fischer-Tropsch process. However, electrocatalysts iron oxides are typically not very active towards OER due to their poor electron transferability. Nevertheless, its combination with Co and Ni can significantly improve the overall efficiency of the electrocatalyst [88, 89].

3.4.1.4 Hydrogen evolution reaction (HER)

Again, there are two main types of HER electrocatalyst: noble metal-based electrocatalysts and non-noble metal based electrocatalysts. For the noble-metal based electrocatalyst, especially Pt-based catalysts, several strategies are being developed to increase HER performance and lower the electrocatalyst price, the commercial application of these noble-metal based catalysts is also hindered by their scarcity.

As a benchmark for Pt electrocatalyst, the activity of HER in alkaline media is usually lower than the activity of HER in acidic media. The water dissociation on the Pt surface is inefficient which results in poor HER activity, coupling Pt with water dissociation promoters is the commonly used strategy to boost the alkaline HER activities

For non-noble metal based HER electrocatalysts, a great deal of attention has been recently drawn to their development largely based on the considerations of the low-cost and earth-abundant characteristics. Metal (Co, Mo, Ni)-encapsulated and heteroatom (N, S, P)-doped carbon represents one new class of non-Pt catalysts for the hydrogen evolution reaction (HER). Nitrogen-doping can dramatically improve the electrocatalytic activity of carbon, and the co-doping with phosphor can further activate the adjacent carbon atom and enhance the reactivity [90].

Bimetallic nickel-cobalt phosphide (Ni-Co-P/NF) self-supported on nickel foam (NF) exhibits a high performance for HER. It requires very low overpotential values of 85, 210 and 350 mV for delivering large current densities of -10, -500 and -1,500 mA cm⁻², respectively. Also displays long-term durability lasting 24 h without obvious deactivation. Yu et al. [91] highlighted that the NiCoP, NiP and Co₂P active phases play a crucial role for the good HER activity.

Lu et al. [92] described a three-dimensional metal network electrocatalyst consisting of a worm-like S-doped RhNi alloy (S-RhNi), which improves the performance for hydrogen evolution reaction (HER). Experimental results reveal that S-RhNi exhibits Pt-like HER activity with an onset potential close to 0 mV and a Tafel slope of 24.61 mV dec⁻¹ in 0.5 M H₂SO₄ aqueous solution, having also good stability.

A catalyst synthesized *via* a one-step chemical vapor deposition (CVD) at different temperatures followed by P-doping treatment (P-doped Ni@CNTs/NF) was reviewed by Jing and co-authors [93]. The corresponding physicochemical and electrochemical results illustrate that the P-doped Ni@CNTs/NF prepared at 600 °C with flower-like structure exhibits excellent activity and

stability for HER in acidic electrolytes. In 0.5 M H₂SO₄ aqueous solution, the sample shows a small overpotential value of -135.2 mV to achieve a current density of -10 mA cm⁻², which also displays acceptable long-term stability for lasting 20 h.

A one-pot method to synthesize boron-doped RhFe alloy with excellent catalytic performance for hydrogen evolution is reported by Zhang et al. [94]. Rhodium-Iron (RhFe) alloy nanoparticles, with diameter ranging from 1 to 5 nm, are distributed uniformly on the carbon support. The corresponding physicochemical and electrochemical results exhibit good catalytic activity comparable to commercially available ones.

In conclusion, the sustainable hydrogen production by water electrolysis is an essential prerequisite of hydrogen economy with zero carbon emission. The implementation of the right catalysts into practical electrolyzers is the vital step to achieve commercial application. Although the design of new inexpensive catalysts for PEM water electrolysis is underway, these new catalysts face considerable challenge to maintain high current density especially at high operational potential and temperature. Therefore, alkaline water electrolysis shows clear advantages versus acidic water electrolysis for large-scale and low-cost hydrogen production.

Some Pt-group materials show excellent HER performances in alkaline electrolytes, but the use of these expensive noble metals will make alkaline water electrolysis lose its cost advantages in compared to PEM water electrolysis. Transition-metal-based catalysts better balance the HER performance and the cost. The currently reported monometallic and non-crystalline multi-metallic borides only show generic and monofunctional catalytic activity. Saad et al. [95] reported that highly crystalline ternary borides, Mo₂NiB₂, is successfully synthesized via a facile solid-state reaction from pure elemental powders. The as-synthesized Mo₂NiB₂ exhibits very low overpotentials for both the oxygen evolution reaction (OER) and hydrogen evolution reaction (HER) of 280 and 160 mV to reach a current density of 10 mA cm⁻², in alkaline media.

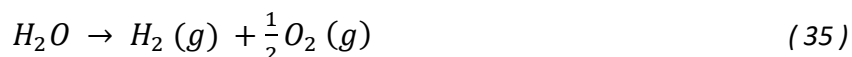
A design of a bifunctional catalyst with high catalytic activity toward both OER and HER in alkaline electrolytes is very important for lowering the manufacturing cost of the resulting hydrogen. Yu and co-authors[91]found that CoNi-OOH-30 After 40 h oxidation to reach ±10 mA cm⁻² requires small overpotentials of -210 and 279 mV, Tafel slopes of 67 and 62 mV dec⁻¹ and exhibit good stabilities for hydrogen evolution reaction (HER) and oxygen evolution reaction (OER) in alkaline solution, respectively. An integration engineering strategy of oxygen-vacancy and core-shell heterojunction to fabricate an anemone-like CoP@CoOOH core-shell heterojunction with rich oxygen-vacancies supported on carbon paper (CoP@CoOOH/CP) benefits from the synergy of CoP core and oxygen-vacancy-rich CoOOH shell [96]. The obtained CoP@CoOOH/CP catalyst displays low overpotentials at 10 mA cm⁻² for HER (89.6 mV/81.7 mV) and OER (318 mV/200 mV) in neutral and alkaline media, respectively. Furthermore, a two-electrode electrolyzer, using CoP@CoOOH/CP as bifunctional catalyst to achieve 10 mA cm⁻², only needs low-cell voltages in neutral (1.65 V) and alkaline (1.52 V) electrolyte.

In neutral pH, an effective strategy to optimize the electronic structure of CoP is copper doping [97]. A neutral electrolyzer, using Cu-CoP NAs/CP as both the anode and cathode, achieves a low cell voltage of 1.72 V at 10 mA cm⁻², superior to that of the typical Pt/C || IrO₂ couple (1.81 V) and of most of the state-of-the-art bifunctional electrocatalysts. Furthermore, the electrolyzer can be driven by a single AA battery (~1.5 V), supporting its practicality in neutral water or seawater splitting.

3.4.2 Photoelectrochemical Water Splitting (Photolysis)

Electrolyzers powered by photovoltaics (PV) are already on the market. These options allow some flexibility because the product can be either hydrogen or electricity. PV-based electrolysis systems are being replaced by direct photoelectrolysis, which is a promising alternative. This is due to the fact that photoelectrolysis produces solar-to-hydrogen (STH) directly in a single apparatus, with no need of a separate device to generate electricity. Photoelectrolysis can reduce the cost of hydrogen production, becoming cheaper than the two-step PV-based electrolysis.

Photo-electrolysis decomposes water into hydrogen and oxygen by using sunlight. The photo-electrolysis systems are the same as the photovoltaic systems, both technologies use semiconductor materials. The reaction of photo-electrolysis is illustrated as follows:



To effectively use sophisticated materials science and build creative systems engineering methodologies, significant research and development is necessary. One of these innovative approaches is photoelectrochemical (PEC) hydrogen generation. PECs are now being investigated all over the world. At least 13 nations in the OECD (Organization for Economic Cooperation and Development) are working on researching and developing PEC systems. In the literature, there are four main PEC systems that are being investigated at the moment: (1) monolithic multijunction cells, (2) two photon tandem cells, (3) one pot two step cells, and (4) dual bed redox cells. The first two systems use thin film coated glass which is immersed in water. Systems (3) and (4) use powder catalysts, that are photoactive, dissolved in water.

Until now, these systems have been able to reach conversion efficiencies of up to 16% STH. The most significant obstacle to bringing PEC cell technology to the market is advancement in materials science and engineering. The development and processing of photoelectrode materials with high efficiency and corrosion resistance properties is critical for paving the way towards smart system engineering. Since there is no-commercially available photoelectrode material ideal for water splitting, tailored materials must be developed. Different photo electrode materials such as WO₃, Fe₂O₃, and TiO₂ in the form of a thin film have been investigated.

Combinatorial chemistry approaches provide quick-tracking experimental options for materials screening, while photooxidation modeling capabilities based on quantum transition theory must be developed. Most importantly, development is needed on research

of semiconductor doping for band gap shifting and surface chemistry modifications, as well as on studies of the associated impacts on both surface and bulk semiconducting. One more challenge that needs to be addressed, is the resistance in corrosion and photo corrosion. In addition to ohmic resistance elimination, current matching between anode and cathode requires system design and sophisticated engineering solutions. Fluid dynamics (and their implications on mass and energy transfer) and gas collection and handling (and their effects on operational safety) will demand significant conceptual and application-specific research and development [38, 98-105].

3.4.3 Photocatalytic Water Splitting

By mimicking natural photosynthesis, photocatalytic hydrogen evolution from water utilizing the photogenerated electrons and holes can accomplish the solar-to-hydrogen energy conversion with relatively lower fabrication and system costs compared to the photoelectrochemical (PEC) or photovoltaic-electrocatalytic junction (PVEC) devices.

3.4.3.1 Photosynthesis

Natural photosynthesis is the process by which sunlight is captured and converted into the energy of chemical bonds of organic molecules that are the building blocks of all living organisms and of oil, gas, and coal. These fossil fuels are the products of photosynthetic activity that occurred millions of years ago.

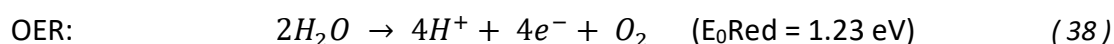
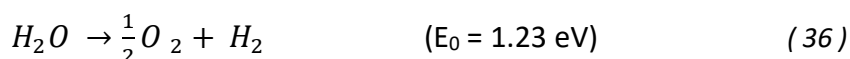
The success of photosynthesis as an energy generation and storage system comes from the fact that the raw materials and power needed for the synthesis of biomass are available in almost unlimited amounts; these are sunlight, water and CO₂. At the heart of the photosynthetic process is the splitting of water by sunlight into oxygen and hydrogen equivalents. The oxygen is released into the atmosphere where it is available for living organisms to breathe and for burning fuels to drive our technologies. The hydrogen equivalents are used to reduce CO₂ to sugars and other organic molecules of various types. When we burn fuels (fossil, biomass, and other biofuels) to release energy, we simply combine the 'hydrogen' stored in these organic molecules with atmospheric oxygen to form water, completing a cycle that began millions of years ago [106].

Chlorophyll of plants is a typical natural photocatalyst. The difference between chlorophyll photocatalyst to man-made nano-photocatalyst (here mentioned as a photocatalyst) is that chlorophyll usually captures sunlight to turn water and carbon dioxide into oxygen and glucose, but on the contrary photocatalysts create strong oxidation agents and electronic holes to break down the organic matter to carbon dioxide and water in the presence of photocatalysts, light, and water. The solar-to-hydrogen STH efficiency of most of the R&D is typically <1%, much below the targeted 5%, thus, the priority in R&D remains to increase the efficiency of photocatalytic hydrogen production.

The procedure requires placing a co-catalyst onto a semiconductor photocatalyst that is needed to reduce the overvoltage for the hydrogen and oxygen development schemes. The production

of hydrogen by photocatalytic water splitting utilizes a variation modification of semiconductors, e.g., graphitic carbon nitride, titanium dioxide (TiO_2), and cadmium sulfide. The oxide materials for the complete decomposition of water based on one-step photoexcitation under UV light mainly include metal oxides with d0 (such as Ti^{4+} , Zr^{4+} , Nb^{5+} , Ta^{5+} , and W^{6+}) and d10 (such as Ga^{3+} , In^{3+} , Ge^{4+} , Sn^{4+} , and Sb^{5+}) structures. However, it is difficult for a single semiconductor to meet the thermodynamic requirements of photocatalytic decomposition of water with a visible light response. The advantage of two-step photocatalytic hydrogen evolution is that it applies many semiconductor photocatalysts with visible light response to the photocatalysis hydrogen evolution but also utilize certain semiconductors with insufficient conduction band potentials, such as WO_3 and $BiVO_4$, as oxygen-producing photocatalysts [107].

Thermodynamically, the overall water splitting is an uphill reaction that requires a larger Gibbs free energy ($\Delta G^0 = 237 \text{ kJ mol}^{-1}$):



3.4.3.2 Mechanism

The overall water splitting reaction on a semiconductor photocatalyst occurs in three steps as illustrated in **Figure 20**. First, the semiconductor catalyst absorbs photon energy greater than the band gap energy of the material and generates electron-hole pairs in the bulk upon photoexcitation, (2) the photo-excited carriers separate and migrate to the surface, a few electrons and holes will recombine in bulk or on the surface, and (3) the rest of the charge carriers will reach the catalysts (or catalytic active site) on the surface where surface redox reactions occur, specifically HER with photoelectrons and donor oxidation with the photo holes.

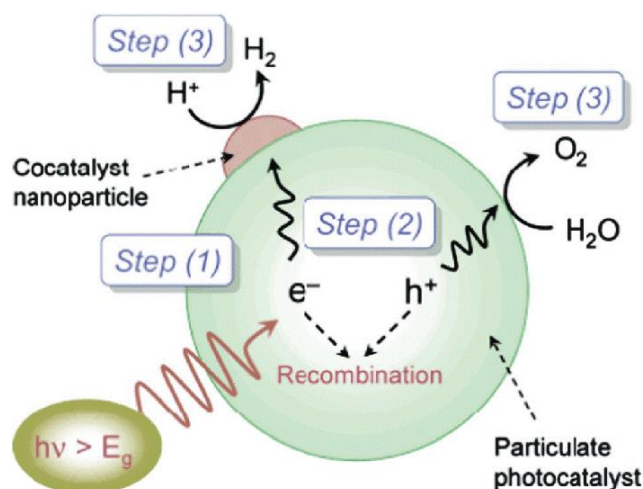


Figure 20: Processes involved in overall photocatalytic water splitting on a heterogeneous photocatalyst [108].

The first two steps are strongly dependent on the structural and electronic properties of the photocatalyst. However, the third step is promoted by the presence of a solid cocatalyst. The cocatalyst is typically a noble metal (e.g., Pt, Rh, Pd) or a metal oxide (e.g., NiO, RuO₂), which is loaded onto the photocatalyst surface as a dispersion of nanoparticles. Generally, a co-catalyst is necessary for the proton reduction and water oxidation in the water splitting process. Apart from intensifying the speed of reaction, a suitable co-catalyst increases the efficiency of the reaction process. The speed of photocatalytic reactions can be accelerated by the suitable preparation of co-catalysts on the surface [109, 110].

3.4.3.3 Photocatalyst Materials

The combination of graphene with semiconductors provides a simple framework for improving behavior and stability. Moreover, graphene is normally inactive when exposed to room temperature. Graphene is a single atom layer made up of hybridized carbon sp² with a distinctive 2D wafer lattice structure. Moreover, it not only renders the thinnest, strongest, and low-cost substance in existence, but also empowers with many exemplary physical and chemical characteristics such as high thermal conductivity, outstanding carrier mobility at room temperature, decent electrical conductivity, excellent environmental stability with exceptionally high theoretical specific surface area and high strength. Other materials proposed are carbon nanotubes, activated carbon and other carbonaceous materials like TiO₂ and cadmium sulfite (CdS).

Photocatalytic water splitting is a strong candidate for future solar hydrogen production. When considering the usage of solar energy, one encounters difficulties due to the low density of the energy. A large area must be used to harvest a reasonable amount of solar energy. The photocatalytic water splitting will be advantageous for the large-scale application of solar hydrogen production because of its simplicity. It is the most promising technology for this purpose, since H₂ could be obtained directly from abundant and renewable water and solar light from the process. Since the discovery of hydrogen evolution over a TiO₂ single-crystal electrode, the technology of semiconductor-based photocatalytic water splitting to produce hydrogen using solar energy has been considered as one of the most important approaches to solving the world energy crisis [111-119].

3.4.4 Hydrogen Production from Wind Energy

The process of producing hydrogen from wind energy is the electrolysis of water, with the main power input being electrical power generated by the conversion of wind energy. Wind energy exists in almost every part of the world. It is a safe, clean, and inexhaustible source of energy with a slight environmental impact caused mostly during the time of installation of its equipment. As a concept, it is a very promising way to produce hydrogen not only because both procedures are renewable and nonpolluting, but also because wind energy conversion systems can become more effective by incorporating an energy storage medium. Wind farms (WFs) may use some part of their energy production for storage by balancing

their load in relation to the current wind conditions and the energy demand of the grid for on-site hydrogen production and distribution.

Wind energy is defined as the kinetic energy of wind converted into mechanical work. This mechanical work can be used to drive an electrical generator to produce electricity. A machine that performs this conversion is called a wind turbine generator (WTG) and a group of these, including the auxiliary equipment, constitute a wind farm (WF). The most common application being studied currently is the stand-alone wind energy system combined with an electrolyzer. This system is shown in **Figure 21**. Others include grid-connected wind energy systems and non-interconnected wind energy systems.

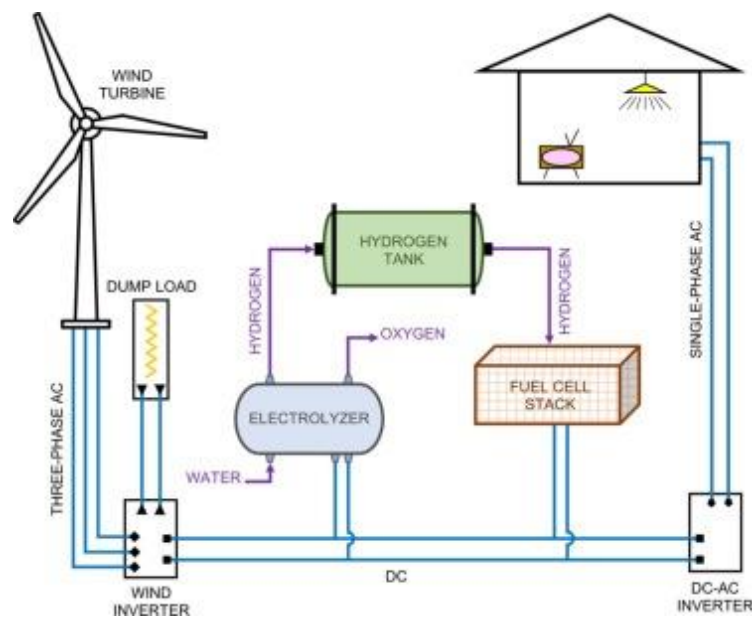


Figure 21: Design of an isolated stand-alone hybrid wind-hydrogen system for a zero-energy house [120].

Use of hydrogen as a carrier for the storage of wind energy presents several advantages. Hydrogen is well adapted for seasonal energy storage without energy loss over time. Water electrolyzers can handle power fluctuations, addressing the problems relative to the intermittent nature of wind power, and allowing wind parks to provide a guaranteed power output. Wind-hydrogen systems present a potential for high-density energy storage with low and predictable operating and maintenance costs. The combination of hydrogen and wind energy systems may contribute to the growth of both technologies while one serves the other for different reasons [120].

3.4.5 High-Temperature Decomposition

High-temperature water splitting happens at around 3000°C. At this temperature, 10% of the water decomposes, leaving 90% of the water to be recycled. There are other processes for high-temperature water splitting that reduce the temperature:

- Thermochemical cycles.
- Hybrid systems that couple thermal and electrolytic decomposition.

- Thermophysical cycle: a direct catalytic water decomposition with separation through a ceramic membrane.
- Plasmachemical water decomposition in a two-stage CO₂ cycle.

Efficiencies of over 50% are expected for these processes, which could result in a significant reduction in hydrogen production costs. There are some technical concerns for the high-temperature processes, that have to do with the: (a) materials development for corrosion resistance at high temperatures, (b) high-temperature membrane and separation processes, (c) heat exchangers, (d) heat storage media, and (e) design and safety [79, 121, 122].

3.4.6 Thermolysis and Thermochemical Water Splitting

The conversion of water into hydrogen and oxygen via a sequence of thermally driven chemical reactions is known as thermochemical water splitting. Water starts to decompose without the need for other chemical materials if a temperature over 2000°C is reached so the thermolysis process can be described as the direct thermal splitting of water at a very high temperature. Thermochemical water splitting cycles have been examined intensively since the late 1970s and 1980s but have received little attention in the last decade. While the technical feasibility and the high-efficiency potentiality are undeniable, commercially viable cycles with proven low cost and high efficiency have yet to be developed.

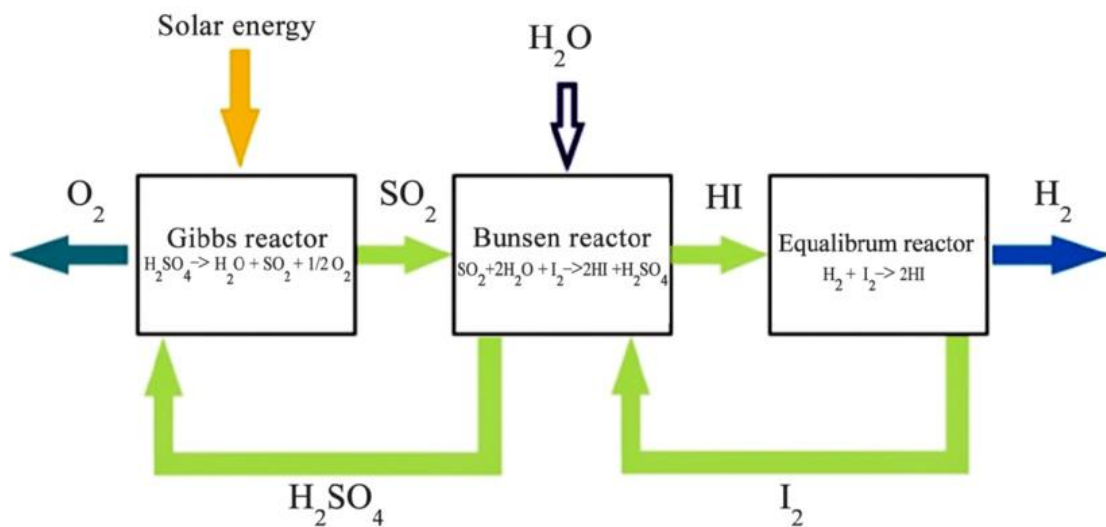
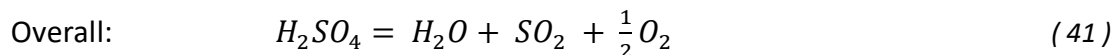
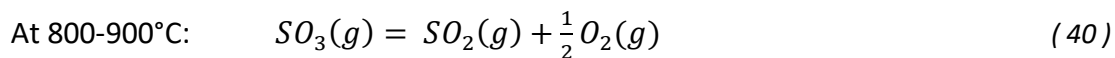
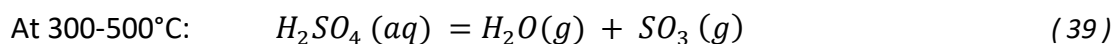


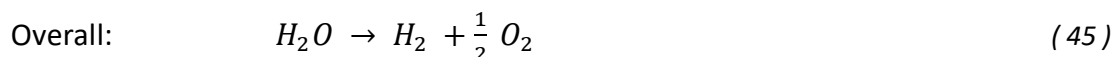
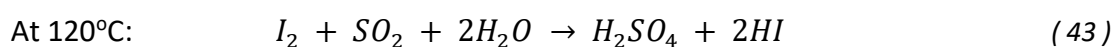
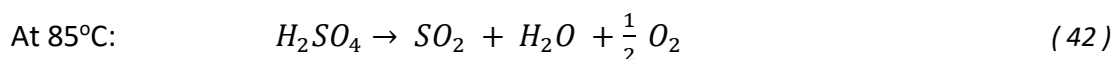
Figure 22: Sulphur-Iodine cycle simplified scheme [123].

The thermochemical water splitting process, combines the thermolysis water splitting process and the chemical reactions so as to reduce the water decomposition temperature to 900°C. While the technical feasibility and the high-efficiency potentiality are great, commercially scaled viable cycles with proven low cost and high efficiency have yet to be developed. The iodine/sulfur (IS) cycle, shown in **Figure 22**, is an example of a thermochemical process. The research and development requirements for this technique focus to collect the thermally split H₂, avoid side reactions, and eliminate the use of toxic compounds. Corrosion issues linked with the handling of such materials are likely to be catastrophic [15, 124-131].

Thermal decomposition of sulfuric acid proceeds in the following two steps:



The acids are then separated and thermally decomposed to produce hydrogen and oxygen. HI-decomposition is a very slow reaction even at a high temperature of 500°C so the use of catalyst will increase the reaction rate. Some common catalysts are Pt, Cu and Fe₂O₃ [132-136].



3.5 Biomass to Hydrogen

Biomass is abundantly available and, compared to fossil fuels, more evenly distributed geographically on a world-scale. It is the solar energy stored in living material and the oldest energy source known to humankind.

A variety of biomass resources can be converted for energy supply. They can be categorized as:

- (i) Agricultural waste including both agricultural food crop residues and animal wastes.
- (ii) Forest residues which encompass all terrestrial trees/shrubs and aquatic plants, wood, and logging residues.
- (iii) Municipal waste including both household and industrial waste and sewage sludge.

The chemical composition of biomass, whether it is lignocellulosic or herbaceous, is characterized by five primary components: cellulose, hemicellulose, lignin, extractives/volatiles, and ash. The carbon content is significantly lower compared to coals, whereas the oxygen content is much higher. Consequently, the heating values of biomasses are generally lower than those of coals. Widely varying moisture contents of biomass are encountered; they may range from 10% to 70%. This water content affects the thermochemical conversion and the volume of gases produced per energy unit. The heating value decreases with an increasing moisture content. Biomass also usually has a low mass and energy density, compared to bulk densities of coals. Even though CO₂ is released during the production of hydrogen from biomass, the amount of gaseous emissions is equal to the amount absorbed by organisms during their lifetime.

Biomass feedstock is an unrefined product with poor quality control and inconsistent quality. Crop type, climate, and location variables all influence production methods. Erratic fuels have hampered technological innovation because less homogeneous and low-quality fuels necessitate more sophisticated conversion devices. Fuel production and processing must be rationalized in order to provide higher-quality, more consistent fuels that can be described using common standards. Large-scale plants are suitable for lower-cost, lower-quality fuels, whereas smaller systems need higher-quality fuels with better homogeneity.

Two groups of conversion technologies are distinguished: biological and thermochemical. The main difference between these routes is the temperature range. The biological processes take place at ambient to slightly higher-temperature levels, whereas the thermochemical conversion routes take place at temperatures of several hundred degrees Celsius [137].

Biomass gasification can be conducted in small, medium, and large-scale gasification units. Large-scale plants are suitable for lower-cost, lower-quality fuels, whereas smaller systems need higher-quality fuels with better homogeneity. In biomass conversion process, hydrogen-containing gas is created in a way similar to coal gasification. However, there are currently no commercial plants that produce hydrogen from biomass. The pathways followed at the moment are steam gasification (direct or indirect), entrained flow gasification, and more advanced techniques, such as gasification in supercritical water, thermochemical cycles application, intermediates conversion (e.g., bio-oil, ethanol, torrefied wood). For hydrogen production, none of the approaches above have reached the demonstration phase.

Biomass gasification is a research and development topic that includes both hydrogen and biofuels production. The most promising medium-term technologies for commercializing hydrogen production from biomass are gasification and pyrolysis. The drying of biomass has great energy requirements; therefore, different routes based on wet biomass are being investigated [138-140].

3.5.1 Thermochemical Biomass Gasification

It is a high temperature partial oxidation process where biomass, which is a solid carbonaceous feedstock, is transformed into a gaseous mixture (CH_4 , CO_2 , H_2 , CO , tar, light hydrocarbons, ash, minor contaminants, and char) using gasifying agents. There are three main types of gasifiers: fixed bed, fluidized bed and entrained flow bed (**Figure 23**).

Thermochemical gasification by partial oxidation is already an old art (well over 150 years), that has been developed to substantially transfer the combustion value of a solid feedstock to a gaseous energy carrier in the form of chemical energy. This is convenient because a gas offers substantial advantages as a heat carrier. Gasification of biomass generates the so-called bio syngas, which contains CO and H_2 in amounts depending on the applied process, oxidation medium, and fuel/oxidizer ratio. Comparatively, low-temperature ($<1000^\circ\text{C}$) gasification processes yield a product gas that contains significant amounts of hydrocarbon compounds. Higher

temperature processes yield a biosyngas that contains almost no hydrocarbons anymore. An advantage of oxygen-based gasification is that it does not require any external source of energy.

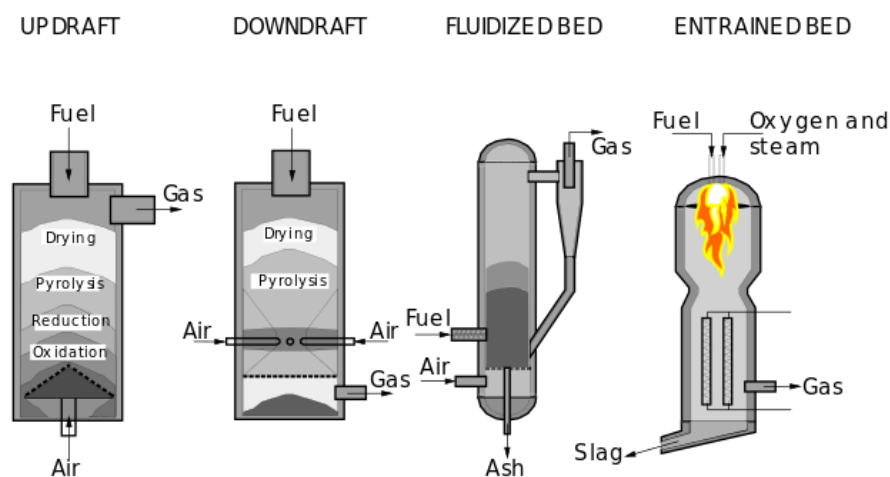


Figure 23: Main gasifier types [141].

The process scheme typically consists of the following basic steps: biomass pretreatment, gasification, gas cleaning, reforming of higher hydrocarbons, shift to obtain suitable $H_2:CO$ ratios, and gas separation for hydrogen production and purification. A gas turbine or boiler to utilize the unconverted gas are optional, as well as a steam turbine to produce electricity.

The pretreatment techniques may include drying, chipping, sizing, densification, and optional torrefaction. The drying of biomass requires a significant amount of energy; therefore, different routes based on wet biomass are being investigated. Since the moisture must be vaporized, the thermal efficiency of the gasification process is typically low.

The reaction is carried out co-feeding O_2 , air or steam, possibly using a catalyst when using the fixed bed and the fluidized bed reactor. The recorded performance of the fluidized bed reactors is higher than the fixed bed type reactors. The produced gas must be cleaned before being upgraded to the downstream application. As gas cleaning options, a choice can be made for either low temperature 'wet' or high temperature 'dry' gas cleaning.

After reforming and shifting of raw syngas is performed and finally hydrogen can be separated and compressed. The hydrogen quality is a major issue for its eventual automotive application. Specifically, CO is a strong poison to polymer electrolyte membrane (PEM) fuel cells. Studies indicate that levels as low as 1-2 ppb will deactivate the platinum anode material of such fuel cells [142, 143].

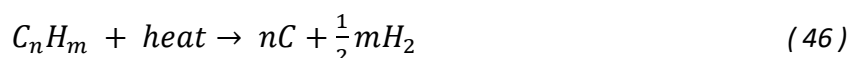
3.5.2 Hydrogen from Pyrolysis-Derived Bio-Oil

Pyrolysis or co-pyrolysis is another promising technique for producing hydrogen. In this technique, heating and gasification of raw organic material occur in a temperature range of 500-900°C at a pressure of 0.1-0.5 MPa. Pyrolysis of biomass is a thermochemical process carried out at typical temperatures in the range 650-800 K and atmospheric or a few bar

pressure, in which the fuel is converted under a supply of heat and principally with the exclusion of oxygen. Consequently, carbon oxides don't appear in the reaction by-products.

The process produces different proportions of liquid (bio-oil), gaseous (H₂-containing) and solid products as the main product in a single-reactor configuration. This is a complex mixture of a multitude of organic compounds including acids, alcohols, aldehydes, esters, ketones, and (oxygenated) aromatics, which can be further converted into different fuels, chemicals, and materials. Bio-oils are already used (practically) commercially as boiler fuels for stationary power and heat production but need upgrading if they are to be used as transportation fuels.

The chemical reaction of the pyrolysis process can be generally expressed as follows:



Pyrolysis can be grouped as high (over 800°C), medium (500-800°C), and low temperatures (up to 500°C). Fast pyrolysis (FP) is a process used to transform organic material into products with higher energy content. Products of FP appear in all three phases, i.e., liquid, solid, and gas [144].

3.6 Biological Production of Hydrogen

Biological hydrogen has several characteristics that make it a suitable energy carrier in meeting future energy needs and a sustainable and clean alternative method for large-scale application. These include its renewable nature, high energy yield, ease of conversion to electricity and CO₂-free combustion.

Biological production of hydrogen from algae can be accomplished through one of the following ways (**Figure 24**):

1. biophotolysis of water by green algae and blue-green algae (cyanobacteria),
2. dark fermentation of algal biomass organic compounds, and
3. light-driven fermentations, or photo-fermentations, of organic compounds in algal biomass by photosynthetic bacteria.

Depending on different basic types of photosynthesis (plant and bacterial types), different light dependent processes have been observed. One approach, biophotolysis, harnesses solar energy to drive water-splitting photosynthesis and derives H₂ from the resultant high-energy electrons. Another approach, photo fermentation, uses bacterial-type photosynthesis to capture light energy and carry out what would otherwise be a thermodynamically unfavorable H₂ production [145-149].

Although it may be possible to engineer plants and other types of photosynthetic organisms (algae) as energy-converting 'machines' and 'chemical factories', the overall efficiency of solar energy conversion will rarely exceed 1 per cent and will usually be much lower, so it is understood that this approach will only make a minor contribution to our future energy needs.

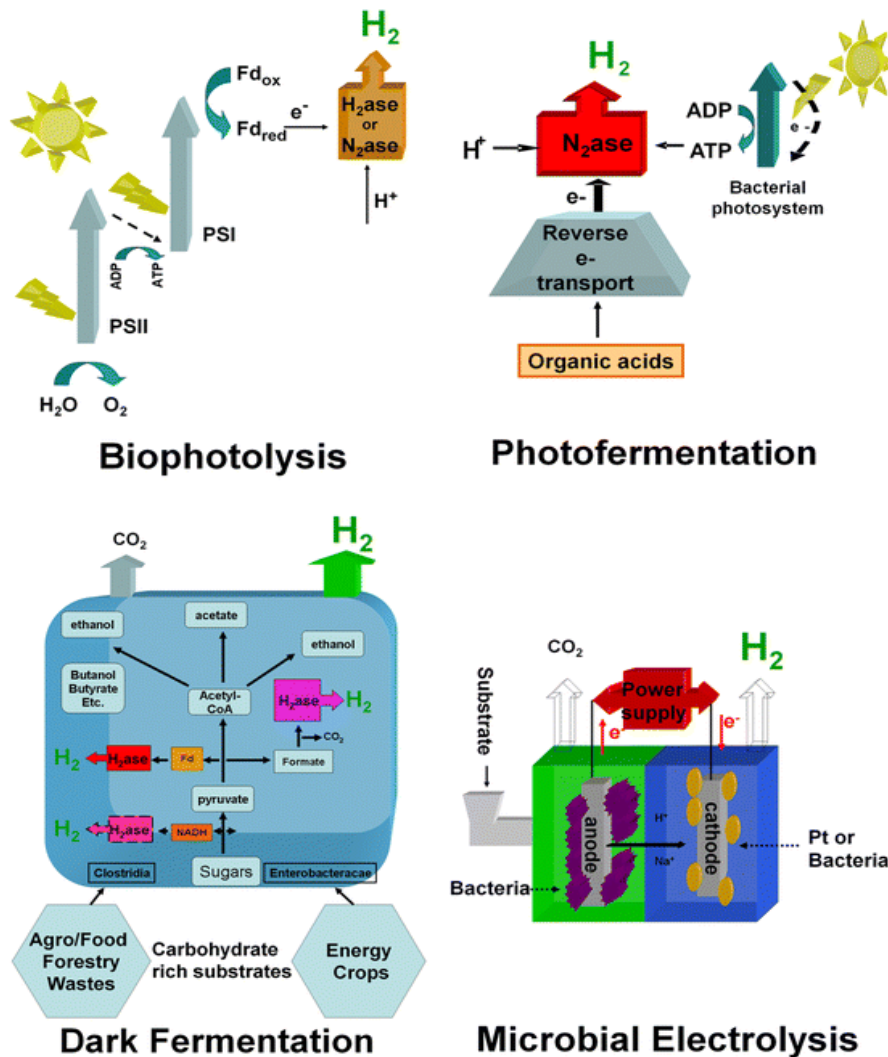


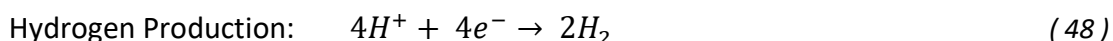
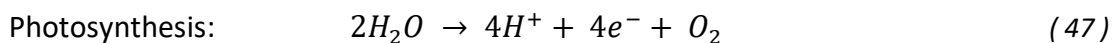
Figure 24: Schematic illustration of biological production of Hydrogen [150].

3.6.1 Photobiological Production (Biophotolysis)

This route of biological hydrogen production is predominant in photosynthetic organisms such as green algae and cyanobacteria, which utilizes enzymes as catalysts to split water in the presence of sunlight. Two specific hydrogenases catalyze these reactions, Fe-Fe hydrogenase in green algae and nitrogenase in cyanobacteria. Based on the mechanism of H₂ evolution, biophotolysis is further categorized as direct and indirect biophotolysis.

During direct photolysis, the electrons generated by water splitting in the presence of light are transferred to photo-system II (PSII), PSI, and the captured solar energy is used to reduce ferredoxin. Reduced Fd acts as an electron carrier and reduces a H₂-evolving enzyme, either a [Fe-Fe]-H₂ase or nitrogenase to produce molecular H₂. Both photosystems (PSI and PSII) and hydrogenase enzymes play an active role in direct bio-photolysis. These enzymes are extremely sensitive to oxygen, and as a result, the oxygen content must be maintained below 0.1%, which is a drawback of this technology. It is a simple process, but one that suffers from the essentially incompatible simultaneous reactions of O₂ evolution and proton reduction by an O₂-sensitive enzyme.

Indirect photolysis is characterized by the conversion of light to biochemical energy, which is stored in cells in the form of carbohydrates, which is later used for H₂ production. Nitrogenase enzyme present in the cyanobacteria catalyzes the H₂ production reaction separately with the reduction of N₂ to ammonia. Bio-photolysis is a two-step process. At first, photosynthesis takes place and then, hydrogen production catalyzed by hydrogenases contained in cyanobacteria and green algae. Another alternative to reproduce the two steps is to use artificial photosynthesis.



The most analyzed species in direct bio-photolysis is the microalgae *Chlamydomonas reinhardtii*. Both photosystems (PSI and PSII) and hydrogenase enzymes play an active role in direct bio-photolysis. These enzymes are extremely sensitive to oxygen, and as a result, the oxygen content must be maintained below 0.1%, which is a drawback of this technology. The process of photosynthesis also occurs in unicellular eucaryotes such as blue green algae and several other bacteria such as cyanobacteria, purple bacteria, and green sulfur bacteria. The photochemical reactions that capture the energy of light are basically the same in bacteria, algae, and plants. Indirect bio-photolysis could be used with many species of cyanobacteria. The process of the photosynthesis is then accompanied by dark fermentation to produce H₂O and H₂.

3.6.2 Dark Fermentation

The dark fermentation is advantageous over light-dependent routes in terms of a high rate of hydrogen production, utilization of various organic substrates, and the presence of a diverse microbial catalyst. It is a complex process that occurs in an anaerobic environment and is characterized by a series of enzymatic reactions. The key enzymes that drive this process in diverse groups of bacteria are mostly Fe only and Fe-Fe hydrogenases.

Dark fermentative H₂ production harnesses the inherent capacity of some microorganisms to rid themselves of excess electrons generated during anaerobic metabolism by evolving H₂ as a product. Both pure substrates and a variety of wastes have been used for dark fermentative H₂ production. Of course, using waste streams is desirable, but this usually necessitates a collaboration of organisms with diverse catabolic activities. Most microbial hydrogen production is driven by the anaerobic metabolism of pyruvate, which is formed during the catabolism of various substrates.

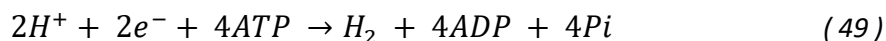
For more than half a century, it has been known that some species of green algae are capable of a short-lived burst of H₂ production, catalyzed by a [FeFe]-H₂ase, upon re-illumination of dark-adapted (anaerobic) cultures. Long considered a laboratory interest, sustained H₂ production by illuminated cultures was finally demonstrated using two stages; a first stage where photosynthesis and growth occur, followed by a stage of sulfur deprivation, providing the anaerobic conditions that support sustained H₂ production.

Anaerobic conditions are established through the concerted effort of two factors: sulfur deprivation, reducing PSII activity under these conditions, cells are unable to replace photo damaged D1 protein, and cellular respiration, augmented when acetate is present, consuming dissolved O₂.

The dark fermentation process is characterized by a massive accumulation of organic acids, which leads to an inhibitory effect on H₂-producing enzymes and the growth of microbes. But the low hydrogen production capacity compared with the unit capital investment has been investigated to be the major challenge of the dark fermentation method. So, different extensive research has been presented to get additional energy by adding and develop a new other two-stage system.

3.6.3 Photo-Fermentation

The photo-fermentation route of H₂ production is distinguished by higher hydrogen yield, the use of organic acids as substrates, and sunlight as a source of energy. During the photo-fermentation, organic acids such as acetic acid and succinic acid are metabolized by photosynthetic bacteria to produce nicotinamide adenine di nucleotide (NADH), which reduces nitrogenase via reverse electron transport. The reduced nitrogenase, in turn, uses photosynthetically produced adenosine triphosphate (ATP) to reduce the protons to molecular H₂.



Although this process has some distinct advantages, it shows poor light conversion efficiency because of the high energy (ATP) requirements of the nitrogenase enzyme. Moreover, photo-fermentative bacteria cannot directly feed on sugar hydrolysates. Instead, they feed on volatile fatty acids, which are major by-products of dark fermentation. Thus, an integrative process of dark and photo-fermentation can be used to produce a generous amount of H₂ from waste biomass.

3.6.4 Microbial Electrolysis

Microbial electrolysis cells (MECs) are based on microbial fuel cells (MFCs), which have been studied for decades. The MEC sector has seen rapid growth in recent years. Organic compound microbial metabolism generates CO₂, protons, and electrons, with the anode acting as an electron sink. An additional voltage can be applied to the current generated to drive H₂ evolution at the cathode. Thus, by applying a relatively low voltage (-0.135 V), acetate (-0.279 V) could be converted to H₂ (0.414 V) against the thermodynamic gradient. However, before MECs can become practical, a number of challenges must be overcome, including the development of efficient and low-cost electrode materials and the reduction of internal resistances.

3.6.5 Factors Affecting Biohydrogen

Temperature is a crucial factor that influences fermentative hydrogen production. As the enzyme kinetics depend on the system temperature, an optimum range is essential for higher

activities of the enzymes that catalyze the metabolic pathways of H₂-producing bacteria. The optimum range of temperature for H₂ production varies with the type of inoculum and substrate used for fermentation. The temperature range of 35-40°C is mostly favorable for microbial H₂ production. The decrease in temperature below 35°C favors the production of other metabolites such as ethanol, acetic acid, butyric acid, and propionic acid.

The pH is also an important factor of fermentative hydrogen production because it influences the growth and enzyme activities of hydrogen-producing microbes. The pH range of 4-7 is optimal for biohydrogen production. The optimum values, however, are determined by the substrate and inoculum used. Hydrogen-producing microbes require acidic pH for growth and metabolism because the hydrogenase enzyme has higher catalytic activity at pH 5-6.

The microbial catalyst used for fermentative hydrogen production is referred to as inoculum. The two factors influencing biological H₂ productivity are inoculum size and type. Mixed culture as inoculum for H₂ production is advantageous over pure culture as it can feed on complex carbon sources like cellulose, food waste hydrolysate, dairy wastewater, corn starch, and other organic wastes [150-154].

3.6.6 Final Comparison

Being a versatile energy carrier, hydrogen can be produced from a variety of feedstocks, including natural gas, coal, biomass, waste, solar, wind, or nuclear sources. The separation of hydrogen from hydrogen-containing feedstocks is the basis of hydrogen production processes. Producing hydrogen from non-fossil energy sources results in zero GHG emissions. **Table 9** demonstrates the different types of feedstocks, as well as the efficiency, the Global Warming Potential (kgCO₂/kgH₂) and the current maturity of every technology. There are two primary methods: thermal (reforming, gasification) and chemical (electrolysis). Other methods (biological, photo-electrochemical) are in the early stages of development.

For decades, natural gas steam methane reforming (SMR) has been used to bulk produce hydrogen. The energy efficiency of SMR is in the 70-85 % range. Scaling down into operationally stable and economically viable distributed generation units has been difficult, but small steam methane reformers, partial oxidation reformers, and auto-thermal reformers are now being manufactured and operated. Continuous operation can achieve energy efficiencies of up to 68 %. Hydrogen can also be produced locally from wastewater or biowaste using anaerobic digestion to produce biogas, which is then reformed into hydrogen.

Electrolysis is a well-known technology. Although large-scale electrolysis using fossil or nuclear generated electricity is still inefficient, it is a key technology for enabling high renewable electricity adoption, particularly in the transportation sector. Electrolyzers are widely used in distributed generation because they can easily meet a variety of smaller

hydrogen needs. Nuclear energy can generate high-quality hydrogen in large quantities at a low cost and with no emissions. In the future, advanced high temperature reactors (HTR) could provide more cost-effective, large-scale hydrogen production while producing less nuclear waste and using less energy. In addition to nuclear heat, concentrated solar thermal power has been successfully demonstrated in a 100kW pilot plant in the EU-funded Hydrosol Project for large-scale thermochemical hydrogen production.

Table 9: Comparison between different biological production methods.

Technology	Feedstock	Efficiency	Global Warming Potential (kgCO ₂ /kgH ₂)	Maturity
Steam reforming	Hydrocarbons	70-85%	2.5	Commercial
Partial Oxidation	Hydrocarbons	60-75%	2.5	Commercial
Autothermal reforming	Hydrocarbons	60-75%	2.5	Near term
Alkaline electrolyzer	H ₂ O+electricity	50-60%	3.33	Commercial
PEM electrolyzer	H ₂ O+electricity	55-70%	3.33	Near term
Solid oxide electrolyzer	H ₂ O+electricity + heat	40-60%	3.33	Med term
Thermochemical water splitting	H ₂ O + heat	NA	9.17	Long term
Biomass gasification	Biomass	35-50%	5.83	Commercial
Bio-Photolysis	H ₂ O + sunlight	0.5%	7.5	Long term
Photocatalytic water splitting	H ₂ O + sunlight	12.4%	9.58	Long term
Dark fermentation	Biomass	60-80%	9.58	Long term
Photo fermentation	Biomass+sunlight	0.1%	9.58	Long term
Microbial electrolysis cells	Biomass+sunlight	78%		Long term

For the time being, hydrogen will continue to be produced by steam reforming natural gas, a well-understood and time-tested technology, and by water electrolysis using electricity from conventional energy resources. In the medium to long term, hydrogen production technologies such as electrolysis, direct renewables (photo-biological, photo-electrochemical, etc.), high temperature nuclear chemical cycles and clean coal will become more cost effective and contribute to the diversification of domestic hydrogen production. Since hydrogen can be produced from a wide range of resources, each region and country may produce hydrogen using a different combination of resources.

CHAPTER IV - HYDROGEN STORAGE

4.1 Background

Hydrogen fuel is the key to a sustainable future, but storage problems are of major concern for further development. For years, hydrogen storage has been at the forefront of research, in the world's most technologically progressive countries. The effort is motivated by the fact that hydrogen can aid in managing the rising energy demand while also slowing global climate change. Furthermore, hydrogen storage is a crucial enabling technology for long-term hydrogen energy development, which is critical for the growth of the future economy. Significant research is being carried out to increase the efficiency of H-storage systems so they can compete with fossil fuels in both transportation and stationary applications. The mobile department is expected to be the largest consumer of hydrogen. Although hydrogen has enough properties for fueling internal combustion engines in cars, it is expected that polymer electrolyte membrane fuel cells (PEMFCs) will replace traditional engines, in the future hydrogen economy.

However, both mobile and stationary storage systems have their own set of requirements and obstacles. In comparison to mobile applications, the weight and volume issues with hydrogen storage are not as important in stationary applications. Stationary storage systems take up more space, operate at higher pressures and temperatures, and have extra capacity to compensate for slow kinetics. Even so, insufficient materials for storage tank pose a technical roadblock to the development of stationary hydrogen storage systems. Mobile applications, on the other hand, have more storage requirements than stationary applications. The Department of Energy (DOE) has proposed new technical system goals, based on a 500-kilometer driving range to develop practical hydrogen-storage technology.

Table 10 summarizes some of these goals for on-board hydrogen storage in light-duty fuel cell vehicles starting in 2020. The DOE targets in mobile applications stress the importance of storage capacity in both gravimetric (weight percent wt %) and volumetric (volume percent v/v %) terms. The gravimetric capacity of storage refers to the amount of hydrogen gas that can be generated by a given volume of storage material, whereas the volumetric capacity of storage conveys the amount of hydrogen gas contained in a given volume of storage material. For a suitable hydrogen storage, high values of both parameters are desired. However, in case of a heavy storage, the vehicle's range will be restricted, and in case of a voluminous storage, luggage capacity will be restricted too. To put it another way, effective balance is needed [45, 155].

Some other important requirements of on-board hydrogen storage requirements are: low operating pressure and temperature between, fast kinetics of uptake and release of hydrogen, low heat of formation in order to minimize the energy required for hydrogen release, low heat dissipation while exothermic hydride forms, limited loss of energy during hydrogen charge and discharge, multicycle reversibility of uptake and release of hydrogen,

high stability against moisture and oxygen for long cycle life, low cost of charging and recycling infrastructures, high safety during operating conditions, and acceptance by the general public.

Table 10: Overview of some selected parts of the U.S. DOE technical system goals for on-board H-storage for light-duty fuel cell vehicles [45].

Storage parameter	Unit	2020	2025	Ultimate
Storage capacities				
Material-based gravimetric capacity	kWh/kg	1.5	1.8	2.2
System-based gravimetric capacity	kgH ₂ /kg system	0.045	0.055	0.065
Material-based volumetric capacity	kWh/L	1.0	1.3	1.7
System-based volumetric capacity	KgH ₂ /L system	0.030	0.040	0.050
Storage system cost	\$/kWh net	10	9	8
Fuel cost	\$/kg H ₂	333	300	266
Durability/Operatability				
Operating ambient temperature	[°C]	-40/60 (sun)	-40/60	-40/60
Min/Max delivery temperature	[°C]	-40/85	-40/85	-40/85
Cycle life (1/4 tank to fill)	[cycles]	1500	1500	1500
Min delivery pressure from tank	[bar]	5	5	5
Max delivery pressure from tank	[bar]	12	12	12
Charging/Discharging rates	[min]	3-5	3-5	3-5
Fuel purity (H ₂ from storage)	[%H ₂]	Meet or exceed applicable standards e.g. SAE J2719 (99.97 dry basis)		

Hydrogen can be stored in a variety of ways, each with its own set of advantages and disadvantages. Gaseous, liquid, and solid-state storage systems are the three major types of storage systems available, depending on the size of the storage and area of application. Although every method has some appealing attributes, none of them meets all the efficiency, weight, size, safety, or cost requirements for car applications. **Figure 25** depicts the volumetric and mass performance of several storage systems. In the next sections the storage systems are going to be reviewed, focusing on the solid-state storage system, since it is the most promising in the field [45, 156].

4.2 Gaseous-State Storage System

Physical hydrogen storage in the form of pressurized gas is the most established hydrogen storage system. As previously noted, hydrogen has a relatively low density of 0.089 kg/m³, which necessitates high pressure or extremely low temperatures for it to be stored. Currently, hydrogen must be pressurized between 35 and 70 MPa for current fuel cell applications. Hypothetically, pressurizing negatively affects between 11 and 13% of the hydrogen energy content. Due to its lightness, there is a risk of hydrogen leaking from containers under high pressure. The traditional types of commercial hydrogen storage vessels are made of steel and aluminum materials. However, in comparison to steel or aluminum vessels, a carbon fiber reinforced plastic composite vessel, with enough strength

and impact resistance needed for safety during accidents, is a lighter alternative but too expensive, posing another problem for cost reduction in the future. In addition, scientists and engineers are looking into new, cost-effective and practical alternatives.

Compressed hydrogen could also be stored in vast underground storages in geological formations such as caverns of salt domes if the amount of hydrogen to be stored is high or the storing time is long. Even under high pressure, the salt caverns are resistant to hydrogen, preventing leakage. On calm and cloudy days when wind and solar power are not as active, hydrogen may then be recovered from the caverns and used in a combined-cycle power plant to create electricity. For a long time, there were no appropriate infrastructures for effectively burning pure hydrogen, but these kinds of infrastructures have recently been developed. The hydrogen underground storage project in Romania that is a part of the HyUnder project, supported by the FCH JU (Fuel Cell and Hydrogen Joint Undertaking), is one of the latest examples. This project aims to make it easier to store enough hydrogen underground in salt caverns for future use, especially in transportation, chemical, and salt industries. Until now, despite promising options, the extremely high gas pressures, the relatively low hydrogen density, cost, and safety issues remain major roadblocks for this technically simple and well-established technology.

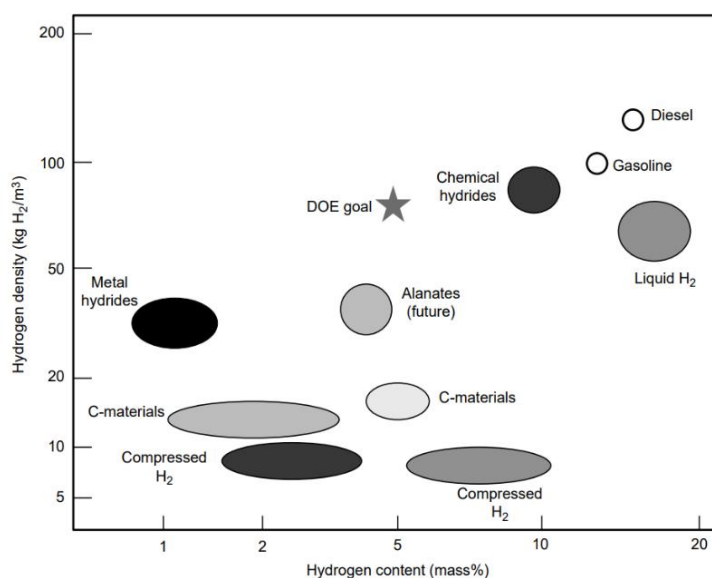


Figure 25: Volumetric versus mass densities achieved by various hydrogen-storage technologies (Modified from [157]).

4.3 Liquid-State Storage System

Cryogenic liquid is another method of physically storing hydrogen. The density of liquid hydrogen is higher. At its normal boiling point of 20 K, liquid hydrogen has a density of around 71 g/L, which is about 1.8 times that of hydrogen pressurized to 70 MPa at 288 K. Because of its low boiling point, liquid hydrogen’s cooling technology demands very low temperatures, which use about 30% of its total energy content. To prevent heat leakage, special double-walled vessels with strong insulation systems are required. Cryogenic pressure vessels are more compact and lighter than compressed hydrogen vessels,

providing higher safety benefits. However, the persistency of hydrogen to boil-off, and the excessive energy required for liquefaction limit the potential use of liquid hydrogen storage systems to applications requiring high energy density as well as uses where the cost of hydrogen is not important, and consumption occurs quickly, such as air, space, and automotive applications [45].

Liquid hydrogen is the simplest form of hydrogen storage; but the cost linked to the low temperatures required for the liquefaction has drawn attention to other liquid carriers that require moderate storage conditions. Two carriers, in particular, have been found to be the most interesting: liquid organic hydrogen carriers (LOHCs) and ammonia. Both with moderate requirements for storage which results in much lower transportation and storage costs. As a result, hydrogen supply networks based on conversion to these compounds are being actively developed. The majority of liquid carrier uses are models of either decentralised hydrogen release at refuelling stations, or centralised dehydrogenation at ports or other facilities for local distribution as hydrogen gas [158].

While the production costs of ammonia and LOHCs is lower than the cost of liquefying hydrogen, use of these carriers sets an extra step which is converting the carrier back to hydrogen. The efficiency and cost losses associated with this reconversion limit their use. As such, lot of research has been devoted to improving the chemistry of hydrogen release via catalyst development.

4.3.1 Liquid Organic Hydrogen Carriers (LOHCs)

The first LOHC carriers investigated were cyclic alkanes such as methylcyclohexane, cyclohexane, which were dehydrogenated to the related aromatic compounds using platinum-based catalysts at 300-350°C. These basic materials, which release up to 6 wt. % hydrogen with a volumetric hydrogen density of 70 MPa hydrogen gas, are appealing since they are already commercially manufactured and have a high technological readiness (e.g. toluene and benzene). However, practical applicability is hindered by high dehydrogenation temperature and high cost of the catalysts required. As a result, studies on these carriers have been concentrated on:

- the temperature reduction of dehydrogenation by modifying the LOHC molecule so that the enthalpy of the reaction is minimized.
- research for more stable, active, and abundant dehydrogenation catalysts.

To modify the dehydrogenation enthalpy, introduction of heteroatoms, particularly nitrogen, into cyclic structures has been used. Many of these materials (for example, N-ethyl carbazole) have been found to have better hydrogen release and storage properties than unsubstituted systems.

To optimize storage properties of hydrogen organic compounds, a metalation strategy is being employed. This happens through replacing the reactive H by alkali/alkaline earth metal in order to form the metalated counterparts. Crystalline lithiated amines are synthesised by ball milling

LiH amines, demonstrating a moderate endothermic dehydrogenation and a superior selectivity to hydrogen release. A sodium phenoxidecyclohexanolate pair is also developed, with a dehydrogenation enthalpy change of 50.4 kJ/mol-H₂, significantly less than that of famous phenol-cyclohexanol pair (64.5 kJ/mol-H₂). This enthalpy change is associated with the delocalization of electrons from oxygen to benzene ring of phenoxide. Hydrogen release and uptake are achieved below 150°C [158].

4.3.2 Ammonia NH₃

Ammonia is also a good liquid carrier for storing hydrogen. Because it is already one of the most important synthetic chemicals as a fertiliser feedstock, with annual production of roughly 180 Mt, current technology of synthesis and delivery infrastructure is mature. There are, however, a number of active research fields aiming to lower the cost and increase the efficiency of ammonia-based hydrogen storage. The release of hydrogen from ammonia, however, is not a well-established technology, since it does not play a major role in the existing ammonia market. Transition metal systems have been explored in depth for ammonia decomposition catalysis as a substitute for catalytic activity of ammonia synthesis. The most active metal is ruthenium, but good performance can also be achieved with more abundant metals including iron, molybdenum, and cobalt.

Temperature is also a factor, since even the most active ruthenium-based catalysts require rather high temperatures (>450 °C) to achieve 100% hydrogen conversion. New catalysts must be developed in order to achieve lower operating temperatures. Metal-nitrogen-hydrogen compounds (mostly light metal imides and amides) have recently been found to effectively mediate decomposition of ammonia, with catalytic activity comparable to ruthenium-supported catalysts. Another challenge is limiting ammonia leakage from storage vessels or hydrogen/exhaust streams to avoid ammonia toxicity in rivers and in the atmosphere, as well as protecting PEM fuel cells from ammonia degradation, and exposure of people to corrosive ammonia gas. Absorption of ammonia by metal halides or zeolites, or filtering H₂ gas streams using membranes, are two methods for purifying hydrogen to guarantee ammonia levels are below the 0.1 ppm limit for mobile applications.

Ammonia can also be stored in sorption materials with a substantially lower vapour pressure. Ammonia concentrations in metal halides ammine complexes are similar to liquid ammonia. It has been found that by modifying the combination of ion-metals in a ternary metal halide system, the ammonia release conditions can fit into the desired application. Mixed-metal systems that best matched a given performance metric were discovered using a combination of evolutionary algorithms and DFT (Density Functional Theory) computations. The barium-strontium-calcium structure was then synthesised, and the behaviour was found to be quite close to the expected ammonia desorption. Metal borohydride amines may store large amounts of ammonia, up to 6 groups of ammonia per molecule in case of 6Mn(BH₄)₂·6(NH₃), and have structures that are often similar to metal halide amines. The decomposition of these compounds gives pure ammonia or ammonia-

mixtures and hydrogen. The relative stability of the metal borohydrides is thought to play an important role, with amines of low-stability borohydrides being more prone to produce mixed gases [158].

4.4 Solid-State Storage System

Storage systems for a hydrogen economy must be safe, efficient, cost-effective, light, and compact. Conventional cryogenic liquid hydrogen and pressurized hydrogen gas though, require a large space for hydrogen storage, have safety issues, and are very expensive; thus, they fail to meet future goals for a hydrogen economy. It is clear that hydrogen storage requires a bigger technological leap. More specifically, for a fuel cell vehicle, there needs to be enough on-board storage space for hydrogen. To realize technically and economically feasible hydrogen-based automobile applications, a hydrogen storage system will need to have a large gravimetric and volumetric capacity. Hydrogen storage in solid materials is currently receiving a lot of attention in order to attain this goal. Solid-state materials can absorb and release hydrogen reversibly, making them a more advantageous option because they are not used up immediately. Exploiting the hydrogen storage potentials for new solid-state technologies could lead to a substantial shift in the faulty hydrogen storage paradigm and have a huge impact on the path to a functioning hydrogen economy.

Hydrogen is stored in solid-state storage systems by either physisorption or chemisorption. In physisorption, molecular hydrogen is adsorbed by van der Waals interactions on solid surfaces of nanostructured materials. The above nanostructured materials are mostly carbon-based materials, such as fibers, carbon nanotubes, fullerenes, zeolites, activated carbon, metal-organic frameworks (MOFs) and more lately polymers with intrinsic microporosity (PIMs), with low density, porosity and ultrahigh surface area [159]. Although the reversibility and quick kinetics make these materials appealing options, their poor storage capacity at ambient temperatures and the demand for extremely low temperatures for high storage capacity are severe limitations on their use in practical applications.

On the other hand, chemisorption is in form of atomic hydrogen chemically reacting with solids to form hydrides (metal, chemical and complex hydrides). While several prototypes of complex hydrides vessels mostly with NaAlH_4 and $\text{Mg}(\text{NH}_2)_2\text{-LiH}$ have been developed and tested with high energy densities, the complexity of the hydrogenation and dehydrogenation reactions of complex hydrides and the deficiency of reversibility presently limit potential applications. Similarly, chemical hydrides, have larger energy densities than other hydrides since they are often composed of lighter elements and can easily release hydrogen under very moderate operating conditions. For example, the hydrolysis process of sodium borohydride (NaBH_4) in an aqueous medium with a catalyst can produce a rather high theoretical hydrogen yield (10.8 wt %). Unfortunately, the use of hydrolysis for hydrogen generation on-board is limited due to the excessive heat generated during the reaction. Also, the dehydrogenation reactions are not reversible, which means that the fuels are used immediately. Furthermore, the by-products must be regenerated off-board the vehicle. Metal hydrides, on the other

hand, have been identified as one of the most viable hydrogen storage alternatives. Metal hydrides have the potential to lead to a hydrogen economy in the future.

Developments in metal hydride technology show that metal hydrides offer a high degree of safety in hydrogen storage, low energy requirements for stationary and mobile applications, low-pressure equipment, and reversibility in hydrogenation/dehydrogenation. Government policies around the world have encouraged thorough research on storage of hydrogen in metal hydrides, focusing on the application of polymer electrolyte membrane fuel cells (PEMFCs) [45].

Due to their large surface area, nanostructured materials such as nanofibers, nanotubes, and nanospheres show considerable promise for hydrogen storage, and may offer numerous benefits for physicochemical reactions such as surface interactions, quick kinetics, hydrogen atom dissociation, low-temperature sorption, and molecular diffusion with the catalyst of the surface. Nanophase materials have naturally large surface areas and exceptional adsorbing capabilities that can assist the gaseous hydrogen dissociation, and the small volume of individual nanoparticles can result in short diffusion paths to the interiors of the materials. The introduction of nanosized dopants allows for greater dispersion of catalytically active species, and consequently, for faster mass transfer reaction. Nanocomposites made of a polymer matrix and functionalized carbon nanotubes have a unique microstructure that allows physisorption of hydrogen atoms and molecules on the surface and inside the bulk. This chapter addresses hydrogen absorption and release properties for polyaniline nanospheres (conducting polymers) at ambient temperatures, as well as a brief discussion of different nanomaterials for hydrogen storage.

Hydrogen storage affects both hydrogen applications and hydrogen production, making it crucial for introducing a hydrogen economy. Fuel cell cars, today, require on-board storage of hydrogen, which is an essential part of the system that must be reengineered. The important properties to look for in materials for automotive applications are (i) light weight, (ii) affordability, (iii) high gravimetric and volumetric density of hydrogen, (iv) low temperature of dissociation, (v) ease of activation, (vi) appropriate thermodynamic properties, (vii) cycle stability in the long run, and (viii) reversibility. All of these properties necessitate a thorough understanding of the fundamental mechanistic behavior of catalyst-containing materials and their physicochemical reactions to hydrogen on an atomic or molecular level. Metal hydrides, chemical hydrides, complex hydrides, adsorbents, nanomaterials (nanofibers, nanotubes, nanospheres, nanoparticles), clathrate hydrates, metal organic frameworks, polymer nanocomposites, and so on, have all been investigated for potential hydrogen storage applications.

Still, none of the materials above meet all hydrogen storage standards, including (1) favorable thermodynamics (30–55 kJ/mol H₂), (2) high hydrogen concentration (>6.0 wt %), (3) on-board refueling for a hydrogen-based infrastructure, (4) H₂ delivery at temperatures under 100°C, (5) cyclic reversibility at mild temperatures (1000 cycles). Among the many hydrogen storage systems, the idea of nanoparticles and their vast range of applications for

energy storage is reviewed in this chapter. By raising the diffusion rate and decreasing the needed diffusion length, nanoscale and nanostructured materials have a significant impact on the kinetics and thermodynamics of hydrogen dissociation and absorption. Furthermore, materials at the nanoscale allow material tailoring to be controlled independently of their bulk counterparts. Also, they lead to the development of lighter hydrogen storage systems with improved hydrogen storage properties [160].

4.4.1 Metal Hydrides

4.4.1.1 Overview

Metal hydrides are chemisorption materials created by the interaction between atomic or ionic hydrogen and various metals (pure or alloy), in the form of metallic, covalent, or ionic bonding, achieving solid-state storage, in moderate temperatures and pressures. Thus, they have a big safety advantage over gaseous and liquid storage. The huge capacity of metal hydrides to accommodate a substantial amount of hydrogen molecules in their structures is a key contributing factor to their widespread use in the field of hydrogen storage. More atoms of hydrogen can be packed into a hydride-lattice metal, than into the same quantity of liquid hydrogen. The reason is the fact that when such metal meets gaseous hydrogen, the molecules of hydrogen are first adsorbed on the surface of the material. If enough energy is given to the system, hydrogen molecules disintegrate into hydrogen atoms, which diffuse into the bulk and fill the interstitial spaces of the metal crystal lattice, forming a solid solution with less amount of hydrogen (a phase). As more energy is applied to the system, the concentration of hydrogen increases, and a hydride phase (b phase) forms, allowing the metal to absorb larger amounts of hydrogen and growing until the metal is saturated in hydrogen. Magnesium hydride, for example, has a way higher hydrogen storage density (6.5H atoms/cm³) than hydrogen gas (0.99H atoms/cm³) or hydrogen liquid (4.2H atoms/cm³). As a result, metal hydride storage is a volume-efficient, and safe storage technology for on-board application [45, 159].

Metal hydrogenation is defined as the creation of metal hydrides by hydrogen absorption, which usually comes with the emission of heat. As hydrogen gas is absorbed by these metal particles, pressure in the tank increases up. However, equal amounts of heat must be applied to the metal hydride for the decomposition and dehydrogenation processes. Because these processes can be repeated indefinitely, reversible metal hydrides can be used to store heat and hydrogen. The hydride tank can be charged and discharged as many times as necessary as long as the hydride material does not get contaminated.

All the reversible hydrides that operate at atmospheric pressure and room temperature consist of transition metals. The electropositive elements, such as actinides, lanthanides and members of the vanadium and titanium groups, are the most reactive. According to the thermodynamics of the reaction, different temperatures need to be applied to different metal hydrides. The following is a typical example of a reversible interaction between hydrogen and a metal/alloy:



, where M is the metal (a solid solution or an intermetallic alloy), MH_x is the produced hydride, x is a positive whole number, and Q is the heat of reaction. **Figure 26** shows a simple concept of hydrogen storage in a metal hydride [45].

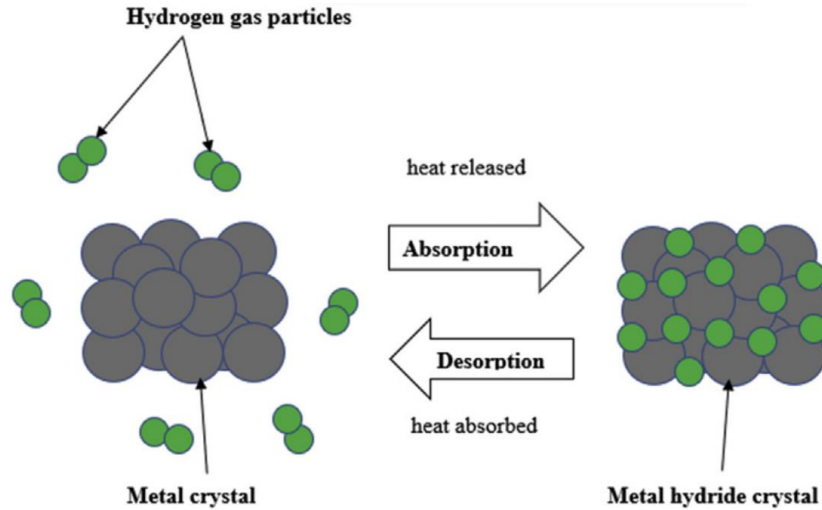


Figure 26: A simplified model of a metal hydride hydrogen storage [45].

Both kinetic and thermodynamic requirements must be met for hydrogen storage to occur. In this situation, a metal that is exposed to hydrogen gas starts to absorb hydrogen until equilibrium is established. The various reaction steps in a hydrogen-storage system may kinetically prevent it from reaching its thermodynamic equilibrium of hydrogen storage in a reasonable amount of time. Thus, the reaction rate of the metal-hydrogen systems is a function of pressure and temperature.

The metal should have the following qualities for optimal hydrogen storage:

- Low dissociation temperature
- High capacity of hydrogen per unit volume and unit mass [161].

Metal hydride hydrogen storage involves a few mechanistic processes and depends on several variables. In order to store hydrogen, the metal's surface needs to be able to dissociate the hydrogen molecule and allow easy movement of hydrogen atoms. Depending on their surface morphologies, structures, and purities, different metals have different ability to dissociate hydrogen. Based on the temperature of hydrogen absorption/desorption, metal hydrides are categorized into high-temperature hydrides and low-temperature hydrides. In low-temperature hydrides, hydrogen is bound through covalent bonding, and the metal hydride is made up of a high molecular weight material with quick kinetics and low hydrogen equilibrium pressures due to their low heat of reaction. At ambient to moderate temperatures, these metal hydrides are primarily intermetallic solid solution or alloy hydrides. In the high-temperature hydrides, on the other hand, hydrogen is ionically bonded, and the metal hydride is made up of low molecular weight material. Although the high temperature limits the types of hydrides that can be used,

high-temperature hydrides have been found to have higher hydrogen storage capacities than low-temperature hydrides.

According to several researchers, the most common hydrides for hydrogen storage at low temperatures can be classified based on the stoichiometries as AB₅-type (e.g. LaNi₅), A₂B-type (e.g. Sb₂Ti, Sn₂Co), AB₂-type (e.g. TiZr alloys), and AB type (e.g. TiFe alloys). A represents elements of high affinity for hydrogen. These are typically alkaline earth or rare-earth metal (e.g., Ca, Y, Ti, Zr, La, Hf, Ce, etc.). B represents elements of low affinity for hydrogen. It is usually a transition metal which forms only unstable hydrides (e.g., Mn, Cr, Fe, Ni, Co). However, their hydrogen storage capacity when combined is relatively low (under 2 wt %) due to the crystal structure and the unit cell volume limitation. For example, LaNi₅ is the most studied intermetallic compound for hydrogen storage because it has great hydrogen storage characteristics (kinetics, pressure and temperature requirements), but at moderate temperatures, the hydrogen storage capacity is quite low (about 1.4 wt %) and it is too expensive for on-board applications. Another well-studied intermetallic compound for storage of hydrogen is FeTi with a maximum storage capacity of around 1.9 wt%. Due to the development of an oxide layer of titanium, activating the material is difficult which makes it impossible to reproduce absorption or desorption of the maximum amount of hydrogen inside the compound without high temperatures and pressures. Therefore, current metal hydride systems are unable to store big quantities of hydrogen and the development of new metal hydrides is necessary. However, magnesium has been highly investigated as a hydrogen storage material by many researchers, because of its many advantages including lightness, resistance to heat, damping capacity, abundant availability, and low cost [45].

Conventional metal hydrides, such as LaNi₅H₆, TiFeH₂, ZrMn₂, were in the spotlight in the past decades, due to their reversibility and fast kinetics under appropriate temperature and pressure. Unfortunately, the application of these materials has been hampered by their limited gravimetric density, which is < 2 % H₂, far from the targets given by DOE, especially in the vehicular H-energy areas. This led to research for new light-metals, such as Mg, Li, N, B, Na, and Al in hydride forms, to use as solid-state storage materials. Light metal-based hydrides (e.g., Mg-based materials or complex hydrides) show great potential in on-/off-board applications, because of their great gravimetric and volumetric hydrogen densities. The H-capacity of Mg-based hydrides and complex hydrides, for example, surpasses the target given by DOE for vehicle applications, with values of 7.6 wt % (MgH₂) and 18.5 wt% (LiBH₄), respectively. However, the majority of hydrides, suffer from adverse kinetic barriers, stable thermodynamics, or low reversibility [159].

Most of the promising hydride-forming alloys and metals, such as the magnesium and magnesium-based alloys, are highly reactive and produce a surface passivation layer (SPL), which consists of metal oxides, hydroxides, water of various thicknesses, carbon-oxygen compounds, which act as a barrier and need to be broken for the hydrogen to diffuse into the surface. To enable practical uses, these materials need to be activated before their kinetics are increased to effectively desorb/absorb hydrogen. This process of activation requires

applying high temperatures or high pressures to overcome the activation barrier. The higher the barrier the more energy is required. Homogenization by complex and slow heat treatment in a vacuum is typically conducted and fresh surface becomes accessible as the SPL is broken up. Still, some of the oxidation which caused the SPL may not be reversed, leaving a part of the sample unable to uptake hydrogen. Besides, the process of the heat treatment is performed at high temperatures and pressures. All these flaws have kept metal hydrides from becoming widely used and commercialized as hydrogen storage devices for a long time [45].

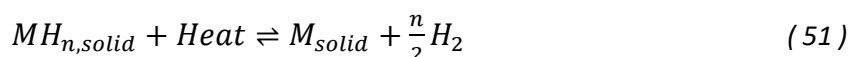
4.4.1.2 Types of Metal Hydrides

There are three different metal-hydrogen bond types, through which metal hydrides are formed: (1) metallic, (2) covalent, and (3) ionic. Metal hydrides are classified into two types based on the strength of their bonds: (1) reversible and (2) irreversible. The following **Table 11** shows some examples of reversible metal hydrides:

Table 11: Energy Content of Various Types of Metal Hydrides [161].

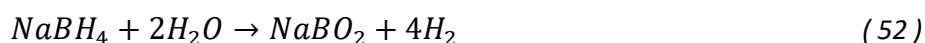
Media Type	Material	Hydride Form	H ₂ Capacity (wt%)	Energy Density (kJ/kg Hydride)	Enthalpy of Hydrogenation (kJ/mol H ₂)
AB ₅	LaNi ₅	LaNi ₅ H ₆	1.3	1,850	30.1
AB	TiFe	TiFeH _{1.95}	1.7	2,560	28.1
AB ₂	ZrMn ₂	ZrMn ₂ H ₄	1.7	2,419	53.2
A ₂ B	Mg ₂ Ni	Mg ₂ NiH ₄	7.0	10,000	64.5
Metal	Mg	MgH ₂	7.7	11,000	74.2

The reversible equilibrium reaction of reversible metal hydrides is shown below:



The forward reaction represents the hydrogen desorption or release, while the backward reaction the hydrogen adsorption or charge. For a long time, reversible hydrides have been used in hydride-based batteries. These hydrides (e.g., LaNi₅H₆ or FeTiH) are standard low-temperature hydrides, which means their dissociation pressure at room temperature is greater than 0.1 MPa. Light metal binary hydrides, on the other hand, work at high temperatures. MgH₂ is an efficient reversible heat storage material that may be applied in solar thermal systems; however, it is the least stable, with an equilibrium pressure of 0.1 MPa at 300°C. LiH and NaH, which are light alkali metal hydrides, are more stable, with decomposition temperatures over 500°C [162, 163].

According to Pant et al. [161], In irreversible metal hydrides, hydrogen is created through a chemical reaction that is difficult to reverse on-board the vehicle. As a result, the by-products are removed from the vehicle and regenerated off the vehicle. The irreversible metal hydrides can involve a transition metal like Mg₂FeH₆ (5.5 wt % hydrogen), a non-transition metal like Be(BH₄)₂ (20.8 wt % hydrogen), or NaAlH₄. The most common reactants are water or an alcohol. Sodium borohydride, for example, can produce hydrogen as:



4.4.1.3 Mg-Based Hydrides

Mg-based hydrogen storage materials have been widely researched due to unlimited amount of Mg, being ~ 0.13 wt % in seawater, and ~ 2.3 wt % in the earth crust (the 8th most abundant element). They can be fell into three categories: pure Mg, Mg-based alloys, Mg-based composites. Especially, more than 300 Mg-based alloys have been extensively investigated because of their relatively better total performance [164]. The theoretical H-capacity of the pure Mg is 7.6 wt %H₂ and 110 g H₂/L [165], and the Mg₂Ni is 3.6 wt %, respectively [159]. Besides the weight of the system, cost is low as well. Magnesium hydride, MgH₂, is inexpensive, so the high H-storage amount of this cheap and readily available host material renders it possible for large-scale applications[164].

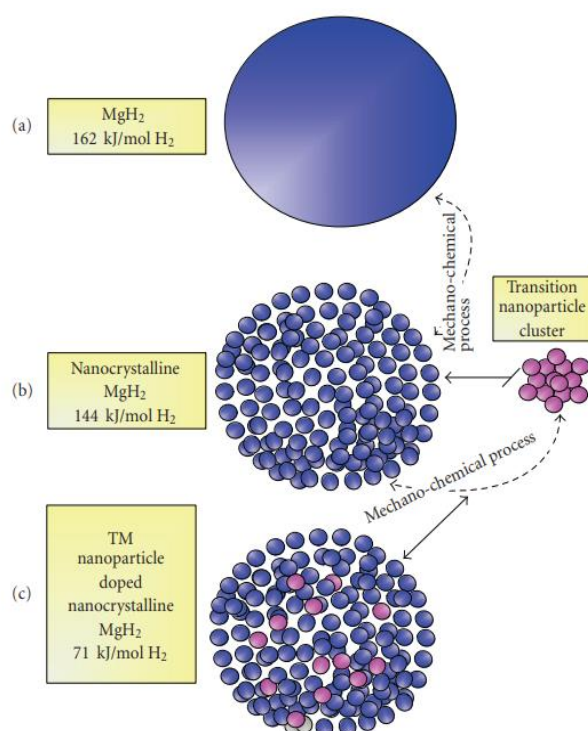


Figure 27: Conceptual model of MgH₂ cluster (a) plain, (b) nanocrystalline, and (c) nanocatalyst-doped materials [160].

However, so far, Mg hydride-based materials have little practical application due to the troublesome kinetics and thermodynamics during hydrogen absorption and desorption. For instance, in hydrogenation, high temperature and pressure of hydrogen is needed. The formation enthalpy ΔH is -74 kJ/mol and entropy ΔS is -130 J/(K·mol) H₂. In dehydrogenation, ambient temperature delivers a low pressure, about 0.1 Pa, due to the high dissociation enthalpy ΔH of 74.5 kJ/mol MgH₂. Thus, the temperature of dehydrogenation equilibrium needs to be $> 289^\circ\text{C}$ in ambient conditions to achieve pressure > 0.1 MPa. Another problem is that MgH₂, like other light metal hydrides, has slow kinetics in hydrogen absorption and desorption. Fast kinetics is important particularly in vehicular applications in order to achieve short refuelling time and appropriate rate of release of hydrogen to fulfil the power requirements when driving [161, 164, 166].

Researchers developed many methods to tailor the thermodynamics and kinetics of Mg-based hydrides for hydrogen release and uptake, such as nanostructuring, alloying with other elements, using catalyst and thin film hydride, forming composites, using different preparation techniques, destabilizing, etc. **Figure 27** shows a MgH_2 nanocluster model and the nanocatalyst distribution in the active surface sites for an efficient hydrogen storage [160].

4.4.1.4 Recent Developments in Improving Hydrogen Storage in Metal Hydrides

Researchers and developers in the field have worked hard over the last three decades to improve the kinetics of hydrogen absorption and desorption in current metal hydrides with large hydrogen storage capacities without raising the temperature. Some of the most important possible approaches that have been reported primarily involve (i) alloying with other elements, (ii) adding catalysts, (iii) nanostructuring, and (iv) nano-confinement.

4.4.1.4.1 Alloying with Other Elements

According to J.O. Abe [45], by adding other elements in the light metals, it is possible to improve the thermodynamics and kinetics of hydrogen sorption in metal hydrides. By doing that, the bond strength between the hydrogen and the metal decreases and it is known that the interphase boundary between interactions of the composite constituents plays a major role. AB_5 , AB, A_2B , and AB_2 are among the several categories of composites based on alloys of various stoichiometries that have been found to be helpful for hydrogen storage applications. Under moderate temperatures and pressures, these chemicals can also ab(de)sorb. Unlike hydride materials, the kinetic reaction of hydrogen at an alloy-based surface is feasible regardless of the occurrence of stable oxide/hydroxide layers or species which are defective in the hydrogen gas. Additionally, the crystal lattice structure of the metal hydride influences the thermal stability and hydrogen ab(de)sorption kinetics because H atoms can fill the interstitial spaces of the crystal lattice. Alloying has effects on the structure of materials which may cause the metal hydride to form various structures, affecting the mechanical properties and, thus, improving its absorption and desorption kinetics.

Transition metals are known to promote the dissociation and recombination of hydrogen so by adding small quantities of these metals could improve limited kinetics and ab(de)sorption reactions. For example, Liang et al. [167] studied the effect additions of transition metals (Ti, V, Ni, Fe, and Mn) have on sorption of hydrogen in nanocrystalline MgH_2 . In the experiment, 5% of the transition metals was ball milled with the MgH_2 alloy for 20 hours. What was observed is that all the additions of transition metals caused a decrease in the activation energy of H desorption from MgH_2 . Titanium addition exhibited the fastest absorption kinetics and vanadium addition the fastest desorption kinetics using a very small activation energy (62.3 kJ/mol), in comparison to that of MgH_2 (120 kJ/mol). Also, Fruchart et al. [168] stated that nanocrystalline compounds based on Mg and other element/elements such as vanadium, titanium and niobium are one of the most promising with vanadium giving the best performance in ab(de)sorption kinetics and reversible storage capacity. The authors worked to improve the activation problem of Mg-based hydrogen alloys for efficient H

uptake and release. First, they made the magnesium-based powder a hydride. Then they added proper amounts of BCC Ti, V and Cr or Mn-based alloy powders, mixed thoroughly and milled. H absorption was executed at 240°C and 10 bar gave up to 5.2 wt % capacity. 4.5 wt % was absorbed in about 2.5 min. On the other hand, H desorption was slower. At 260°C, 4.5 wt % of hydrogen was released in 5 min. Based on the result, the issue of slow kinetics of the Mg-based alloys was solved, but that of the high temperatures remained unresolved.

4.4.1.4.2 *Catalysis*

Catalysis is a process which enhances the hydrogen sorption kinetics in metal hydride systems by dissociating hydrogen molecules or recombining hydrogen atoms quickly and effectively. The most common catalysts used are transition metals (e.g., Ti, V, Pd, Ni, Pt, Rh, Ru, etc), metal oxides (e.g., Cr₂O₃, Nb₂O₅, TiO₂, Fe₃O₄), non-metals like carbon, and compounds. Catalyst addition can reduce the reaction energy barrier, hence accelerating the absorption and desorption rate. But the heavy transition metals are only necessary on the surface of the Mg clusters, where hydrogen gas dissociates, and not in the interior of the grains. A catalytic transition metal which can naturally migrate to the surface of clusters and coats them can ease this issue. Another serious problem is the high formation enthalpy of the hydride that can be improved through adding Cu or Ni to Mg. The desorption temperature of the Mg₂Ni alloy, for example, is around 50°C lower than the one of pure Mg, but this is still insufficient. Unfortunately, the use of heavy transition metals reduces storage capacity significantly from 7.6% to 3.6 wt % [161, 166].

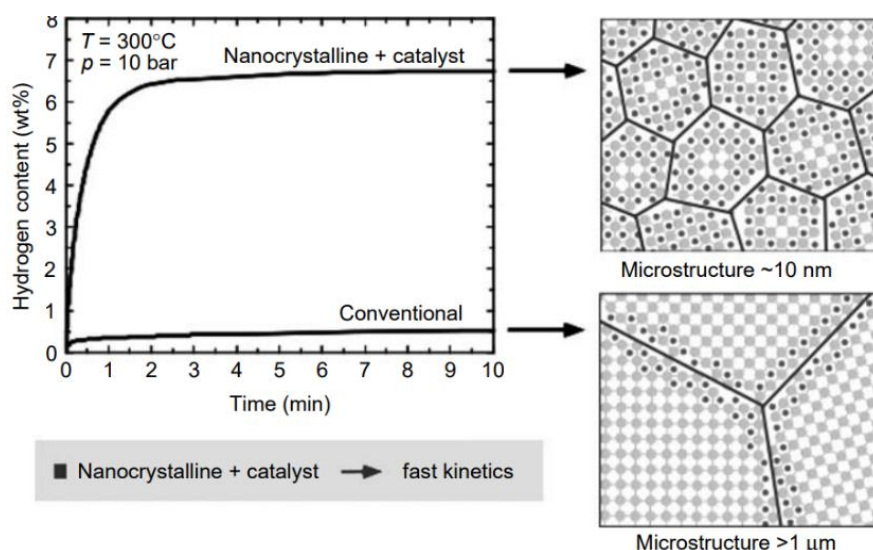


Figure 28: Hydrogen storage in reversible light metal hydrides (Reproduced from [169]).

Palladium, for example, is an excellent catalyst for metal hydrides with remarkable properties necessary for hydrogen applications because it demands little or no activation energy and has better dissociative ability, according to Adams et al. [170]. Palladium at room temperature and atmospheric pressure can absorb significant amounts of hydrogen still in its primary α -phase, and then forms Pd-hydride as more hydrogen is absorbed. The authors developed a theoretical model of MgH₂ clusters in pure, Pd-doped, and nanocrystalline forms. What they found was that Pd-doped Mg reaches the same hydrogen capacity three times faster than pure Mg.

Platinum is another potential catalytic material. Particularly, carbon-based platinum is often used in low-temperature fuel cells as electrocatalyst. However, the widespread usage of palladium and platinum remains impractical because of their prohibitive cost. Nevertheless, if proper and cost-efficient methods like alloying with cheaper metals and using nanoscale materials can be employed (see **Figure 28**), these could be very useful elements to purify hydrogen and harness hydrogen energy through fuel cells [45].

4.4.1.4.3 Nanostructuring

According to Chen et al. [171], and Yu et al. [172], stability and reactivity of metal clusters depend on their size (especially in the nanoscale range). Nanomaterials exhibit significantly different properties than the coarse-grained equivalents, owing to their short diffusion distances, large surface area, and multiplied grain boundary atoms. Nanostructuring has been shown to improve mechanical and thermal stability, thermodynamic properties, and hydrogen sorption kinetics. Development of many nanocrystalline structures with improved hydrogen absorption and desorption properties has been accomplished. Examining Mg hydrides, for example, many studies have shown that reducing the size into nanometers can increase the ratio of surface to volume, therefore simultaneously offering more nucleation sites that promote rapid hydrogen diffusion alongside the boundary of Mg and MgH₂ or internal interfaces and defects of hydrides, thus delivering quicker hydrogen diffusion path. The ideal temperature for the hydrogenation/dehydrogenation steps is a range between 50°C and 100°C. Temperatures for MgH₂ can be decreased by making a composite of small Mg crystals, which are loosely agglomerated together, rather than having a big chunk of Mg crystals. This happens because channels with smaller migration barriers for hydrogen and a lower binding energy are seemingly formed and sustained throughout the hydride, hence enabling fast loading/unloading. Some theoretical estimates and experimental results showed that the introduction of additional boundary/surface reduces the reaction enthalpy of Mg-based systems [161, 166].

High-energy ball milling is the most common method to achieve nanostructuring, since it is cost-effective and obtains good surface properties on metal hydrides. Rahmaninasab et al. [173], in a recent work, applied ball milling to create a magnesium hydride + nanostructured composite of an alloy of rare-earth elements (mischmetal) using magnesium hydride plus 6% wt. and 10 wt. % mischmetal. Ball milling was found to be effective in producing nanostructured composite with increased grain boundaries and free surface, decreased grain sizes, porous structure with high active sites on the surface for hydrogen adsorption/desorption, defects, and micro-strains on the surface and within the Mg-hydride + mischmetal grains and crystals. These defects accelerate the hydrogen diffusion into the material by reducing the diffusion activation energy, decreased crystallite sizes, enhanced kinetics, and improved sorption properties. In general, more grain boundaries are proportional to smaller crystallite sizes. Multiple interfaces and grain boundaries in nanocrystalline materials provide favourable hydrogen diffusion paths and accelerate hydrogen absorption/desorption rates [45].

4.4.1.4.4 Nanoconfinement

As mentioned above, nanostructuring is an established method for improving hydrogen sorption kinetics. Recently, a new technology of nanoconfinement has sparked interest in energy storage for the production of nanomaterials, and it has been tested on a variety of metal hydride systems. Nanoconfinement can be achieved by confining the active material within light porous scaffold hosts that need to be light for the hydrogen gravimetric storage, have a large surface area or porosity to allow high loadings, be non-reactive to avoid unnecessary reactions, be abundant, cheap, and have suitable purity, like ordered mesoporous silicas and carbon-based materials. Other scaffold materials are being studied for active storage usage like zeolites, ordered mesoporous oxides, metal-organic frameworks, and thin-film systems, but with slow progress due to their unsuitable weight and cost. Nanoscale carbon materials (e.g., nanotubes, nanofibers, nanowires, nanoribbons, and nanorods) have been gaining popularity many years now, due to their large surface areas, that promote physisorption kinetics, bulk adsorption, surface interactions, hydrogen dissociation, and desorption temperature. The nanoconfinement method has shown considerable potential in improving dehydrogenation kinetics and thermodynamics of metal hydrides, both of which are required for the reversibility of hydrogen storage in on-board applications. Nanoconfinement, added to the general impacts of nanostructuring, could also prevent particle agglomeration and phase separation in the composite system through restricting the movement of the particles within the scaffold hosts [45].

4.4.1.4.5 Altering reaction pathway

One of the most successful methods to tailor poor thermodynamics of metal hydrides is altering reaction pathway. For Mg-based hydrides, for example, one way of doing that is by alloying with Si in order to weaken the strongly bound MgH_2 , out of which forms a more stable Mg_2Si after dehydrogenation (i.e., $2\text{MgH}_2 + \text{Si} \rightarrow \text{Mg}_2\text{Si} + 2\text{H}_2$). This results in the equilibrium pressure which ranges from 1.8 bar to >7.5 bar at 300°C. The dehydrogenation enthalpy of the MgH_2 -Si system is decreased from 75.3 kJ/mol to 36.4 kJ/mol H_2 , and the H-capacity is ~5.0 wt % H_2 . Unfortunately, it was found that the MgH_2 -Si composite suffers from slow kinetics and poor reversibility [166].

4.4.1.5 Applications

Metal hydrides is an excellent choice for storing hydrogen in cases where space is limited. Hydrogen stored in metal hydrides occupies one-third of the volume, compared to the typical high-pressure cylinders. Additionally, the pressure of absorption and desorption is just 1–25 bar, as opposed to the cylinder storage pressure of 200 bar. Fuel candles of metal hydride are used in handheld burners. Usage of couples of metal hydride alloys with different plateau pressures, makes it possible to now realize applications of thermal engineering like refrigeration and air conditioning, heat transformer, heat pump, and solar heat harvest system. The hydrogen produced by metal hydrides has a high purity (usually >99.9%), making it suitable for a wide range of applications. Metal hydrides can be employed to load-level electric supply and demand in large-scale stationary applications. At

low demand, the hydride is charged, and at high demand, more electricity is provided by utilizing the hydrogen stored [161].

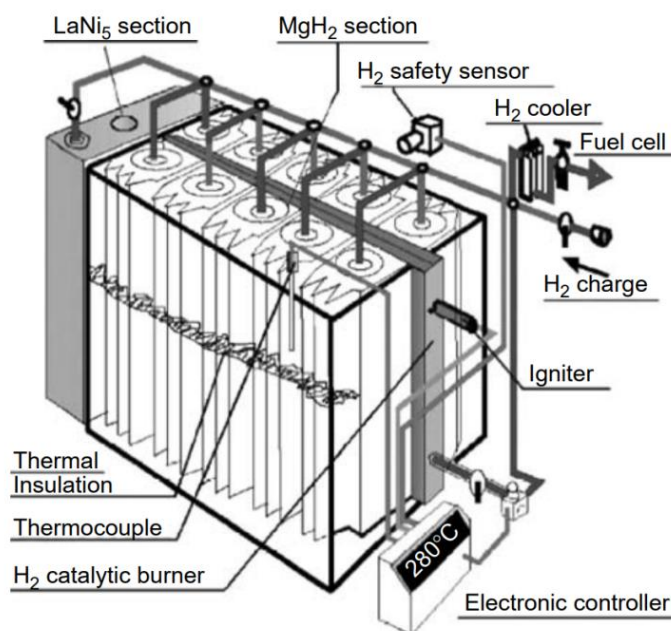


Figure 29: Schematic of a two-stage metal hydride reservoir [161]

Batteries is the most common application of hydrogen storage metal hydrides. Nickel–metal hydride (Ni-MH) type, which is activated or charged with hydrogen is a hydride-forming alloy. Several hydriding and dehydriding cycles occur during the battery's lifespan. Portable electronics and computers, such as power tools and cell phones, typically employ Ni-MH batteries. They are also being utilized in hybrid vehicles. Ni-MH batteries both supply and draw energy from the gas motor, not needing a separate recharging station. Hydrogen loading for automotive applications must be done quickly (within 5 min) and at a temperature close to ambient. The storage can be configured for hydrogen usage in both internal combustion engines (IC) and fuel cells. A fuel cell vehicle is almost 2.5 times more efficient than an internal combustion engine. The energy efficiency of an internal combustion engine is only 25%, opposing to a fuel cell with a (DC) direct current motor, which is almost 80% [162, 174, 175].

However, a hydride with a storage capacity of at least 9.1 wt % is required, so only hydrides with the best possible gravimetric storage capacity are viable for vehicular use. Practical metal hydrides can store a maximum of 3.5 wt % H₂ that is insufficient for automobile applications due to the inconvenience of carrying the heavy metal while transit. It will be difficult to realize commercial use of metal hydrides in automotive applications unless a storage level of 6 wt % H₂ is reached. As a result, complex materials like alanates of magnesium or sodium are being investigated. However, to release hydrogen, Mg-based alloys need a high temperature (300°C), which necessitates the use of a heating equipment and the associated energy cost [176, 177].

Metal hydride hydrogen storage tanks resemble heat exchangers. Thermal jackets or conduits must be used as a heat transfer medium to cool and heat the material. Heat wasted from the engine, or the fuel cell coolant is used to provide heat during discharge. The heat causes hydrogen desorption, resulting in a pressure that feeds the fuel cell. The bed is connected to a source of hydrogen gas during refuelling and is cooled by an external or internal coolant. For speedy absorption and refuelling, high pressure and rapid cooling are required. **Figure 29** depicts a typical design for a metal hydride reservoir prototype[176].

The main stage is made up of containers filled with doped MgH_2 , while the primer stage contains $LaNi_5$. The flow of hydrogen from the main-stage reservoir to the fuel cell and the continuous refilling are electronically controlled. The hydrogen burner stage, which is part of the main stage, contains two supply inlets: for hydrogen and air [161]

Figure 30 depicts a metal hydride-based fuel cell-powered system in which the vehicle's original gasoline engine power train has been replaced by an electric motor and a hydrogen fuel cell. The system is consisted of the hydrogen storage system, the fuel cell stack, the air loop, the water loop, and the coolant loop.

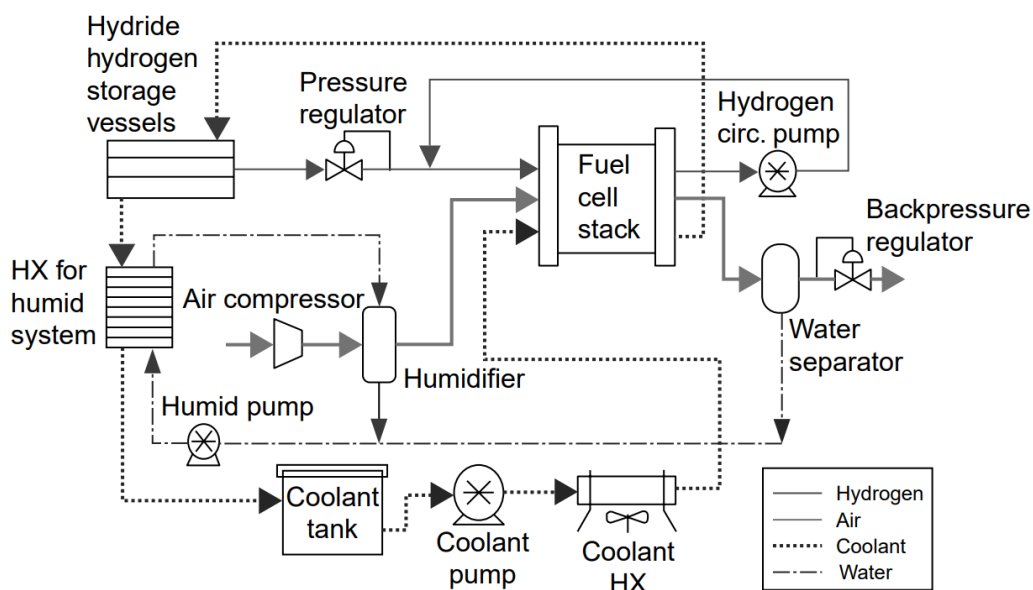


Figure 30: Metal hydride hydrogen-fuel-cell-powered system [161].

During operation, the fuel cell stack coolant heats the metal hydride system, resulting in a discharge pressure of 0.2 to 2 MPa. Ahluwalia [39] investigated if Ti-catalyzed sodium alanate is a reversible storage medium of hydrogen for automotive polymer-electrolyte FCs under the constraint of meeting certain performance criteria such as the amount of recoverable H_2 required for vehicle driving range, minimal full-flow requirement, minimum H_2 -delivery pressure, and maximum refuelling time.

According to the findings, a 10-fold improvement of published desorption kinetics is required to achieve 90% reversible H_2 storage capacity while meeting the minimal full-flow requirement of 0.02 g H_2 /kW. The higher the peak heat transfer rate and the lesser the

amount of recoverable H₂, the faster the refuelling rate is. The maximal heat transfer rate during refuelling for a system with 5.6 kg recoverable H₂ can surpass 1 MW [178].

4.4.1.6 Challenges

The main challenge in using hydrogen as an automotive fuel is the development and demonstration of a practical hydrogen storage technology. Low-cost, off-board hydrogen storage solutions are required to support hydrogen infrastructure in the stationary, transportation, and portable power markets. The following are the key technical obstacles to using metal hydrides for hydrogen storage [161]:

1. **Cost.** Low-cost materials and components, as well as low-cost, high-volume manufacturing methods, are desired for hydrogen storage systems.
2. **Weight and volume.** There is a need for materials and components that enable compact and lightweight hydrogen storage while allowing a driving range of 500km for automobiles.
3. **Efficiency.** It takes a lot of energy to absorb/desorb hydrogen in the metal hydride. To improve total efficiency, releasing hydrogen from the storage system and thermal management for charging must be optimized.
4. **Durability.** Materials with a lifetime of 1500 cycles and tolerance to fuel impurities are required.
5. **Refuelling time.** Development of hydrogen storage systems with refilling times of less than 3 minutes for 5 kg of hydrogen is needed.

Metal hydrides have the ability to store up to 12 wt. % hydrogen which is higher than any other solid storage method. However, these metal hydrides are heavy, and in order to break the ionic connections to release the hydrogen they require a lot of energy and high temperatures. Metal hydrides that are currently useable can only hold 1.8 wt. % hydrogen.

Figure 31 shows a typical hydrogen content that can be obtained using several approaches.

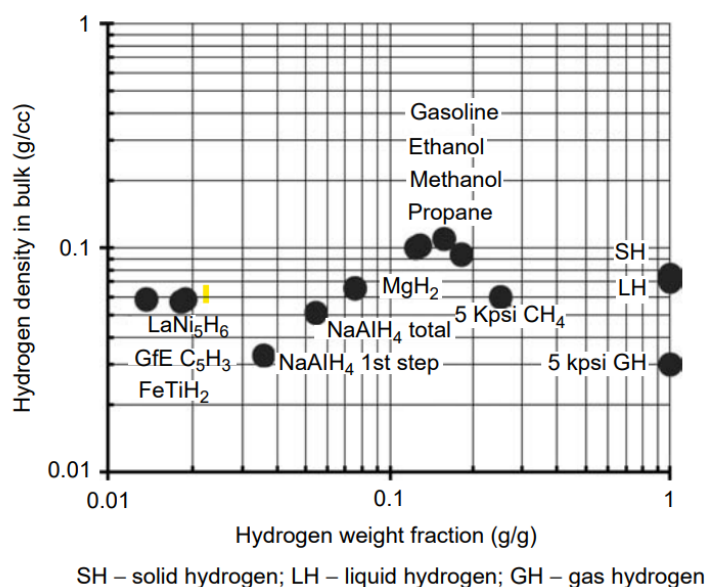


Figure 31: Hydrogen content in various storage options (Adapted from [178]).

Also, light solids like magnesium and sodium aluminum hydride have a high hydrogen weight ratio but a low volumetric density.

The metal hydride absorbs hydrogen in an exothermic process, therefore the sluggish heat removal during refuelling becomes a controlling issue. Another issue with the usage of metal hydride is the container size. A hydrogen-powered car consumes about 1.2 kilogram of hydrogen per 100 kilometres. Metal hydrides require an excellent heat management system due to the high heat of hydrogen absorption/desorption, which adds to the weight. By adding catalyst and producing nanostructures, storage qualities like as temperature, pressure, and rate of absorption/desorption are improved [161].

4.4.2 Complex/Chemical Hydrides

4.4.2.1 Overview

In addition to metal hydrides, complex and chemical hydrides (see **Figure 32**), have been studied for on-board hydrogen storage applications. Complex hydrides, such as $[\text{AlH}_4]^-$ (alanates), $[\text{BH}_4]^-$ (borohydrides), and $[\text{NH}_2]^-$ (amides) are made up of an alkali or alkaline earth metal cation and a coordination complex anion with the hydrogen covalently bound to the central atom (Al, B, N, etc.).

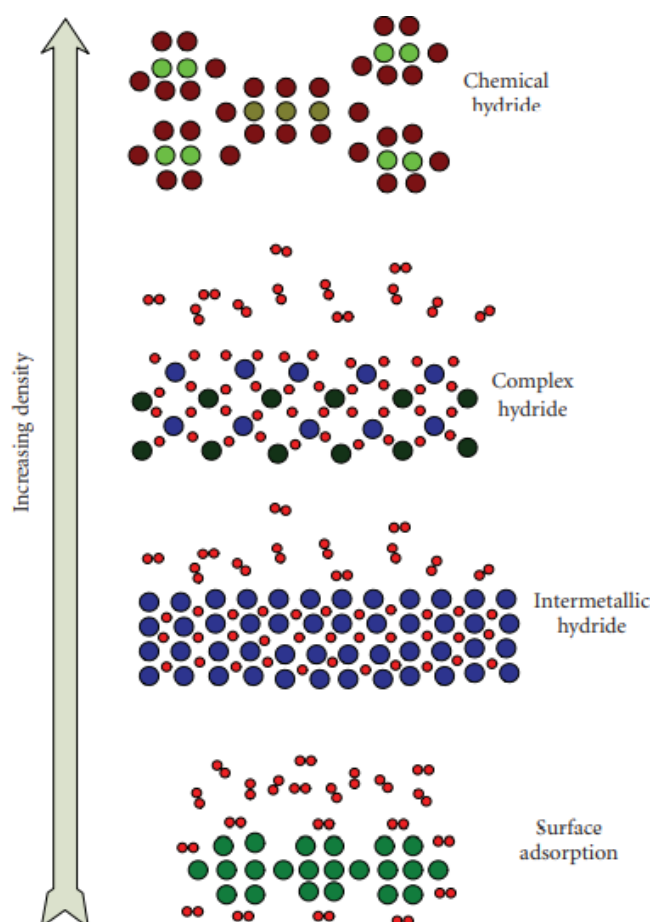


Figure 32: Hydrogen storage density in physisorbed materials, metal/complex, and chemical hydride [160].

Complex hydrides have been in the spotlight as solid-state hydrogen materials over the last few decades, in comparison to Mg-based compounds and other classic metal hydrides. Their potential hydrogen densities are unparalleled, making them promising candidates for a range of on/off-board hydrogen storage applications. Hydrolysis or thermolysis could be used to achieve hydrogen supply. Hydrolysis provides precisely regulated hydrogen release, a mild working temperature, high purity H₂, and more benefits, when compared to thermolysis. The hydrolysis reactions, however, are irreversible and cannot be used in rechargeable hydrogen storage devices.

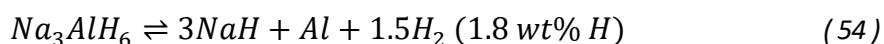
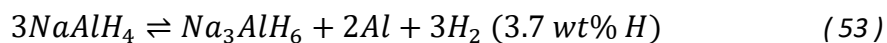
Similarly, the difficulties in absorption of reversibly hydrogen pyrolysis products under moderate temperatures makes vehicular commercial application impossible. Not until 1997, when Bogdanovic et al. [179] discovered that the reversible hydrogen sorption and desorption reaction of NaAlH₄ can be improved by adding a small amount of titanium-based catalysts such as TiCl₃. Then, P. Chen et al. [180] in 2002, discovered reversible nitrogen-based complex hydrides, such as LiNH₂-Li₂NH-LiH, while A. Zuttel, et al. [181], in 2003, were the first to study metal tetrahydroborates, such as LiBH₄ [159, 182].

4.4.2.2 Types of Complex/Chemical Hydrides

4.4.2.2.1 *Alانات (LiAlH₄, NaAlH₄, and Mg(AlH₄)₂)*

Alانات, is one of most typical categories of complex hydrides. They are made up of a metal cation and a tetrahedron [AlH₄]⁻, connected through the ionic bond (the four H-atoms are bonded covalently to an aluminum atom in the centre). Some examples of alانات are LiAlH₄, NaAlH₄, and Mg(AlH₄)₂, etc. **Figure 33** shows the crystal structures of the above alانات, where Li cations are surrounded by five isolated [AlH₄]⁻ tetrahedral, Na atoms by eight [AlH₄]⁻ tetrahedral, and Mg(AlH₄)₂ has four-coordinated Al and six-coordinated Mg in a distorted MgH₆ octahedral geometry[159]. **Table 12** shows gravimetric and volumetric H₂ densities and the standard heat of formation of alانات. The theoretical gravimetric and volumetric H₂ densities are 4.3-7.9 wt % and 2.7-3.7 kg H₂/100 L, respectively. KAlH₄ can also desorb and absorb hydrogen reversibly. The heat of formation of KAlH₄ is -84.9 kJ/mol H₂, which mean that it is a stable hydride [182].

Sodium alانate (NaAlH₄), with a reversible storage capacity of roughly 5.5 wt %, is a promising material for hydrogen storage. It is a recognized complex hydride with good thermodynamics and a suitable gravimetric storage capacity to use it in a polymer electrolyte membrane (PEM) fuel cell system operating at around 90°C. The inclusion of titanium and/or zirconium dopants improves the reversibility kinetics of NaAlH₄, resulting in a substantial reduction in the primary crystal size. Sc-doped NaAlH₄ has comparable kinetics and a larger hydrogen storage capacity than Ti-doped NaAlH₄, depending on the temperature, cycle, and the metal dopant amount. The elemental segregation of Na and Al in particles after many absorption/desorption cycles could explain the low absorption capacity. Hydrogen is released from NaAlH₄ in two steps:



So, NaAlH₄ decomposes to produce molecular hydrogen and the intermediate product Na₃AlH₆, which then decomposes to produce NaH and more metallic aluminum and hydrogen. The first reaction is thermodynamically advantageous and can release 3.7 wt % hydrogen at ambient pressure and at 33°C, and the second reaction takes place above 110°C, releasing an additional 1.8 wt. % hydrogen. Rehydrogenation should be carried out at a pressure of 10 MPa and at a temperature of just above 100°C. At higher temperatures, the kinetics are faster, but this is countered by an increase in the hydrogen equilibrium pressure as temperature rises. As a result, a balance between fast rate and proximity to equilibrium must be found.

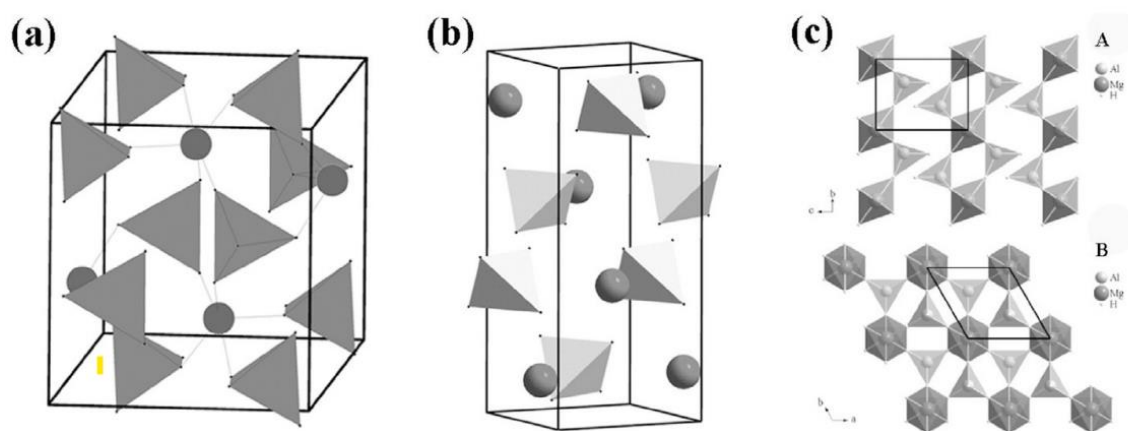


Figure 33: The crystal structures of (a) LiAlD₄, where Li cations are surrounded by five isolated [AlD₄] - tetrahedra. Copyright 2002 Elsevier; (b) NaAlD₄, in which Na atoms are surrounded by eight [AlH₄] - tetrahedra in a distorted square antiprismatic geometry. Copyright 2003 Elsevier; (c) Mg(AlH₄)₂, showing six-coordinated Mg and four-coordinated Al in a distorted MgH₆ octahedral geometry. Views along (A) the a-axis and (B) the c-axis. Copyright 2005 Elsevier [159].

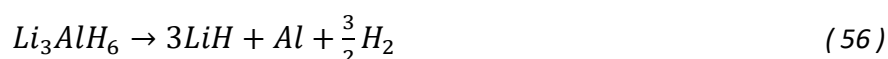
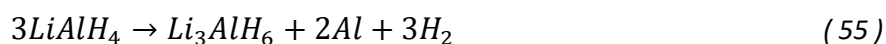
Wang et al. [183] showed that graphite cocatalyst with Ti has an effect on both the dehydrogenation and hydrogenation kinetics of NaAlH₄ over a wide temperature range (90–250°C). Co-doping of 2 mol% Ti-doped NaAlH₄ with 10 wt % graphite, for example, significantly enhanced the kinetics of the first and second hydrogen evolution events by lowering the dehydrogenation temperature over the critical range of 90–150°C by as much as 15°C compared to the control. Similarly, adding graphite to a sample doped just with Ti improved the dehydrogenation kinetics at 90°C and 110°C by factors of 6.5 and 3.0, respectively, when compared to a sample doped only with Ti [161].

Only NaAlH₄ offers good thermodynamic characteristics for hydrogen storage among the well-researched alanates. For instance, kinetically stabilized LiAlH₄, due to thermodynamic instability, decomposes immediately under room temperature. Lithium alanates appear to be appealing for hydrogen storage, because of their high hydrogen content.

Table 12: Density, H₂ densities & standard heat of formation of complex hydrides.

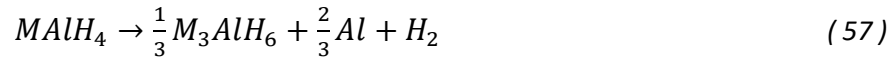
Complex Hydrides	Density g/cm ³	Gravimetric density wt% ^a	Volumetric density kgH ₂ /100L ^b	Standard heat of formation ΔH ⁰ /kJ/kmolH ₂
Alانات				
LiAlH ₄ → LiH + Al + 3/2H ₂	0.917	-(7.97)	-(3.65)	-14.6
NaAlH ₄ ⇌ NaH + Al + 3/2H ₂	1.24	4 (5.60)	2.5 (3.47)	-35
KAlH ₄ ⇌ KH + Al + 3/2H ₂	1.25	3.5 (4.31)	2.2 (2.70)	-84.9
Mg(AlH ₄) ₂ → MgH ₂ + 2Al + 3H ₂	1.05	-(7.01)	-(3.68)	-14
Ca(AlH ₄) ₂ → CaH ₂ + 2Al + 3H ₂	1.17	-(5.92)	-(3.46)	-13
Borohydrides				
LiBH ₄ ⇌ LiH + B + 3/2H ₂	0.66	-(13.9)	-(4.58)	-66.9
NaBH ₄ → Na + B + 2H ₂	1.07	10 (10.7)	5.4 (5.70)	-108
Mg(BH ₄) ₂ ⇌ MgH ₂ + 2B + 3H ₂	0.78	6.1 (11.2)	2.4 (4.37)	-57
3Ca(BH ₄) ₂ ⇌ 2Ca ₂ H ₂ + CaB ₆ + 10H ₂	1.12	5.8 (9.63)	3.2 (5.39)	-53
				^a Theoretical value ^b Packing ratio: %

LiAlH₄ and Li₃AlH₆ have total hydrogen concentration of 10.5 and 11.2 wt. %, respectively. Unfortunately, even at ambient temperature, LiAlH₄ has an unusually high hydrogen equilibrium pressure. LiAlH₄ is a highly unstable hydride that easily decomposes but cannot be rehydrogenated. Its desorption occurs in two stages:



The decomposition of LiAlH₄ and Li₃AlH₆ releases 5.3 and 2.65 wt % of total hydrogen, respectively, at temperatures between 160°C and 200°C. After the reaction, about 2.65 wt% of the total hydrogen content in LiAlH₄ remains unreleased in the form of LiH, which can only be desorbed at very high temperatures (680°C). Thus, commercializing lithium-based compounds is difficult due to their slow kinetics and the requirement for high-temperature [161].

A great feature of alانات is the fact that both sodium and lithium salts are commercially available. Additionally, to synthesize Mg(AlH₄)₂, a metathesis reaction between NaAlH₄ and MgH₂ can be used. Nevertheless, alkali metal alانات release hydrogen at a relatively high temperature due to their innate nature of mixing both ionic and covalent bonds. For example, NaAlH₄ does not begin to release hydrogen until it reaches a temperature of over 220°C. Also, the hydrogen desorption of MAlH₄ (where M is Na, Li, K) is a complex and multi-step process (eqs (57)-(59)) that begins with the melting of the hydride and the tri-alkali metal, with hexahydroaluminate (M₃AlH₆) as an intermediate.



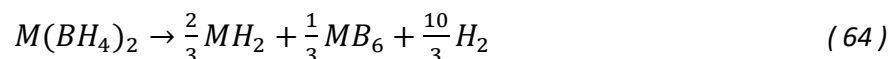
Because of its extraordinarily high decomposition temperature, MH may be improper for use as a hydrogen storage material in practical vehicles. But efforts are being made, including catalysis, nanostructuring, and composite systems in order to overcome the challenges of hydrogen thermodynamics and kinetics in sorption and desorption [159].

4.4.2.2 Borohydrides ($LiBH_4/NaBH_4/Mg(BH_4)_2$)

Borohydrides are complex hydrides which are stable and based on the standard heat of formation value. The reactions of hydrogen desorption in borohydrides are very attractive for hydrogen storage materials, due to their high hydrogen density (>9.6 wt %). In **Table 12**, gravimetric/volumetric densities, as well as the heat of formation of borohydrides are shown[182]. All elements in the boron group produce polymeric hydrides $(MH_3)_x$, as the MH_3 monomers are unstable strong Lewis acids. Borane (BH_3) dimerizes into diborane, which achieves electronic saturation (B_2H_6) [161]. Light-metal borohydrides, such as $LiBH_4$, $Mg(BH_4)_2$, and $NaBH_4$, have a larger theoretical hydrogen content (>10 wt % H_2 , see **Table 12**) than alanates. Light-weight metal borohydrides are one of the best solid hydrogen materials, due to their extraordinary hydrogen densities, which far exceed the DOE's target of 6.5 wt % [159]. The hydrogen storage capacity of the reversible lithium tetrahydroborate ($LiBH_4$) is 18.4 wt%, which is the largest gravimetric storage capacity of all the complex hydrides[181, 184]. In $LiBH_4$ the end products are B and LiH, and the absorption of H_2 happens at 963 K and 20 MPa, forming $LiBH_4$ [182]. The crystal structures of some borohydrides are demonstrated in **Figure 34**, with the high- and the low-temperature phases of $LiBH_4$ being orthorhombic and hexagonal, respectively, the structure of $NaBH_4$ being cubic, and the one of $Mg(BH_4)_2$ hexagonal [159]. According to Orimo et al. [185], the decomposition reaction of alkali metal borohydrides is:



However, thermodynamic properties of these materials are not useful for mobile storage applications. Except for hydrolytic storage, in which hydrides are more stable than the equivalent alanates. According to Ouyang et al. [159], the thermal processes of decomposition of alkaline earth borohydrides are the following:



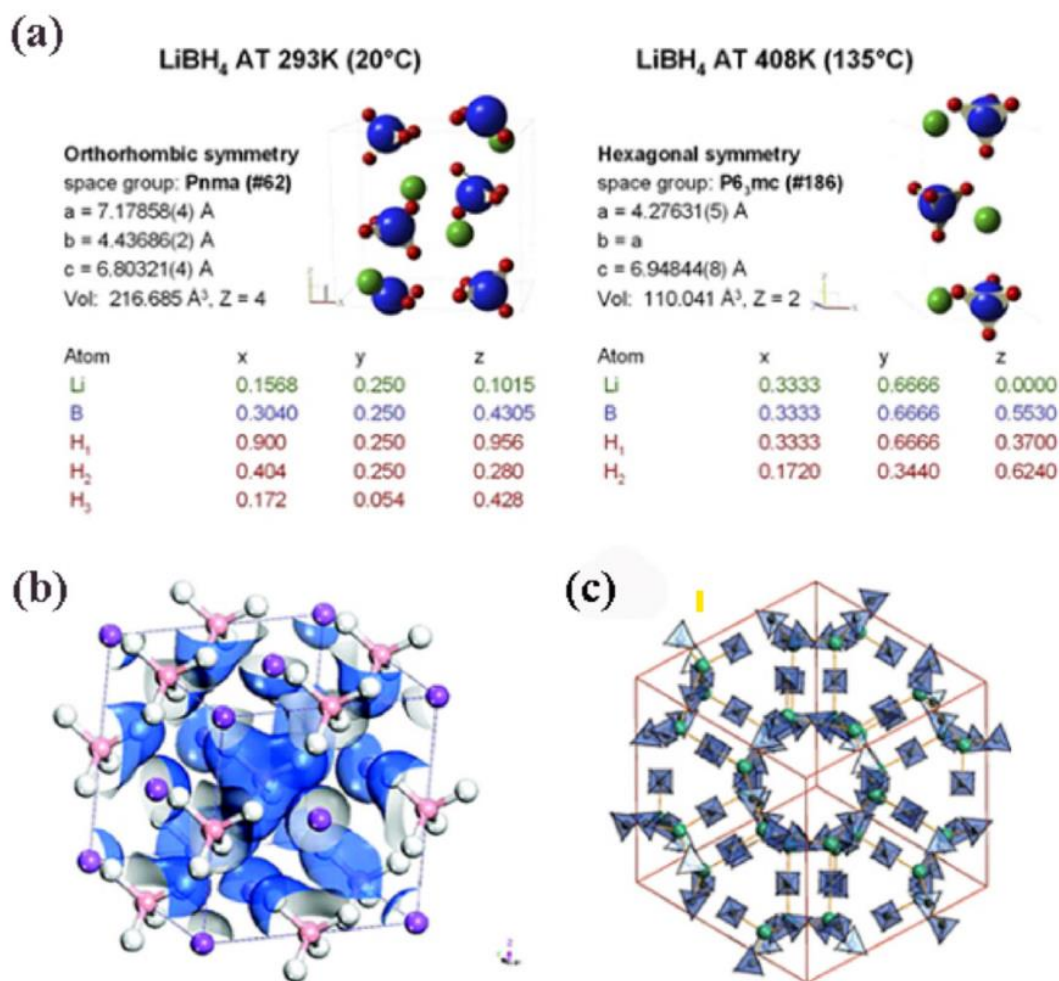


Figure 34: (a) Low- and high-temperature structures of LiBH₄ determined from XRD. Blue, green, and red spheres represent boron, lithium, and hydrogen, respectively. Copyright 2007 Elsevier. Crystal structure of cubic (b) α -NaBH₄. Copyright 2010 ACS Publications, (c) γ -Mg(BH₄)₂ [159].

Another problem is that it is possible for some toxic borane to develop, which can damage consequent aggregates in a fuel cell system, resulting in a decrease of storage capacity over time. Above 320°C, LiBH₄ begins to thermally decompose, with the major decomposition happening above 400°C. Typically, the total amount released is around half of the theoretical capability. According to Zuttel et al.[181], adding SiO₂ powder can lower the onset temperature of decomposition and allow for the release of 9 wt % hydrogen below 400°C. In theory, decomposing stable hydrides could become an easier process, by adding compounds which form stable complex either with the boron produced from the borohydride decomposition or with the produced LiH, thereby giving an extra thermodynamic driving force [184].

4.4.2.2.3 *Alane (AlH₃)*

Because of its high hydrogen capacity of 7.47 kgH₂/100 L (10.1 wt %), aluminum hydride, also known as "alane", is an appealing covalent hydride to use hydrogen storage. However, the reversibility requires GPa-scale H₂ pressure $\Delta H^0 = -6.6, -7.6$ kJ/mol H₂, AlH₃, so it is a thermodynamically unstable material [182].

4.4.2.2.4 Amides ($\text{LiNH}_2/\text{NaNH}_2/\text{Mg}(\text{NH}_2)_2$)

There have been fewer investigations on amides as H storage materials, in comparison to alanates and borohydrides, owing to NH_3 development during heat decomposition. In organic chemistry, alkali-metal amides are being utilized as reagents. Chen was the first to announce the possibility of Li_3N as a reversible hydrogen material in 2002, which sparked a lot of interest in amides as solid hydrogen carrier. Using amides and hydrides, scientists and researchers have created a variety of complex hydrogen storage systems. **Table 13** summarizes some common composites and their hydrogen content theoretically. A recent review could provide detailed information on the de-/rehydrogenation performance of amide-based hydrides systems [159].

Table 13: Hydrogen release and uptake properties of some metal N-H systems.

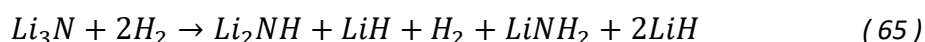
Systems	Reaction mechanism	Theoretical H content (wt %)
$\text{LiNH}_2\text{-LiH}$	$\text{LiNH}_2 + 2\text{LiH} \rightleftharpoons \text{Li}_3\text{N} + 2\text{H}_2$	10.3
	$\text{LiNH}_2 + \text{LiH} \rightleftharpoons \text{Li}_2\text{NH} + \text{H}_2$	6.5
$\text{LiNH}_2\text{-MgH}_2$	$2\text{LiNH}_2 + \text{MgH}_2 \rightarrow \text{Li}_2\text{Mg}(\text{NH})_2 + 2\text{H}_2 \rightleftharpoons \text{Mg}(\text{NH}_2)_2 + 2\text{LiH}$	5.6
	$2\text{LiNH}_2 + \text{MgH}_2 \rightarrow \text{Mg}(\text{NH}_2)_2 + 2\text{LiH} \rightleftharpoons \text{Li}_2\text{NH} + \text{MgNH} + 2\text{H}_2$	5.6
$\text{LiNH}_2\text{-LiBH}_4$	$2\text{LiNH}_2 + \text{LiBH}_4 \rightleftharpoons \text{Li}_3\text{BN}_2 + 4\text{H}_2$	11.9
$\text{LiNH}_2\text{-LiAlH}_4$	$2\text{LiNH}_2 + \text{LiAlH}_4 \rightleftharpoons \text{Li}_3\text{AlN}_2 + 4\text{H}_2$	9.6
$\text{Mg}(\text{NH}_2)_2\text{-LiH}$	$\text{Mg}(\text{NH}_2)_2 + 8/3\text{LiH} \rightleftharpoons 1/3\text{Mg}_3\text{N}_2 + 4/3\text{Li}_2\text{NH} + 8/3\text{H}_2$	6.9
	$\text{Mg}(\text{NH}_2)_2 + 4\text{LiH} \rightleftharpoons 1/3\text{Mg}_3\text{N}_2 + 4/3\text{Li}_3\text{N} + 4\text{H}_2$	9.1
$\text{Mg}(\text{NH}_2)_2\text{-MgH}_2$	$\text{Mg}(\text{NH}_2)_2 + 2\text{MgH}_2 \rightleftharpoons \text{Mg}_3\text{N}_2 + 4\text{H}_2$	7.4
	$\text{Mg}(\text{NH}_2)_2 + \text{MgH}_2 \rightleftharpoons 2\text{MgNH} + 2\text{H}_2$	4.9
$\text{NaNH}_2\text{-NaBH}_4$	$2\text{NaNH}_2 + \text{NaBH}_4 \rightleftharpoons \text{Na}_3\text{BN}_2 + 4\text{H}_2$	6.9
$\text{NaNH}_2\text{-NaAlH}_4$	$\text{NaNH}_2 + \text{LiAlH}_4 \rightleftharpoons \text{NaH} + 0.67\text{Al} + \text{LiAl}_{0.33}\text{NH} + 2\text{H}_2$	5.2

4.4.2.2.5 Ammoniates of Borohydrides

Various ammine complexes of borohydrides, such as $\text{LiBH}_4 \cdot \text{NH}_3$ ($x = 1-4$), $\text{M}(\text{BH}_4)_2 \cdot 2\text{NH}_3$ ($\text{M} = \text{Mg}, \text{Ca}, \text{and Zn}$), $\text{Mg}(\text{BH}_4)_2 \cdot 6\text{NH}_3$, $\text{Mg}(\text{BH}_4)_2 \cdot 2\text{NH}_3\text{-MgH}_2$, $\text{Ca}(\text{BH}_4)_2 \cdot \text{NH}_3$ ($x = 1, 2, \text{and } 4$), and $\text{Al}(\text{BH}_4)_3 \cdot 6\text{NH}_3$, have recently been developed, inspired by the $\text{Mg}(\text{BH}_4)_2 \cdot 2\text{NH}_3$ system, in which the hydrogen evolution is forced through the combination of H^- and H^+ starting at $\sim 120^\circ\text{C}$. $\text{LiBH}_4 \cdot \text{NH}_3$ has the highest hydrogen density (~ 18 wt %) among these ammoniates of borohydrides, with a peak emission temperature of 280°C . However, at lower temperatures, the coordinate bond $\text{N} \rightarrow \text{Li}^+$ in $\text{LiBH}_4 \cdot \text{NH}_3$ is easily broken, releasing ammonia. Guo et al. [186], used MgCl_2 , ZnCl_2 , and AlCl_3 to create stable metal ammonia complexes and restrict ammonia release, improving hydrogen desorption from the ammoniate. Particularly, by 150°C the $\text{AlCl}_3/\text{LiBH}_4 \cdot \text{NH}_3$ composite can release

the majority of H₂. Al(BH₄)₃·6NH₃, another promising complex hydride with long-term air stability and an optimum H-capacity of 17.4 wt %, is only slightly inferior to LiBH₄·NH₃[187]. Al(BH₄)₃·6NH₃ was found to be capable of releasing over 10 wt % H₂ at temperatures below 140°C. They also discovered that the dehydrogenation of Al(BH₄)₂·xNH₃/LiBH₄ composites can be adjusted by changing the coordination number and by doping mixed cations[188], with Al(BH₄)₂·4NH₃-LiBH₄ releasing almost 12 wt % pure H₂ at 120°C. Tang et al.[189] looked at the dehydrogenation properties of Al(BH₄)₃·6NH₃ when it was combined with various metal borohydrides M(BH₄)_n (M = Li, Na, Mg, Ca) and chlorides MCl_n (M = Ni, Sc, Zn, Cu, Ca, Mg, Li). They discovered that adding metal cations significantly improved dehydrogenation kinetics, with 0.5 Mg(BH₄)₂/Li₂Al(BH₄)₅·6NH₃ releasing more than 10% high-purity H₂ in 30 minutes at below 120°C. However, the difficulty in regenerating borohydride ammoniates limits their use as mobile hydrogen carriers, despite the fact that they may release large amounts of hydrogen at low temperatures [159].

Chen et al. [180] studied the hydrogen absorption of a lithium nitride Li₃N, in which Li₃N undergoes the following reaction:



,at a packing density of 0.635 g/cm³, the reversible hydrogen storage densities are 11.5 wt % and 7.35 kgH₂/100 L [ΔH^0 : 81kJ/molH₂] (Li₃N+2H₂ →LiNH₂+2LiH) [180].

Ammonia borane (NH₃BH₃) is another solid material suitable for hydrogen storage due to its high hydrogen capacity of 19.6 wt % (volumetric density: 7.64 kgH₂/100 L and packing density: 0.39 g/cm³). It is also highly stable under ambient conditions, nontoxic, and highly soluble in common solvents. Hydrolysis of ammonia borane seems to be the most efficient way to release hydrogen stored in it. Because ammonia borane is quite stable against hydrolysis in an aqueous solution, the hydrolytic dehydrogenation at room temperature can only be achieved in the presence of an appropriate catalyst [190]. After desorption of hydrogen from ammonia borane, spent fuel (polyborazylene) could convert back to ammonia borane if put in liquid ammonia with hydrazine. Many kinds of AB-based materials have been synthesized, such as NaH-NH₃BH₃ (H₂: 5.2 wt %), NaNH₂BH₃ (H₂:7.5 wt %), and LiNH₂BH₃ (H₂:10.9 wt %) [182].

4.4.3 Nanoporous Carbon Materials

4.4.3.1 Overview

The development of innovative storage systems with bigger capacity, lighter weight, and greater stability have been the main objectives of many technological initiatives, particularly in the fields of portable devices and moving vehicles. As a result, it has become clear that a secure, efficient, and cost-effective storage system is required for the future use of hydrogen as a clean energy carrier. Metal hydrides have the upper hand in terms of safety, but they fall short when the weight of the tank system is considered. Carbon materials could overcome this hurdle, due to their low atomic weight and microporous character that adsorbs un-dissociated H-molecules at their surface via van der Waal's forces. Hydrogen storage capacities, synthesis, and techniques

to improve storage capacity of some kinds of carbon materials, like activated carbons, graphite, fullerene, carbon nanotubes, and carbon nanofibers, are covered in this chapter [191].

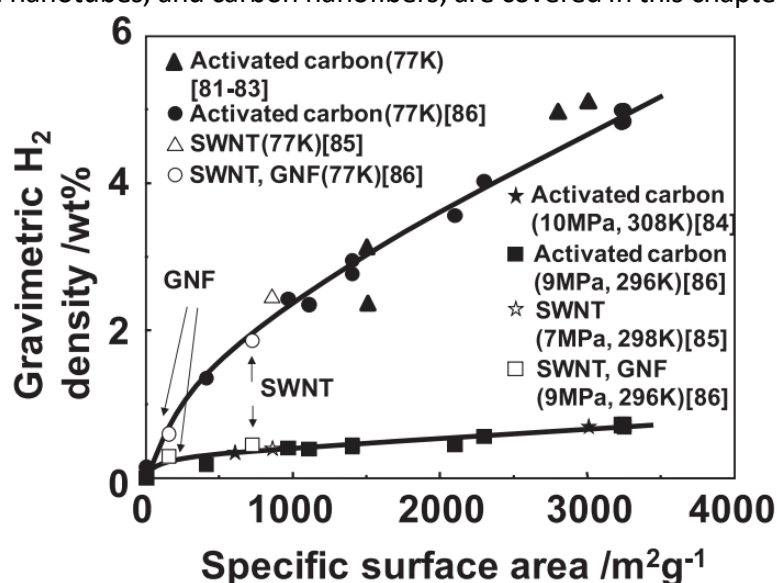


Figure 35: H₂ absorption capacities at 77 and 296-308K as a function of surface area of carbon materials [182].

Materials with a large specific surface area appear to be promising for storing hydrogen. In **Figure 35**, gravimetric H densities of several carbon nanostructures are demonstrated with their specific surface area. For activated carbons, single-walled carbon nanotubes (SWNT), and graphite nanofibers (GNF), the association of surface area and hydrogen adsorption amount demonstrates an increase in hydrogen absorption capacity and the BET (Brunauer-Emmett-Teller) surface area. At 77 K, super-activated carbon with a specific surface area of around 3000 m²/g can adsorb and desorb reversibly 5 wt % and 1.3 wt % H₂, respectively. Due to the low packing H₂ density of 0.3 g/cm³, the volumetric density at 77 K is only 1.5 kgH₂/100L. Conventional activated carbon, graphite nanofiber, and single-walled carbon nanotubes all have lower values. The standard heat of formation (heat of absorption) on superactivated carbon is calculated -6 kJ/mol H₂, via the Clausius-Clapeyron equation, and is unstable at ambient temperature. At 20 K, the volumetric and gravimetric H₂ densities of superactivated carbon are 7.5 kgH₂/100L and 10 wt %, respectively [182].

$$\ln\left(\frac{P_1}{P_2}\right) = \frac{\Delta H_{vap}}{R} \left(\frac{1}{T_2} - \frac{1}{T_1}\right) \quad (66)$$

4.4.3.2 Recent Advances of Nanoporous Carbon Materials

The main difficulty in achieving a “hydrogen economy” is hydrogen's low volumetric energy density, which means that moving a vehicle requires a larger fuel tank than gasoline-fueled vehicles. Storage and transport of hydrogen is a major barrier in the development of technologies based on hydrogen, such as fuel cells. A critical step toward realizing a hydrogen economy is the development of feasible technologies and materials for safe, stable, and effective hydrogen storage. High-pressure tanks, cryogenic liquefaction of molecular hydrogen, chemical solid storage materials, and physically adsorbing porous materials are among the approaches to hydrogen storage. For hydrogen compression, high

pressure storage tanks require 350–700 bar pressures; however, even at high pressures like these, the energy density is lower than that of conventional energy sources. The tanks must be made of strong lightweight materials which can endure pressurized conditions, something that increases the application cost. The car industry has examined cryogenic liquefaction of hydrogen as a viable on-board storage solution; however, hydrogen liquefaction happens only at extremely low temperatures (20 K). Heat flow from the environment in the storage tank quickly evaporates hydrogen, increasing the internal pressure, causing fuel loss (boil-off) and posing safety challenges.

Chemical solid-state storage is safer than liquefaction or compression and it relies on dissociative hydrogen adsorption on metals (often magnesium, lithium, or aluminum). At ambient temperatures and pressures, this approach gives a high gravimetric storage capacity. Unfortunately, the desorption of hydrogen from those materials has a high endothermic energy barrier (MgH_2 : $-75.3 \text{ kJ mol}^{-1}$), necessitating excessively high temperatures to release the desired hydrogen, reducing the energy efficiency. This means poor release kinetics and inadequate storage material recycling. Another option for hydrogen storage without energy inefficiencies is to use porous materials via physical absorption. One issue is that adsorption processes are based on van der Waals interactions that are low-energy interactions by nature. Nevertheless, most current attempts to develop hydrogen storage materials have focused on the development of nanomaterials that can reversibly store hydrogen particles at conditions close to ambient.

In low-stringency conditions, physisorption (physical adsorption) in porous substances allows for hydrogen storage. Hydrogen molecules physically adsorbed to a surface are weakly bonded to it and hence easily released. Porous carbons seem to be the most efficient hydrogen storage candidate among the many surface candidates, with the added benefit of being relatively inexpensive to produce and simple to prepare. In this chapter, the pore properties, preparation methods, storage capacities of nanoporous carbons, such as zeolite-templated carbon, activated carbons, and carbide-derived carbon are discussed [192].

Until recently, methods for hydrogen storage based on physically adsorbing materials have maximized the adsorbent's surface textural properties. In general, hydrogen storage capacities are governed by the pore characteristics (shape and size distribution) and the SSA (Specific Surface Area). Microporous materials, like zeolites, activated porous carbons, porous polymers, and metal–organic frameworks (MOFs), are target materials that meet these requirements.

Highly porous adsorbents that are based on carbonaceous materials are thoroughly investigated due to their appealing characteristics, which include decent thermal and chemical stabilities, high SSA, and mass production (they can be easily produced from a wide range of organic precursors). Carbonaceous adsorbents which are lightweight, provide excellent kinetics as well as a high SSA. As a result, they've gotten a lot of attention for their potential use in hydrogen storage. The categories of the major carbonaceous adsorbents are: (1) carbon nanomaterials, nanotubes, and fullerene, (2) carbide-derived carbons (CDCs),

and (3) zeolite-templated carbons (ZTCs). The newly produced MOF-derived carbons (MDCs) are described in the next section, and they have promising H₂ storage capabilities that are superior to the previously reported porous adsorbents. To provide suggestions for the design of acceptable porous carbon materials, we focus on the preparation and the pore properties of MDCs [192].

4.4.3.3 Carbon Materials for Hydrogen Storage

4.4.3.3.1 *Graphite*

Graphite can be created by heating coal pitch or petroleum coke to a temperature of 2200°C. It is one of the four carbon allotropes. Other carbon allotropes are diamond and fullerene. Each graphite carbon atom is bonded covalently to three other carbon atoms (**Figure 36**) and carbon atom sheets (layers) are linked together to form hexagonal structures. The layers are not covalently bonded to the layers around them; rather, they are held together by weak van der Waals forces [156].

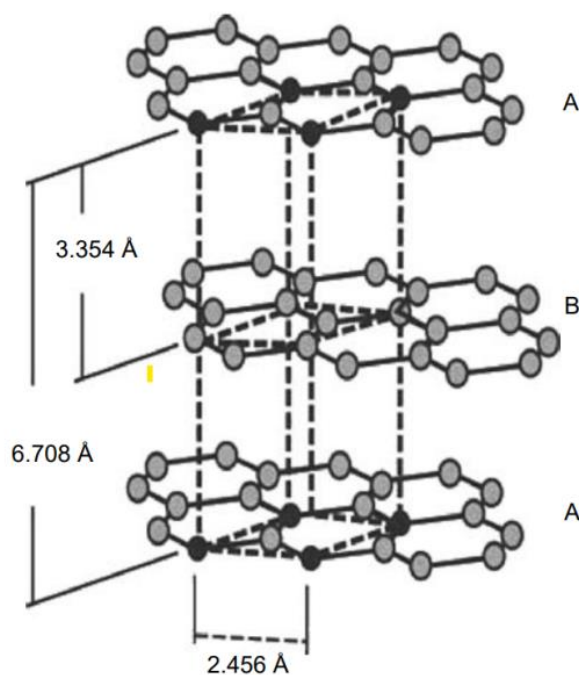


Figure 36: Molecular structure of graphite [156].

Graphite, pyrolytic carbon, carbon fiber, in their pure glassy synthetic forms (isotropic), are very strong, heat-resistant materials (up to 3000°C) used in rocket engines, solid pebble bed reactors, electric motor brushes, re-entry shields for rocket nose cones, electrodes in electrical discharge machines, and brake shoes. Expandable graphite is used in firestops, in the form of gaskets and plastic pipes fitted around the fire door perimeter. During a fire, expansion and charring of the graphite happens resisting fire penetration and lowering the risk of fire and fumes spreading. Exfoliated graphite (**Figure 37**), a key raw material in the industrial manufacture of flexible graphite sheets, is appealing due to its high sorption capacity. It is usually made by rapidly heating the residual compound of natural graphite flakes in sulfuric acid at 1200°C [193].

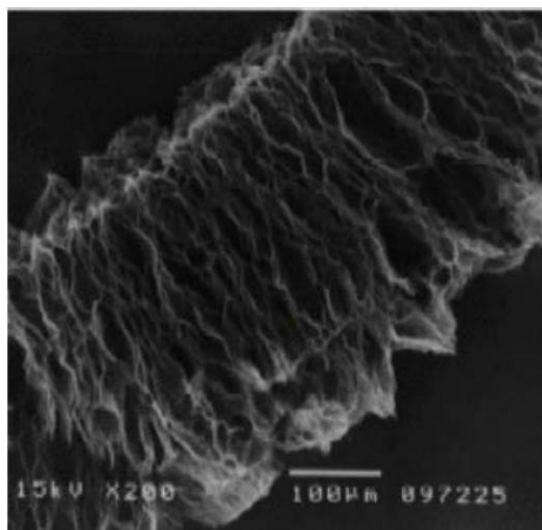


Figure 37: SEM micrographs of graphite after exfoliation [156].

Graphite has a low hydrogen-storage capacity due to its small interlayer distances and specific surface area (SSA), despite its comparatively high polarizability. Ball milling, however, can increase the surface area. For example, according to Schlappbach [194], after 80 hours of ball milling in a 10-bar hydrogen atmosphere, graphite nanostructures hold up to 7.4 wt %, or 0.95 hydrogen atoms per carbon atom, of which 80% can be desorbed at temperatures over 300°C. Furthermore, by slightly extending the interlayer gap, hydrogen can be intercalated into graphite at room temperature and mild pressures [156].

4.4.3.3.2 Graphene

Graphene is a single atomic sheet of graphite that consists of sp_2 bonded atoms of carbon, which is the same as a single isolated layer of the graphite structure (**Figure 38**).

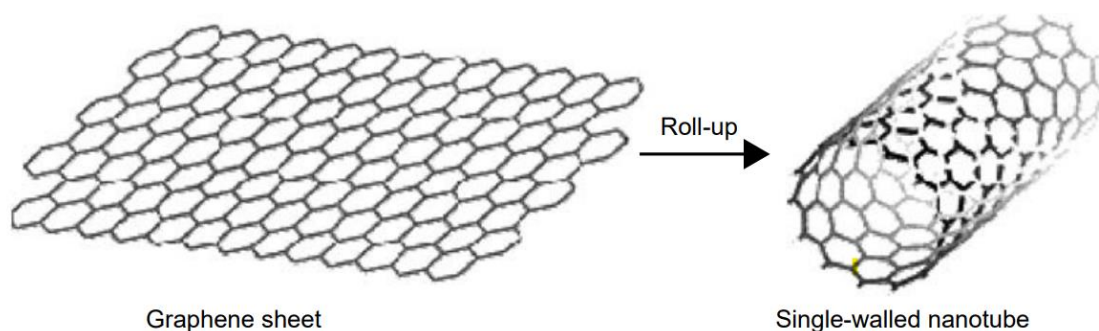


Figure 38: Molecular structure of grapheme [156].

Non-carbon elements can appear on the sheet's edge since it has a finite size. Graphene in nature is aromatic and mostly consists of hexagonal cells. The chemical formula for a typical sheet is $C_{62}H_{20}$, with hydrogen employed to terminate the dangling bonds. The plane is warped into a conical shape if a pentagonal cell is present. To isolate a single graphene sheet and examine its electrical properties, mechanical exfoliation of tiny fragments of pyrolytic graphite has been used. The maximum concentration for a graphene sheet with an

SSA equal to $1315 \text{ m}^2/\text{gas adsorbent}$ is 0.4 hydrogen atoms per surface carbon atom, or 3.3 wt % hydrogen on sheets with the hydrogen atoms on one side [156, 195].

The use of graphene-based nanomaterials has increased dramatically over the last decade [196]. Apart from hydrogen storage, graphene is being researched as a promising material to use in the sector of electrochemical sensors for detecting glucose, dopamine, or even SARS CoV-2 RNA [197, 198].

4.4.3.3 *Carbon Nanotubes (CNTs)*

CNTs are made from rolled graphite sheets with inner diameters ranging from 0.7 nm to several nanometers and a length range of 10–100 μm . CNTs are typically closed on both sides by a hemisphere, which is half of a fullerene. **Figure 39** [199] shows typical TEM (transmission electron microscopy) and SEM (scanning electron microscopy) of CNTs. Single-walled CNTs are tubes made up of only one concentric layer, whereas Multiwalled CNTs are made up of many concentric layers. SWNTs have diameters ranging from 0.7 to 3 nm, whereas MWNTs range from 30–50 nm.

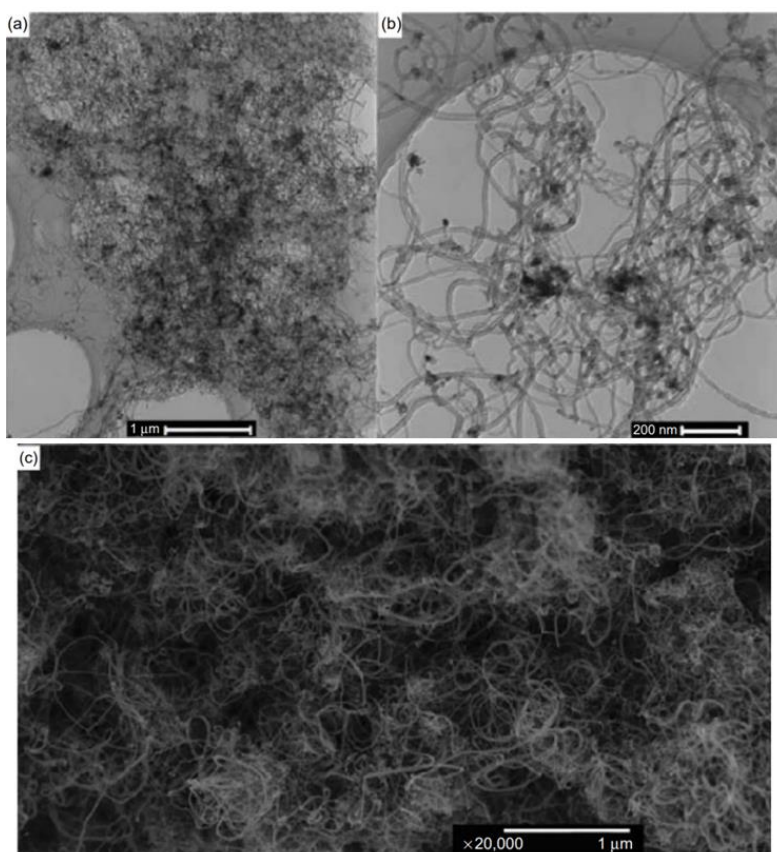


Figure 39: Typical TEM (a,b) and SEM (c) images showing the morphologies of the MWNTs (CNT) [199].

SWNTs are empty cylinders rolled-up sheets of graphene in one or more concentric layers (**Figure 38**). They feature a rare form of elemental carbon that gives them distinctive properties, such as the diameter and chirality of the carbon atoms, which can affect hydrogen adsorption. SWNTs are excellent prospects as hydrogen adsorbents because of their narrow pore-size distribution, and their cylindrical form can lead to a greater potential well. Based on calculations utilizing a continuum cylindrical Lennard–Jones potential, in order to minimize the energy of a hydrogen

molecule placed at the center of a SWNT with 6.4 Å internal-diameter, the lowest sorption binding energy inside it would be 12.3 kJ/mol. This binding energy is between two and three times that of AC. However, very small SWNT radii might cause repulsive interactions in the nanotube. Early SWNT studies showed adsorbed levels of 0 to 10% H by weight [195, 200-202].

SWNTs can be produced in an electric arc heater, where a cobalt catalyst and graphite are co-evaporated. The fibres are typically made up of 7–14 bundled SWNTs with a diameter of 10–15 Å. SWNTs can also be created by laser vaporization with a high yield. The predicted amounts of hydrogen absorbed in the cavity and at the surface of the nanotubes are shown in **Figure 40**. The bulk absorption in the hollow is proportional to the tube diameter and is the highest for SWNT. Furthermore, because hydrogen would condense in the nanotube, the wt % of adsorbed hydrogen in the tube cavity increases with tube diameter. Although the tube volume grows as the square of the radius, hydrogen uptake is linear to the tube diameter. This is because absorption is related to surface area, or the quantity of carbon atoms, which grows linearly with tube diameter [203].

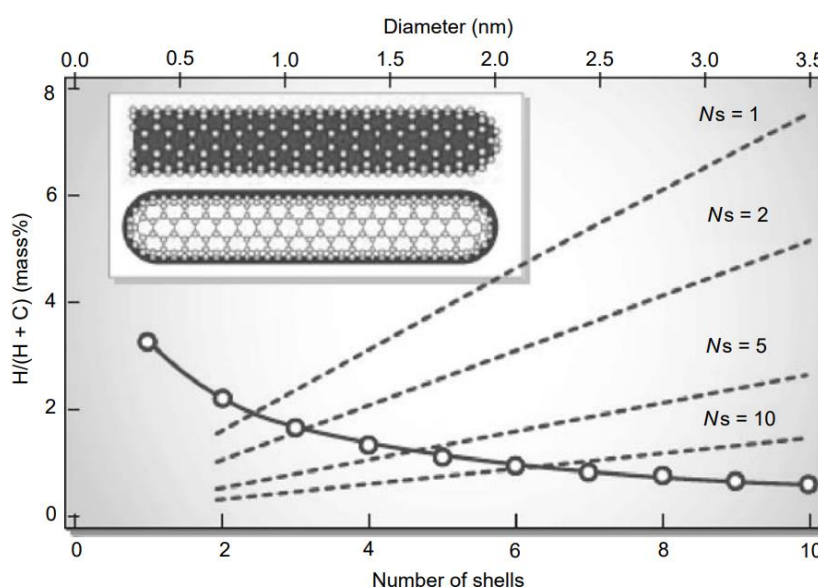


Figure 40: Calculated amount of adsorbed hydrogen in weight percent on CNTs, assuming condensation of hydrogen: (a) Monolayer adsorbed at the surface of nanotubes as a function of the number of shells (NS) (markers and line, axis: left and bottom) (b) hydrogen condensed in the cavity of nanotubes as a function of the diameter (dashed lines, axis: left and top) for various number of shells, NS=1 (SWNT), NS=2, NS=5, NS=10 [194].

MWNTs are made up of nested concentric cylinders of graphite with a hollow center. The number of shells varies from 2 to 50, and the distance between each cylinder is close to the interplanar spacing in graphite. MWNTs typically have inner and outer diameters of 2–10 and 15–30 nm, respectively, and a length of 5–100 microns. Large bundles of MWNTs of diameters up to 200µm, as well as lengthy individual tubes of over 2 mm have been recorded. MWNTs can be created by carbon vaporizing in an electric arc, decomposing acetylene with metal catalysts, or pyrolyzing benzene. The majority of MWNT shells are inactive for adsorption of hydrogen, serving solely to increase carbon mass and thus decrease hydrogen storage capacity [204-207].

4.4.3.3.4 Fullerene

Fullerenes are closed-cage molecules of carbon C_{2n} ($n > 10$) that are made up of trigonal carbon atoms, organized in 12 pentagons and $(n-20)/2$ hexagons. Fullerenes are soluble in toluene and carbon disulfide solvents. In the presence of metal catalysts, spherical fullerenes, which are known as "buckyballs," and cylindrical fullerenes, known as "buckytubes" or "nanotubes", are formed. The smallest complete fullerene molecule possible could be produced from 32 carbon atoms. A truncated icosahedron with 20 hexagons and 12 pentagons is a shape of spherical fullerene that resembles a soccer ball [208, 209]. Fullerenes, both spherical and cylindrical, are hollow. C_{60} , the most common fullerene, is made up of 60 carbon atoms linked together in a roughly spherical configuration. Aside from this, several additional fullerenes exist, such as C_{70} , C_{76} , and C_{84} , C_{240} and C_{540} . **Figure 41** depicts the usual structures of two most common fullerenes. Fullerenes are created by vaporizing carbon using a pulsed laser or an arc discharge, mixing it with an inert gas, and then slowly condensing it.

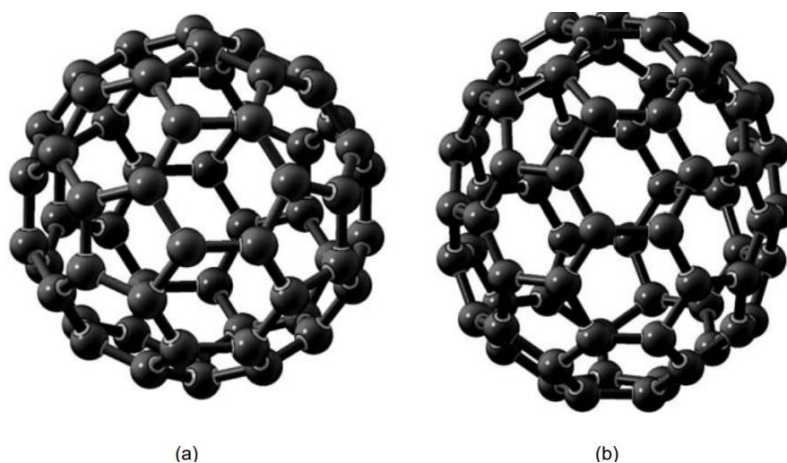


Figure 41: Molecular structures of fullerenes: (a) C_{60} and (b) C_{70} (Modified from [210]).

Fullerenes, such as C_{60} , are the only type of carbon that can be reversibly hydrogenated and dehydrogenated, due to their unique molecular structures. Reduced fullerenes can be made using dissolving-metal reductions or transfer hydrogenation having dihydroanthracene as the hydrogen donor, which produces $C_{60}H_{36}$ isomers with about 5% hydrogen content. Transfer hydrogenation hydrides are favoured for hydrogen storage because the $C_{60}H_{36}$ isomers produced by this method are more stable than those produced by dissolving-metal reductions. Fullerene is the simplest hydrofulleride, which has vicinal bond between hydrogen atoms. Because adjacent pentagons put too much strain on the cages, stable fullerenes cannot have them. It is a family of carbon molecules in which the carbon atoms are organized into 12 pentagonal faces and 2 or more hexagonal faces, and it is a great model for the thermally induced hydrogen removal from a fullerene [156, 210].

The possibility of localisation of hydrogen within the fullerene frame as a strategy for increasing hydrogen capacity is intriguing. At 77 K, around 3 mol H_2 /mol C_{60} can be found as H_2 molecules in the interstitial sites of $C_{60}H_x$ and can be ejected from the sample during its heating to 293 K. The C–H bond is weaker than the C–C bond, according to theoretical estimations (68 VS 83 kcal/mol bond energy). As a result, the C–H bond will break faster

than the C–C bond when heated, releasing hydrogen while maintaining the fullerene structure, making such a structure useful for hydrogen storage [210].

C₆₀ can be treated mechanically and chemically to produce a structurally robust material. However, the specifics of the structural modifications have yet to be determined. According to studies of C₆₀ polymers generated by chemical techniques, the linking of C₆₀ molecules with rigid covalent bonds leads in a decrease in cell volume and an increase in density when compared to the pristine C₆₀. In the case of milling-driven modifications the opposite effect was observed. Due to milling, hydrogen adsorption by C₆₀ rises, peaking at the milling time, which leads to complete amorphization of the material [156, 211].

4.4.3.3.5 *Carbon and Graphite Nanofibers (CNFs & GNFs)*

To achieve larger storage densities, various carbon nanostructures are being researched. Carbon nanofibers (CNFs) are layered nanostructures of graphite that sparked a lot of attention and debate when they first came out. At moderate temperatures and pressures, the hydrogen-storage capacity of these structures was found to range from less than 1% to tens of weight percentages. On catalysts made mostly of iron and nickel-based alloys, CNFs are generated from a combination of hydrogen and carbon-containing gases, or from hydrocarbons alone, at high temperatures. Variable forms of CNFs with different morphology, shape, and crystallinity can be generated depending on the shape and nature of the catalyst, the ratio of the hydrogen/hydrocarbon reactant mixture, and the reaction circumstances. The fibers are normally 5–100 μm long and 5–100 nm in diameter [212]. These ordered crystalline solids have an SSAs (BET) between 100 and 300 m²/g, but can occasionally approach 700 m²/g. CNFs hydrogen-storage capacity is determined by their structure, geometry (tube diameter, surface area, and length), defects on the structure, purification, pretreatment, tube arrangement in bundles or "ropes", temperature, and storage pressure etc.

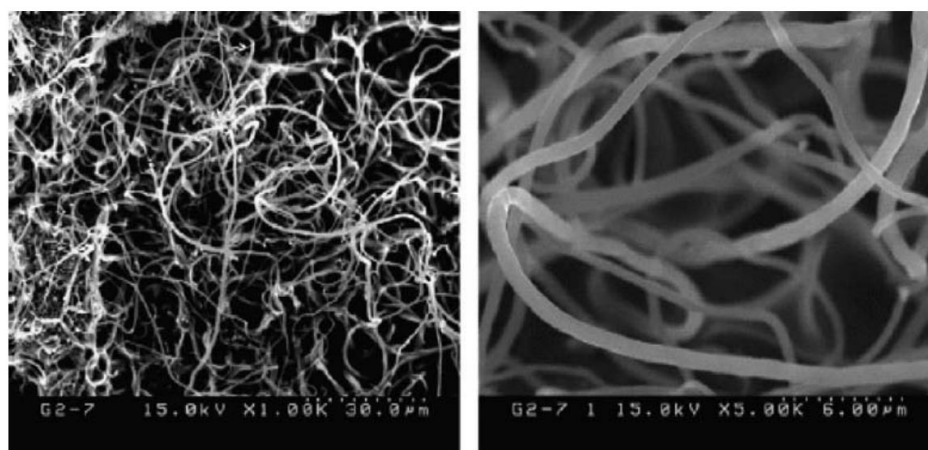


Figure 42: SEM of graphitic nanofiber prepared by decomposition of C₂H₄:H₂ = 1:4 gas flow over NiCu alloy powder [213].

GNFs made up of stacks of graphene plates and cones, with a length between 10–100 μm, a section range of 10–50 nm, and an interlayer spacing of 0.337 nm, contain lots of open edges that can encourage hydrogen sorption. GNFs produced via pyrolysis of C₂H₂ on

Fe:Ni:Cu = 85:10:5 absorb 6.5 wt % H₂. GNFs derived from C₆H₆ or CH₄ absorb 4–5.7 wt % H₂. GNFs with a parallel-bladed structure can absorb 10–13 wt % H₂. In a recent research, Xu et al., used a NiCu catalyst to synthesize GNF by decomposing C₂H₄:H₂ = 1:4 gas flowing at 873 K. These GNFs (**Figure 42**) were found to adsorb hydrogen similarly to the SWNHs with a relatively high pore volume and surface area.

Because the platelet structure provides multiple edges on a nanofiber, which constitutes a broad surface with many adsorbate-interaction sites, the interlayer distance can play a significant role. The proposed configurations for hydrogen adsorption on GNFs show a phase with a nearest-neighbour spacing of 4.26 Å, for low hydrogen coverage; 3.51 Å, for a denser and incommensurate close-packed structure at higher pressure; and only 0.98 Å, for a possible storage density of 60 wt % H₂, within the monolayer required if five layers were present between every two sheets of graphite. At temperatures ranging from 77 to 300 K, hydrogen adsorption experiments that were carried out on similarly manufactured fibers, showed that the GNF absolute level of hydrogen desorption is generally <0.08 weight% [156, 213, 214].

4.4.3.3.6 *Activated Carbons (ACs)*

Activated carbon is a cheap material, available in the industry, with a typical pore diameter of <1nm and a possible specific surface area of 3000 m²/g that is available at the industrial level. AC is made up of amorphous carbon of tiny graphite crystallites with nanoporosity and some and macro- and meso-porosity. It is created by dry distillation of carbon-rich organic precursors into carbonized organic precursors, which can then be activated with thermal or chemical treatments to increase pore volume. Carbon is heated between 700°C and 1000°C in the presence of oxidizing gases like steam, CO₂, air, or CO₂/steam mixes, during the thermal activation method. Carbon is heated between 500°C and 800°C with the presence of dehydrating chemicals like ZnCl₂, KOH, or H₃PO₄ (which are leached out later), during the chemical activation process. **Figure 43** depicts a typical AC molecular structure [215].

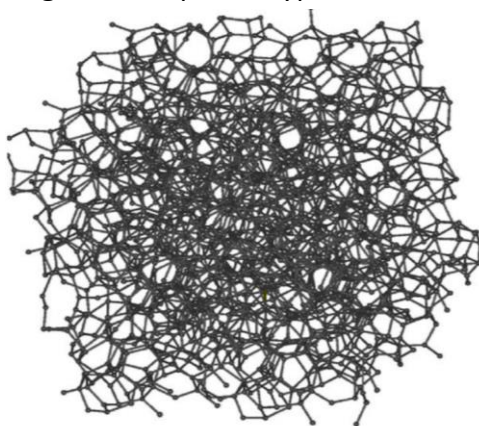


Figure 43: Molecular structure of activated carbon [215].

The amount of hydrogen adsorbed in ACs correlates well with the surface area, which, at room temperature and moderate pressures, is very low. For example, despite a large surface area (2800 m²/g), at 100 bars and 298 K, hydrogen adsorption is less than 1%. Although physical contact is the primary method of hydrogen sorption, surface groups and

other reactive sites can be introduced into the AC to aid hydrogen sorption. However, such technologies are largely based on chemisorption and are not a good way to improve reversible hydrogen storage [156].

4.4.3.3.7 Zeolite-Template Carbons

Microporous carbons with highly ordered pore arrays have been created through inorganic frameworks and hard templating procedures, as an alternative to ACs' chaotic pore structures. Carbon porosities can be managed with hard templating materials like zeolites and aluminosilicates, are desirable due to their uniform and ordered interconnecting pore channels which are readily accessible to many carbon precursors. The usual manufacturing of zeolite-templated carbon (ZTC) was described by Kyotani et al. as follows [216]:

- (i) Using either liquid impregnation or chemical vapor deposition (CVD), a carbon precursor was integrated into the channels and pores of chosen zeolites.
- (ii) The inserted carbon precursors were polymerized, then carbonized.
- (iii) Afterwards, the zeolite template used, was totally destroyed using a series of strong acids like hydrochloric acid.

The microporous ZTCs produced had high BET SSAs ($42000 \text{ m}^2/\text{g}$). Unlike ACs, ZTCs had morphologies that were identical to the original zeolite template particles, as observed by scanning electron microscopy. Transmission electron microscopy (TEM) could characterize the thin carbon walls due to the well-ordered microstructure. The ZTCs had a relatively high micropore volume ($41 \text{ cm}^3/\text{g}$), indicating that a considerable fraction of the pores in the carbon were micropores. Another textural characteristic of the ZTC is that the majority of the micropores have diameters between 1-2 nm. The large pores (40.6–0.7 nm) of the chosen zeolite ensured the great structural regularity of the pores in the ZTCs. As a result, despite the fact that pore size might be lowered by using zeolite with smaller pores, most reported ZTCs with higher structural ordering had a pore size distribution of 1–2 nm in width. Mokaya et al.[217] created microporous ZTCs by impregnating them with furfuryl alcohol, then carbonizing and then further carbonizing them using CVD techniques in argon under an acetonitrile flow. With nitrogen atom doping, the resultant ZTCs had micropore volumes ($40.8 \text{ cm}^3/\text{g}$) and high BET SSAs ($42000 \text{ m}^2/\text{g}$). At 77 K and 20 pressure, the ZTCs showed a hydrogen uptake of 5.4 wt %. Kyotani et al.[218] used chemical activation methods to introduce ultramicropores into the ZTCs, resulting in very porous activated ZTCs (CA850, Ac-ZTC₁, and P7(2)-H showed BET SSAs of 3189, 3064, and $3800 \text{ m}^2/\text{g}$, respectively). Due to the growth of ultramicropores, the activated ZTCs showed increased H₂ storage uptakes, which was helpful for hydrogen storage [192, 205, 216, 219].

4.4.3.3.8 Carbide-Derived Carbons

Carbide-derived carbon (CDC) is formed by selective etching of metal-carbide atoms, resulting in porous carbon with a density lower than graphite. CDCs were first assumed to be an unwanted by-product, but Gogotsi et al.[220] discovered that they can be used as molecular sieves, catalysts, gas storage adsorbents, and supercapacitors. This group created

methods for CDC mass production. CDCs were primarily made by chlorinating metal carbide using the following reaction: $\text{MeC}_x + \frac{1}{2} \text{Cl}_2(\text{g}) = \text{MeCl}_x + \text{C}$, where Me represents an extracted metal atom (see Fig. 3). The microstructures of the resulting CDCs were considerably impacted by the carbide employed during processing (e.g., TiC, SiC, B₄C, ZrC, Mo₂C, and TaC) and the heating temperature used during the chlorination process. The pore structure of CDCs is unique because it is adjustable at the atomic level, and the pore size distribution is narrow. CDCs, unlike ACs and ZTCs, have a large ultramicropore volume and an extremely small pore size distribution. Despite the ultramicropores' appealing tunability, CDCs do not have high BET SSAs (<2000 m²/g), and their SSAs are lower than those of ACs and ZTCs. Many experimental and theoretical approaches have shown that hydrogen preferentially adsorbs in ultramicropores; thus, the pore properties of CDCs were predicted to be particularly suitable for hydrogen storage applications [192, 221, 222].

4.4.3.3.9 Metal-Organic Frameworks/-Derived Carbons (MOFs/MDCs)

CNTs can be combined with other hydrogen-storage materials to take advantage of synergetic effects based on crystal and electronic structure modifications. Metal organic frameworks (MOFs), for example, consist of metallic ions or clusters combined with multidentate organic functional groups. They deliver exceptionally large surface areas (SSA > 5000 m²/g) and tuneable properties. It has been found that titanium alloys containing SWNT have a hydrogen uptake of 2–8 wt %, which is significantly higher than the 2.5 wt % of the alloy alone. Physisorption accounts for the majority of hydrogen uptake in nanoporous materials like carbon nanostructures and MOFs. However, the hydrogen absorption upon those porous materials only happens at cryogenic temperatures, due to the weak interaction between the sorbents and H₂. Thus, at ambient conditions, the storage capacity of hydrogen in these materials is very low, approaching that of liquid hydrogen, usually less than 2 mass %. Any further increase in storage density would require storing hydrogen at densities higher than liquid hydrogen in the porous structure. Going beyond present carbon and MOF nanostructures to increase the operating temperature of a physisorption storage device will be necessary [159, 205, 223].

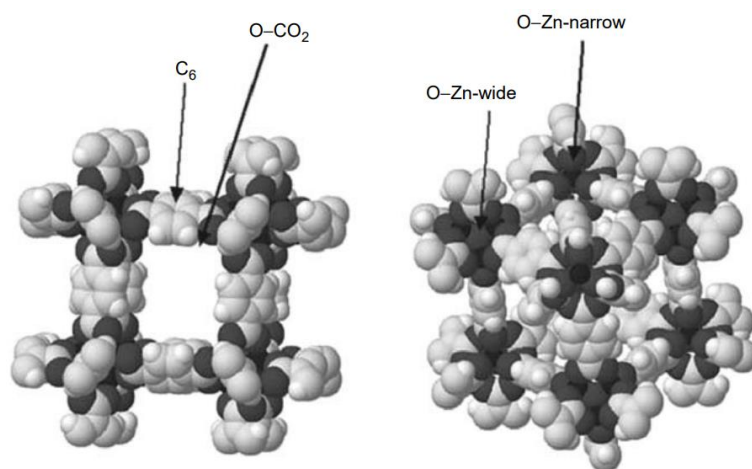


Figure 44: The minimized unit cell of MOF5 viewed from two different directions. In the left image the open pore structure is visible. White spheres, hydrogen; light gray, carbon; dark gray, oxygen; black, zinc. The hydrogen-adsorption sites are indicated by arrows [224].

One option is to dope carbon nanostructures with certain metals to increase their sorption capacity. That could lead to non-dissociative hydrogen molecule binding and enabling reversible usage for hydrogen storage. The adsorption enthalpy is highest for SWNTs and lowest for MOFs, implying that SWNTs have stronger adsorbate-adsorbent interactions. Both values congregate to below 5 kJ/mol at high coverage, which is consistent with physisorption [156].

If volumetric considerations are not crucial, increasing the specific surface of the adsorbent appears to remain the best technique for designing materials for hydrogen storage. For MOF adsorbents, the adsorbate-adsorbent interaction was found to be important in the low-pressure region of the adsorbent isotherms, resulting in a reverse trend with respect to the higher-pressure region [156].

Typical frameworks are made up of rigid organic spacer molecules bound together in three dimensions by metal complexes that fix the spacers' direction. **Figure 44** shows the unit cell for MOF5, one of the first MOF materials to show potential hydrogen adsorption. Aromatic rings in the spacer molecules make them stiff building components. Because MOFs have such large internal surfaces, increasing the adsorption interaction strength through chemical modification might pave the road for practical hydrogen storage [224].

4.4.3.4 Comparison of Hydrogen Storage Capacity of Different Carbon Materials

Due to the fact that solid-state hydrogen storage has been shown to be more reliable in terms of transportation and safety, various researchers around the world are working to build a suitable solid-state hydrogen storage system, in order to meet the estimated deadlines set by the DOE, for on-board automobile storage applications. Metal hydrides have been extensively studied for their hydrogen storage properties throughout the last several decades. Despite their strong reversibility, storage capacity of metal hydrides at room temperature does not meet the target.

Next, the hydrogen storage characteristics of carbon nanostructures are studied. Several researchers have found important hydrogen storage capabilities, but only at high pressures and cryogenic temperatures. Many researchers have experimentally found large storage capacities, in materials like CNF (10 wt %), K-doped MWCNT (14 wt %), and Li-doped MWCNT (20 wt %), at near room temperature. However, other scholars throughout the world dispute these findings. As a result, except for these remarkable results, none of the carbon materials have been found suitable for meeting the US DOE's aim (7.5 wt %).

Figure 45 compares the hydrogen storage capabilities of various carbon materials at room temperature, as well as the 2020 US DOE target and the UFF. All other carbon nanostructured materials, with the exception of graphite and SWNT, have achieved the hydrogen storage capacity predicted for 2020. (5.5 wt %).

Carbon materials failed to meet the UFF DOE objective despite various treatments and changes (7.5 wt %). This finding necessitates additional research into carbon-nanostructure flaws, doping, treatment, and other properties in order to improve hydrogen storage

capacity. The maximum hydrogen storage capacity (17 wt %) has been reported in 2004 for graphite nanofibers with acetylene thermal decomposition using a palladium catalyst. It appears to be a very appealing experimental discovery that can meet the DOE target; however, such results have not been replicated by any other researcher globally to explain these interesting hydrogen storage capacity numbers. Hydrogen storage capacity in carbon materials can be increased by catalyst doping, ball-milling, thermal treatment, and other methods, but it appears to be very difficult to attain the needed storage qualities for on-board use at ambient temperatures. This finding necessitates additional research in the field of carbon material structure modification in order to attain the hydrogen storage capacity necessary for future applications [191].

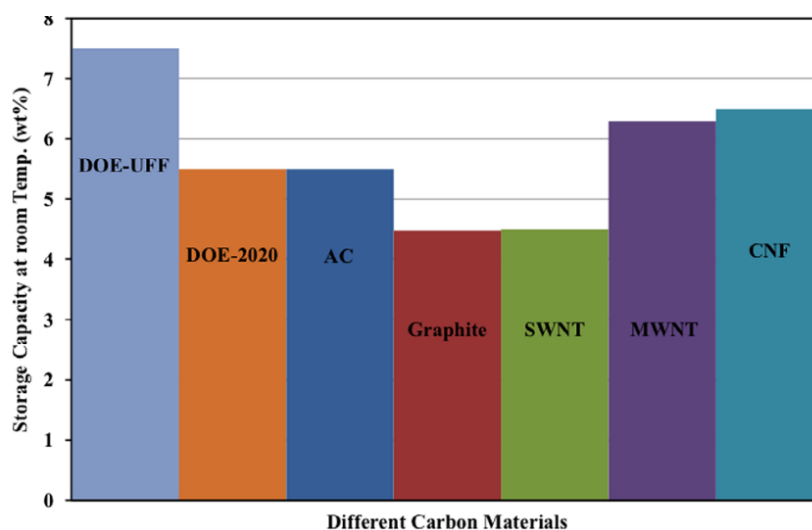


Figure 45 Hydrogen storage capacity of different carbon materials [191].

4.4.3.5 Challenges

Hydrogen-storage capacity of carbon materials is currently limited. CNFs and nanotubes appear to be the carbons that should be further investigated. The development of appropriate carbon materials for hydrogen storage requires:

- (i) a comprehension of the hydrogen-adsorption mechanism, so that the adsorption energy is increased up to 20–40 kJ/mol,
- (ii) a suitable method to produce materials with a high gravimetric density of sites exhibiting such interactions, and
- (iii) approaches to arrange the sites in space to allow high-volumetric storage densities.

Because pure and hybrid SWNT materials can be formed into tight nanoporous solids and exhibit properties that can be controlled by nanotube geometry, such as the attachment of electronic species, the introduction of defects, the introduction of adventitious dopants or catalytic species, and the elemental replacement on the nanotube lattice, they remain prime candidates for development. Other nanostructured carbon materials, such as MWNTs and metal oxide frameworks, are particularly interesting as well, because they offer additional systems for studying and controlling hydrogen adsorption interactions [156].

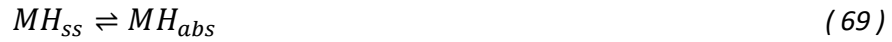
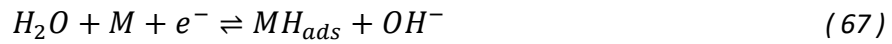
The construction of CNTs, for one storage tank with 5 kg hydrogen, (e.g., with a 10% H₂ capacity) would take roughly 1.2 GW of electricity. This indicates that producing the storage system would use the same amount of energy as running a vehicle for 3.6 million km. This is 20 times the vehicles life span and a prohibitable factor of 400 above the acceptable level. The disadvantages of existing production methods are emphasised by the fact that producing carbon material for a single storage tank would take around 27 years if done on a single production line. SWNTs are currently available commercially at roughly \$60 per gram, which would result in a tank cost of over \$3 million per vehicle [195, 200].

Carbon is a safe chemical in general, however breathing nanotubes is likely to be dangerous. The results of various in vitro and in vivo investigations suggest that exposure to these substances could pose a significant risk, but the potential dangers of inhaled CNTs have not been adequately investigated. Inhalation of nano-sized (i.e., smaller than 100 nm) carbon black particles has been shown to cause significant lung damage in rats. The toxicity of nano-sized black carbon particles is even higher. Within 24 hours after receiving a high dose of SWNT (5 mg/kg), the blockage of the major airways by the infused aggregate, rather than toxicity, caused 15% mortality to the instilled rats. Injecting MWNT into the lungs of the rats caused pulmonary lesions and inflammatory and fibrotic effects. Furthermore, the toxicity of the materials utilized in the preparation still poses a health risk during the production process. However, when nanostructured carbons are manufactured as monolithic bulk materials, many of the toxicity risks are minimized [225, 226].

4.4.4 Electrochemical Hydrogen Storage

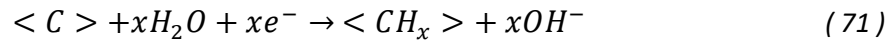
Solid-state hydrogen storage could be a game-changer in realizing the unique potential of hydrogen as a green fuel. It can be done chemically, physically, and electrochemically. Among the possible methods mentioned above, electrochemical hydrogen storage is one of the most promising ways since it can be conducted reversibly at low temperatures and pressures with a simple device, via physical hydrogen absorption (van der Waals bond) on the working electrode, directly. In the literature, it has been overshadowed by physical hydrogen storage, even though it seems that hydride form has disadvantages, including condensation heat release during the absorption and contraction-expansion of the metal lattice during the hydrogen adsorption, which cause pressure in the lattice. On the other hand, storing hydrogen in solid material via H₂ form seems to not have these drawbacks [227].

During the electrochemical breakdown of an aqueous solution, atoms of hydrogen adsorb onto hydrogen storage material [228]. The process of electrochemical hydrogen sorption involves Volmer and Tafel's reactions. In the Volmer process, hydrogen atoms are initially adsorbed on the electrode's surface, and water is reduced to generate hydroxyl ions (Eq. 67). After the adsorption of H atoms onto the host material (Eq. (68)), subsurface hydrogen (MH_{ss}) is produced. Eq. (69) shows how hydrogen atoms diffuse from the subsurface of the electrolyte to its bulk. The Tafel reaction (Eq. (70)) involves the forming of gaseous hydrogen from atomic hydrogen [229].



In this process, molecular hydrogen does not disintegrate into atomic hydrogen, hence important drawbacks of hydrogen storage are absent. Furthermore, applications of this type of hydrogen storage are quite high because of its accuracy and its availability [230].

A process has been proposed where carbons are utilized to sorb hydrogen created in situ by water electrolysis, similar to the creation of metal hydrides. Carbon is employed as a negatively polarized electrode in this experiment. The method itself is appealing in terms of energy efficiency since it produces hydrogen from water electrolysis and immediately stores it in the carbon substrate in a single step, thanks to the driving force given by negative polarization. The following reaction depicts the charge/discharge phenomenon:



, where $\langle CH_x \rangle$ is the hydrogen added to the carbon (charging) or oxidized (discharging). Given the strong hysteresis between sorption (reduction) and desorption (oxidation), it was thought that hydrogen diffuses throughout the carbon material after adsorption, occupying high-energy sites. The carbon material, electrolyte, and charge/discharge conditions all influence hydrogen storage capacity. The charge reaction is generally carried out via an adsorbed atom, so hydrogen might also be incorporated into carbon compounds, atomically without having to overcome the dissociation barrier. The electrolyte is the most significant component in electrochemical devices. The electric current in electrolytes is carried by ions, whereas in metals it is carried by electrons. Solid electrolytes are used in many electrochemical devices such as fuel cells, batteries, supercapacitors, and electrochemical gas sensors [231].

According to Pant et al. [156], electrochemical hydrogen storage on very pure single-walled nanotubes is found to be appealing. The electronic characteristics of CNTs are improved by incorporating conductive elements such as gold, copper, nickel, or palladium into the nanocarbon electrode in the form of micrometre-sized powders. The hydrogen electrochemical storage typically has a capacity of 0.3–3 wt %; however, capacities of even up to 7.7 wt % have been reported [195, 232], which has to be further validated.

Three popular methods of electrochemical storage of hydrogen are cyclic voltammetry (CV), electronic impedance spectroscopy, and chronopotentiometry (CP). In the latest decades, the CP method has been employed as the primary method in measuring the electrochemical hydrogen storage capacity of materials, because it is a simple, accurate, and safe procedure. This method is a three-electrode system in which current is applied and the capacity is determined as a function of time. The current is applied between the working and the counter (auxiliary) electrode. Then, the working electrode's changes are measured over

time. The auxiliary electrode is used to apply the desired current to the working electrode because the current cannot pass through the reference electrode, which is a polarized.

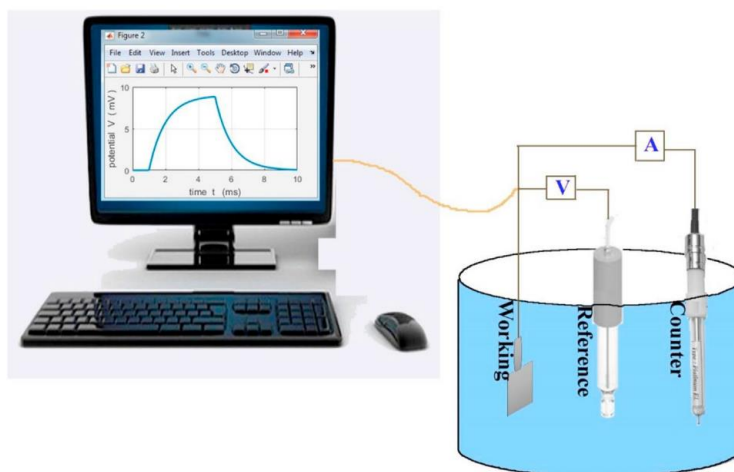


Figure 46: Schematic of three-electrode CP system [228].

As shown in **Figure 46**, applying current to the working electrode causes reduction and oxidation reactions, which are translated as potential changes which can be measured using the reference electrode. The Sand equation is the most important equation in the CP method. It shows the connection between the transition time (when the concentration of the reduction species reaches maximum and the concentration of the oxidizing species reaches zero), the concentration of the experimental species, and the used current:

$$\tau^{1/2} = \frac{nFAC\pi^{1/2}D^{1/2}}{2i} \quad (72)$$

, where t : transition time, n : number of transition electrons, F : Faraday constant, A : electrode surface area, D : diffusion coefficient, C : concentration of electroactive species, and i : applied current. The transition time can be the endpoint of the charging or the discharging process in the electrochemical hydrogen storage process [228].

Electrochemical hydrogen storage is also the foundation for other electrochemical power sources like batteries, supercapacitors, and fuel cells. For example, available hydrogen storage materials can be used to build supercapacitors with extraordinarily high specific capacitances. Generally, electrochemical hydrogen storage, will play a significant role in the future of both hydrogen storage and electrochemical power sources [227, 228].

CHAPTER V - CONCLUDING REMARKS

In this essay, hydrogen production, storage, and treatments for improving storage capacities of different materials were presented. The review led to the following conclusions:

- The realization of a “hydrogen economy” in the near future is considered to be a possible solution to the looming energy crisis.
- Hydrogen is a colourless, tasteless, odourless, and nontoxic gas.
- Hydrogen is the lightest of all the elements, with a small density per unit volume (around 14 times less than that of air).
- Due to its lightness, there are issues with transport and storage of hydrogen.
- Hydrogen is more flammable, buoyant, explosive, and diffusive than gasoline.
- Hydrogen as a fuel has a huge potential in the transportation sector, energy storage, power supplies, and renewable hybrid energy systems.
- It is an innovative alternative to the fossil fuels since it is clean, green, and has a higher energy density.
- However, it demands advancement in a number of industries, including production, storage, delivery, and end use. A practical, safe, and economical hydrogen energy system is critical to achieve a hydrogen economy.
- A crucial factor that needs to be considered is the combustion rate of hydrogen gas. Public awareness in the usage of hydrogen is required due to the safety issues.
- Hydrogen production can be achieved by a range of sources, including coal, natural gas, biomass, sun, wind, nuclear energy, and waste.
- Hydrogen produced from renewable sources or from fossil fuels with carbon capture emits no greenhouse gases.
- Hydrocarbon fuels are likely to continue playing a large role in hydrogen production in the near future, due to their availability, competitive cost, and ease of storage and distribution.
- To produce pure hydrogen from coal, coal gasification and CO₂ separation are combined with CO to H₂ conversion via the water-to-gas shift reaction. The most costly part of the process is coal gasification.
- Hydrogen can be produced by nuclear energy in a variety of ways, including (1) nuclear-heated natural gas steam reforming, (2) nuclear-powered water electrolysis, (3) HTE

using major electricity and minor heat from a nuclear reactor, and (4) thermochemical water splitting using minor electricity and major heat from a nuclear reactor. The current light water reactor is only suitable for water electrolysis and has a 30% efficiency.

- The production of hydrogen via water electrolysis using wind power is an intriguing method because it does not require the usage of fossil fuels and is environmentally friendly. Energy storage with high-density and little operation and maintenance costs is possible with wind-hydrogen systems.
- Biomass provides a possibly sustainable and certainly renewable source of hydrogen. It is one of the most significant CO₂-neutral energy production methods.
- For large-scale hydrogen production, thermochemical conversion seems to be the most promising biomass conversion technology.
- Gasification is still the most advanced method for large-scale hydrogen production, but it requires integrated demonstration plants with catalytic gas upgrading on a large scale. Gasification routes for hydrogen production have higher process efficiencies than liquid transportation fuels.
- Pyrolysis techniques aimed at producing hydrogen gas are currently being tested on a smaller scale.
- Supercritical water gasification is in its early stages of research and development, as the corrosive medium sets challenges to the reactor material, among other features.
- More sunlight energy hits the earth in one hour, than is consumed on the world in a year. Photovoltaics (PVs; solar electricity) is the most successful technology for utilizing this resource, with an annual growth rate of 35–40 %.
- Additionally, when compared to the renewable sources (biomass, wind, geothermal, and solar thermal), PVs have the greatest potential to lower the costs.
- At the moment, only around 5% of commercial hydrogen is produced primarily through water electrolysis, with the other 95% predominantly derived from fossil fuels.
- Hydrogen storage is a vital enabling technology for long-term development of hydrogen energy, which is essential for future economic growth.
- The most well-known hydrogen storage technique is physical hydrogen storage, formed in compressed gas. Because of its light weight, there is a risk of leakage from high-pressure containers.

- The liquid state is considered to be a viable option for large-scale transport and storage of hydrogen, in the direction of a global hydrogen-based energy market.
- Solid-state materials are able to absorb and release hydrogen in a reversible manner, so they are a better option since they are not used up instantly.
- Hydrogen is stored in solid materials by either chemisorption or physisorption.
- In physisorption, molecules of hydrogen are adsorbed on surfaces of solid nanostructured materials, which are mostly carbon materials like fibers, fullerenes, carbon nanotubes, zeolites, metal-organic frameworks (MOFs), activated carbon, and polymers with intrinsic microporosity (PIMs), which have low density, porosity and ultrahigh surface area.
- One of the key approaches being examined for automobile applications is hydrogen physisorption on porous materials. The goal is to store big amounts of hydrogen at temperatures close to ambient and at safe pressures.
- The hydrogen storage capacity of carbon materials is mostly determined by surface area, which is influenced by micropore size distribution.
- Thermal treatments and metal doping on carbon nanostructures can help increase H storage capacity, however the best storage capacities are achieved at high pressures and cryogenic temperatures. Further research into carbon nanostructures would be beneficial in achieving the 7.5 wt % storage target for automotive applications.
- Despite their high surface area, particularly that of nanostructured carbons, carbon materials have a storage capacity of less than 3 wt %.
- While many typical carbon materials are cheap and lightweight, nanotubes and similar materials are prohibitively expensive for mass-production storage systems.
- Carbon materials have quick adsorption and desorption kinetics, which is important for practical applications. Carbon or metal hybrid materials are showing promise, but further study is needed to obtain a storage capacity that is acceptable.
- Chemisorption materials (metal, complex and chemical hydrides) mix with H in the form of metallic, covalent, or ionic bonding, achieving solid hydrogen storage
- Metal hydrides have a greater hydrogen storage density (e.g., $6.5 \text{ H}_{\text{atoms}}/\text{cm}^3$, for MgH_2) than liquid hydrogen ($4.2 \text{ H}_{\text{atoms}}/\text{cm}^3$), or hydrogen gas ($0.99 \text{ H}_{\text{atoms}}/\text{cm}^3$). Metal hydrides take up much less space in storage than pressurized tanks do.

- Low hydrogenation/dehydrogenation enthalpies, high hydrogen capacity, reversibility, and low temperature of desorption are the most important properties for a metal hydride-based hydrogen storage material, all of which are difficult to achieve simultaneously due to thermodynamic and kinetic constraints.
- Magnesium hydride, with a storage capacity of 7.6 wt %, and sodium alanate, with a storage capacity of 5.5 wt %, are promising as materials of interest.
- So far, however, magnesium hydride-based materials have limited practical applications, because hydrogenation/dehydrogenation reactions are slow, requiring high temperatures.
- The weight, however, of metal hydrides remains high, necessitating further material development. Once the weight is decreased, using them in mobile applications will be possible. Metal hydrides require an excellent heat management system (which adds to the weight) due to the high heat of hydrogen absorption/desorption.
- Adding catalyst and forming nanostructures improves storage properties such as temperature, pressure, and rate of absorption and desorption.
- Organic chemical hydrides with adequate properties have been proposed as a hydrogen storage material in this study. Their potential densities of hydrogen are incomparable, which makes them great candidates for a range of hydrogen storage applications
- Another possible solid-state storage method is electrochemical hydrogen storage via physical absorption of hydrogen (van der Waals bond) directly on the working electrode. It can be conducted at low pressures and temperatures, reversibly, with a simple device.

BIBLIOGRAPHY

- [1] U. Bossel, "Does a hydrogen economy make sense?," *Proceedings of the IEEE*, vol. 94, pp. 1826-1837, 2006.
- [2] N. Tajitsu and M. Shiraki, "Toyota plans to expand production, shrink cost of hydrogen fuel cell vehicles," *Business News; Reuters: London, UK*, 2018.
- [3] M. K. Singla, P. Nijhawan, and A. S. Oberoi, "Hydrogen fuel and fuel cell technology for cleaner future: a review," *Environmental Science and Pollution Research*, vol. 28, pp. 15607-15626, 2021.
- [4] H. Kobayashi, A. Hayakawa, K. D. K. Somarathne, and E. Okafor, "Science and technology of ammonia combustion," *Proceedings of the Combustion Institute*, vol. 37, 2018.
- [5] E. Lopez-Alonso, "A proposed methodology for passive autocatalytic recombiners sizing and location in LWR containment," 2016.
- [6] I. Jain, "Hydrogen the fuel for 21st century," *International Journal of Hydrogen Energy*, vol. 34, pp. 7368-7378, 2009.
- [7] H. Kobayashi, A. Hayakawa, K. D. Kunkuma A. Somarathne, and Ekenechukwu C. Okafor, "Science and technology of ammonia combustion," *Proceedings of the Combustion Institute*, vol. 37, pp. 109-133, 2019.
- [8] S. Masoudi Soltani, A. Lahiri, H. Bahzad, P. Clough, M. Gorbounov, and Y. Yan, "Sorption-enhanced Steam Methane Reforming for Combined CO₂ Capture and Hydrogen Production: A State-of-the-Art Review," *Carbon Capture Science & Technology*, vol. 1, 2021.
- [9] A. Kumar, T. Singh, S. Singh, and Y. Liu, "A Comprehensive Review of Fuel Cell and its Types," 2013.
- [10] G. W. Crabtree and M. S. Dresselhaus, "The hydrogen fuel alternative," *Mrs Bulletin*, vol. 33, pp. 421-428, 2008.
- [11] A. Shokuhi, N. Nariman-Zadeh, and M. Naghash-Zadegan, "Model Development And Optimization Base On Generalized Steady-State Electrochemical Equations For A PEM Fuel Cell," *Proceedings - 23rd European Conference on Modelling and Simulation, ECMS 2009*, 2009.
- [12] J. R. Anstrom, "17 - Hydrogen as a fuel in transportation," in *Advances in Hydrogen Production, Storage and Distribution*, A. Basile and A. Iulianelli, Eds., ed: Woodhead Publishing, 2014, pp. 499-524.
- [13] M. T. Gencoglu and Z. Ural, "Design of a PEM fuel cell system for residential application," *International Journal of Hydrogen Energy*, vol. 34, pp. 5242-5248, 2009.

- [14] J. Kim, K. Boo, J. Cho, and I. Moon, "Key challenges in the development of an infrastructure for hydrogen production, delivery, storage and use," in *Advances in Hydrogen Production, Storage and Distribution*, ed: Elsevier, 2014, pp. 3-31.
- [15] S. Song, V. Maragou, and P. Tsiakaras, "How far are direct alcohol fuel cells from our energy future?," 2007.
- [16] J. Harrison, *Micro CHP: The Big Picture*: Big Picture Publishing, 2010.
- [17] I. Staffell, D. Scamman, A. V. Abad, P. Balcombe, P. E. Dodds, P. Ekins, N. Shah, and K. R. Ward, "The role of hydrogen and fuel cells in the global energy system," *Energy & Environmental Science*, vol. 12, pp. 463-491, 2019.
- [18] N. P. Brandon and Z. Kurban, "Clean energy and the hydrogen economy," *Philosophical Transactions of the Royal Society A: Mathematical, Physical and Engineering Sciences*, vol. 375, p. 20160400, 2017.
- [19] C. Guerreiro, A. G. Ortiz, F. de Leeuw, M. Viana, and J. Horálek, *Air quality in Europe-2016 report*: Publications Office of the European Union, 2016.
- [20] M. McGrath, "Four major cities move to ban diesel vehicles by 2025," *BBC news*, vol. 2, 2016.
- [21] D. Hart, J. Howes, F. Lehner, P. E. Dodds, N. Hughes, B. Fais, N. Sabio, and M. Crowther, "Scenarios for deployment of hydrogen in contributing to meeting carbon budgets and the 2050 target," *CCC – Committee on Climate Change*, vol. Final Report, 2015.
- [22] G. D. Clercq. (2019, JUNE 11). France to uphold ban on sale of fossil fuel cars by 2040. Available: <https://www.reuters.com/article/us-france-autos-idUSKCN1TC1CU>
- [23] T. Mitrova, Y. Melnikov, and D. Chugunov, *The Hydrogen Economy- a path towards low carbon development*, 2019.
- [24] M. Di Paolo Emilio. (2020, EC to Bet on Hydrogen Fuel-Cell Vehicles. *EE Times Europe*. Available: <https://www.eetimes.eu/ec-to-bet-on-hydrogen-fuel-cell-vehicles/>
- [25] M. Z. Jacobson, W. Colella, and D. Golden, "Cleaning the air and improving health with hydrogen fuel-cell vehicles," *Science*, vol. 308, pp. 1901-1905, 2005.
- [26] K. Hemmes, G. Barbieri, Y. M. Lee, E. Drioli, and H. J. De Wit, "Process intensification and fuel cells using a Multi-Source Multi-Product approach," *Chemical Engineering and Processing: process intensification*, vol. 51, pp. 88-108, 2012.
- [27] H. Ritchie, M. Roser, and P. Rosado, "CO₂ and greenhouse gas emissions," *Our world in data*, 2020.
- [28] H. R. Ritchie, Max; Rosado, Pablo (2020, CO₂ and Greenhouse Gas Emissions. Available: <https://ourworldindata.org/co2-and-other-greenhouse-gas-emissions>
- [29] P. Dodds and A. Hawkes, *The role of hydrogen and fuel cells in providing affordable, secure low-carbon heat*, 2014.

- [30] A. Ahmed, A. Q. Al-Amin, A. F. Ambrose, and R. Saidur, "Hydrogen fuel and transport system: A sustainable and environmental future," *International Journal of Hydrogen Energy*, vol. 41, pp. 1369-1380, 2016.
- [31] F. Gutiérrez and F. Méndez, "Entropy generation minimization for the thermal decomposition of methane gas in hydrogen using genetic algorithms," *Energy conversion and management*, vol. 55, pp. 1-13, 2012.
- [32] S. S. Pokharel, G. A. Bishop, and D. H. Stedman, "An on-road motor vehicle emissions inventory for Denver: an efficient alternative to modeling," *Atmospheric Environment*, vol. 36, pp. 5177-5184, 2002.
- [33] K. Ota, S. Mitsushima, K. Matsuzawa, and A. Ishihara, "Assessing the environmental impact of hydrogen energy production," *Advances in Hydrogen Production, Storage and Distribution*, pp. 31-42, 2014.
- [34] R. F. Service, "The hydrogen backlash," ed: American Association for the Advancement of Science, 2004.
- [35] O. Omoniyi, T. Bacquart, N. Moore, S. Bartlett, K. Williams, S. Goddard, B. Lipscombe, A. Murugan, and D. Jones, "Hydrogen gas quality for gas network injection: State of the art of three hydrogen production methods," *Processes*, vol. 9, p. 1056, 2021.
- [36] I. Dincer and C. Zamfirescu, "Potential options to greenize energy systems," *Energy*, vol. 46, pp. 5-15, 2012.
- [37] I. Dincer and C. Acar, "Review and evaluation of hydrogen production methods for better sustainability," *International Journal of Hydrogen Energy*, vol. 40, pp. 11094-11111, 2015.
- [38] M. I. El-Shafie, S. Kambara, and Y. Hayakawa, "Hydrogen Production Technologies Overview," *Journal of Power and Energy Engineering*, vol. 7, pp. 107-154, 2019.
- [39] R. K. Ahluwalia, "Sodium alanate hydrogen storage system for automotive fuel cells," *International Journal of Hydrogen Energy*, vol. 32, pp. 1251-1261, 2007.
- [40] M. Balat and H. Balat, "Recent trends in global production and utilization of bio-ethanol fuel," *Applied Energy*, vol. 86, pp. 2273-2282, 2009.
- [41] R. K. Ahluwalia, X. Wang, and A. Rousseau, "Fuel economy of hybrid fuel-cell vehicles," *Journal of Power Sources*, vol. 152, pp. 233-244, 2005.
- [42] C. Thomas, "Fuel cell and battery electric vehicles compared," *International Journal of Hydrogen Energy*, vol. 34, pp. 6005-6020, 2009.
- [43] M. A. Rosen and S. Koohi-Fayegh, "The prospects for hydrogen as an energy carrier: an overview of hydrogen energy and hydrogen energy systems," *Energy, Ecology and Environment*, vol. 1, pp. 10-29, 2016.
- [44] H. Idriss, "The Merit and the Context of Hydrogen Production from Water and Its Effect on Global CO₂ Emission," vol. 12, ed: MDPI, 2022, p. 231.

- [45] J. O. Abe, A. Popoola, E. Ajenifuja, and O. Popoola, "Hydrogen energy, economy and storage: review and recommendation," *International Journal of Hydrogen Energy*, vol. 44, pp. 15072-15086, 2019.
- [46] A. Herbst, T. Fleiter, M. Neuwirth, M. Rehfeldt, and J. Wachsmuth, "Options for achieving a close-to climateneutral EU industry and their implications," Working Paper Sustainability and Innovation 2021.
- [47] B. Breitschopf, L. Zheng, M. Plaisir, J. Bard, R. Schröer, D. Kawale, J. Koornneef, Y. Melese, M. Schaaphok, and J. Gorenstein Dedecca, "The role of renewable H₂ import & storage to scale up the EU deployment of renewable H₂," 2022.
- [48] T. Mitrova and Y. Melnikov, "Energy transition in Russia," *Energy Transitions*, vol. 3, pp. 73-80, 2019.
- [49] M. Nagashima, *Japan's hydrogen strategy and its economic and geopolitical implications*: Ifri, 2018.
- [50] IEA. (2018, World Energy Outlook 2018. Available: <https://www.iea.org/reports/world-energy-outlook-2018>
- [51] J. J. Romm, *The hype about hydrogen: fact and fiction in the race to save the climate*: Island Press, 2004.
- [52] G. A. Olah, "Beyond oil and gas: the methanol economy," *Angewandte Chemie International Edition*, vol. 44, pp. 2636-2639, 2005.
- [53] E. Serrano, G. Rus, and J. Garcia-Martinez, "Nanotechnology for sustainable energy," *Renewable and Sustainable Energy Reviews*, vol. 13, pp. 2373-2384, 2009.
- [54] R. Navarro, R. Guil, and J. Fierro, "Introduction to hydrogen production," in *Compendium of Hydrogen Energy*, ed: Elsevier, 2015, pp. 21-61.
- [55] J. Ren, N. M. Musyoka, H. W. Langmi, M. Mathe, and S. Liao, "Current research trends and perspectives on materials-based hydrogen storage solutions: a critical review," *International Journal of Hydrogen Energy*, vol. 42, pp. 289-311, 2017.
- [56] M. Felderhoff, C. Weidenthaler, R. von Helmolt, and U. Eberle, "Hydrogen storage: the remaining scientific and technological challenges," *Physical Chemistry Chemical Physics*, vol. 9, pp. 2643-2653, 2007.
- [57] H. Reardon, J. M. Hanlon, R. W. Hughes, A. Godula-Jopek, T. K. Mandal, and D. H. Gregory, "Emerging concepts in solid-state hydrogen storage: the role of nanomaterials design," *Energy & Environmental Science*, vol. 5, pp. 5951-5979, 2012.
- [58] M. P. Stracke, G. Ebeling, R. Cataluña, and J. Dupont, "Hydrogen-storage materials based on imidazolium ionic liquids," *Energy & fuels*, vol. 21, pp. 1695-1698, 2007.
- [59] D. W. Himmelberger, L. R. Alden, M. E. Bluhm, and L. G. Sneddon, "Ammonia borane hydrogen release in ionic liquids," *Inorganic chemistry*, vol. 48, pp. 9883-9889, 2009.

- [60] M. Twigg and V. Dupont, "Hydrogen production from fossil fuel and biomass feedstocks," *Advances in Hydrogen Production, Storage and Distribution*, pp. 43-84, 2014.
- [61] D. Fino, "Hydrogen production in conventional, bio-based and nuclear power plants," in *Advances in Hydrogen Production, Storage and Distribution*, ed: Elsevier, 2014, pp. 85-122.
- [62] N. Muradov, "Production of Hydrogen from hydrocarbons, Included in Hydrogen Fuel: Production, Transport and Storage, edited by RB Gupta," ed: CRC Press, Boca Raton, FL, 2009.
- [63] P. B. Abdalla and T. Hamed, "Simulation of a Multi Functions Methane Steam Reforming Reactor [MSRR]," *NUJES Al Neelain University Journal of Engineering Sciences*, vol. 2, p. 5, 2014.
- [64] J. N. Armor, "The multiple roles for catalysis in the production of H₂," *Applied Catalysis A: General*, vol. 176, pp. 159-176, 1999.
- [65] P. L. Spath and M. K. Mann, "Life cycle assessment of hydrogen production via natural gas steam reforming," National Renewable Energy Lab., Golden, CO (US)2000.
- [66] P. Van Beurden, "On the catalytic aspects of steam-methane reforming," *Energy Research Centre of the Netherlands (ECN), technical report I-04-003*, 2004.
- [67] Y. H. Hu and E. Ruckenstein, "Catalytic conversion of methane to synthesis gas by partial oxidation and CO₂ reforming," *Advances in catalysis*, vol. 48, pp. 297-345, 2004.
- [68] S. Z. Baykara, "Hydrogen: A brief overview on its sources, production and environmental impact," *International Journal of Hydrogen Energy*, vol. 43, pp. 10605-10614, 2018.
- [69] R. M. Navarro, M. Pena, and J. Fierro, "Hydrogen production reactions from carbon feedstocks: fossil fuels and biomass," *Chemical reviews*, vol. 107, pp. 3952-3991, 2007.
- [70] K. Aasberg-Petersen, I. Dybkjær, C. Ovesen, N. Schjødt, J. Sehested, and S. Thomsen, "Natural gas to synthesis gas—Catalysts and catalytic processes," *Journal of Natural gas science and engineering*, vol. 3, pp. 423-459, 2011.
- [71] J. Pina and D. O. Borio, "Modeling an simulation of an autothermal reformer," *Latin American applied research*, vol. 36, pp. 289-294, 2006.
- [72] M. Korobitsyn, F. Van Berkel, G. Christie, J. Huijsmans, and C. van der Klein, "SOFC as a Gas Separator," *Final Report NOVEM contract*, 2000.
- [73] I. Dincer, *Comprehensive energy systems*: Elsevier, 2018.
- [74] J. D. Bethel Afework. (2018, Coal types [Online]. *Energy Education*. Available: https://energyeducation.ca/encyclopedia/Coal_types
- [75] IEA. (2021, Global Hydrogen Review 2021. Available: <https://www.iea.org/reports/global-hydrogen-review-2021>

- [76] P. Choudhary, *Carbon Capture and Storage Program(CCSP) Final report 1.1.2011–31.10.2016*, 2016.
- [77] B. Metz, O. Davidson, H. De Coninck, M. Loos, and L. Meyer, *IPCC special report on carbon dioxide capture and storage*: Cambridge: Cambridge University Press, 2005.
- [78] C. W. Forsberg, P. F. Peterson, and P. S. Pickard, "Molten-salt-cooled advanced high-temperature reactor for production of hydrogen and electricity," *Nuclear Technology*, vol. 144, pp. 289-302, 2003.
- [79] Z. Y. Yu, Y. Duan, X. Y. Feng, X. Yu, M. R. Gao, and S. H. Yu, "Clean and affordable hydrogen fuel from alkaline water splitting: past, recent progress, and future prospects," *Advanced Materials*, vol. 33, p. 2007100, 2021.
- [80] C. Molochas and P. Tsiakaras, "Carbon Monoxide Tolerant Pt-Based Electrocatalysts for H₂-PEMFC Applications: Current Progress and Challenges," *Catalysts*, vol. 11, 2021.
- [81] P. Tsiakaras, C. Athanasiou, G. Marnellos, M. Stoukides, J. E. ten Elshof, and H. J. Bouwmeester, "Methane activation on a La_{0.6}Sr_{0.4}Co_{0.8}Fe_{0.2}O₃ perovskite: Catalytic and electrocatalytic results," *Applied Catalysis A: General*, vol. 169, pp. 249-261, 1998.
- [82] P. Tsiakaras and C. Vayenas, "Oxidative coupling of CH₄ on Ag catalyst-electrodes deposited on ZrO₂ (8 mol% Y₂O₃)," *Journal of Catalysis*, vol. 144, pp. 333-347, 1993.
- [83] D. Medvedev, V. Maragou, E. Pikalova, A. Demin, and P. Tsiakaras, "Novel composite solid state electrolytes on the base of BaCeO₃ and CeO₂ for intermediate temperature electrochemical devices," *Journal of Power Sources*, vol. 221, pp. 217-227, 2013.
- [84] E. Gorbova, V. Maragou, D. Medvedev, A. Demin, and P. Tsiakaras, "Influence of Cu on the properties of gadolinium-doped barium cerate," *Journal of Power Sources*, vol. 181, pp. 292-296, 2008.
- [85] S. I. Sinar Mashuri, M. L. Ibrahim, M. F. Kasim, M. S. Mastuli, U. Rashid, A. H. Abdullah, A. Islam, N. Asikin Mijan, Y. H. Tan, and N. Mansir, "Photocatalysis for organic wastewater treatment: From the basis to current challenges for society," *Catalysts*, vol. 10, p. 1260, 2020.
- [86] S. S. Shah, T. Najam, C. Molochas, M. A. Nazir, A. Brouzgou, M. S. Javed, A. U. Rehman, and P. Tsiakaras, "Nanostructure Engineering of Metal–Organic Derived Frameworks: Cobalt Phosphide Embedded in Carbon Nanotubes as an Efficient ORR Catalyst," *Molecules*, vol. 26, 2021.
- [87] R. C. Jakobs, "Tafel plot. Overpotential η as a function of $10\log i$," ed: Wikimedia Commons, the free media repository, 2020.
- [88] M. S. Burke, M. G. Kast, L. Trotochaud, A. M. Smith, and S. W. Boettcher, "Cobalt–iron (oxy) hydroxide oxygen evolution electrocatalysts: the role of structure and composition on activity, stability, and mechanism," *Journal of the American Chemical Society*, vol. 137, pp. 3638-3648, 2015.

- [89] M. W. Kanan and D. G. Nocera, "In situ formation of an oxygen-evolving catalyst in neutral water containing phosphate and Co^{2+} ," *Science*, vol. 321, pp. 1072-1075, 2008.
- [90] G.-f. Long, K. Wan, M.-y. Liu, Z.-x. Liang, J.-h. Piao, and P. Tsiakaras, "Active sites and mechanism on nitrogen-doped carbon catalyst for hydrogen evolution reaction," *Journal of Catalysis*, vol. 348, pp. 151-159, 2017.
- [91] C. Yu, F. Xu, L. Luo, H. S. Abbo, S. J. Titinchi, P. K. Shen, P. Tsiakaras, and S. Yin, "Bimetallic Ni-Co phosphide nanosheets self-supported on nickel foam as high-performance electrocatalyst for hydrogen evolution reaction," *Electrochimica Acta*, vol. 317, pp. 191-198, 2019.
- [92] J. Lu, Z. Tang, L. Luo, S. Yin, P. K. Shen, and P. Tsiakaras, "Worm-like S-doped RhNi alloys as highly efficient electrocatalysts for hydrogen evolution reaction," *Applied Catalysis B: Environmental*, vol. 255, p. 117737, 2019.
- [93] S. Jing, D. Wang, S. Yin, J. Lu, P. K. Shen, and P. Tsiakaras, "P-doped CNTs encapsulated nickel hybrids with flower-like structure as efficient catalysts for hydrogen evolution reaction," *Electrochimica Acta*, vol. 298, pp. 142-149, 2019.
- [94] L. Zhang, J. Lu, S. Yin, L. Luo, S. Jing, A. Brouzgou, J. Chen, P. K. Shen, and P. Tsiakaras, "One-pot synthesized boron-doped RhFe alloy with enhanced catalytic performance for hydrogen evolution reaction," *Applied Catalysis B: Environmental*, vol. 230, pp. 58-64, 2018.
- [95] A. Saad, Y. Gao, K. A. Owusu, W. Liu, Y. Wu, A. Ramiere, H. Guo, P. Tsiakaras, and X. Cai, "Ternary Mo_2NiB_2 as a Superior Bifunctional Electrocatalyst for Overall Water Splitting," *Small*, vol. 18, 2022.
- [96] B. Zhang, J. Shan, W. Wang, P. Tsiakaras, and Y. Li, "Oxygen Vacancy and Core-Shell Heterojunction Engineering of Anemone-Like $\text{CoP}@/\text{CoOOH}$ Bifunctional Electrocatalyst for Efficient Overall Water Splitting," *Small*, vol. 18, 2022.
- [97] L. Yan, B. Zhang, J. Zhu, Y. Li, P. Tsiakaras, and P. K. Shen, "Electronic modulation of cobalt phosphide nanosheet arrays via copper doping for highly efficient neutral-pH overall water splitting," *Applied Catalysis B: Environmental*, vol. 265, p. 118555, 2020.
- [98] M. Yu, C. K. Chan, and H. Tüysüz, "Coffee-Waste Templating of Metal Ion-Substituted Cobalt Oxides for the Oxygen Evolution Reaction," *ChemSusChem*, vol. 11, pp. 605-611, 2018.
- [99] H.-L. Chou, B.-J. Hwang, and C.-L. Sun, "Chapter 9 - Catalysis in Fuel Cells and Hydrogen Production," in *New and Future Developments in Catalysis*, S. L. Suib, Ed., ed Amsterdam: Elsevier, 2013, pp. 217-270.
- [100] Z. Li, M. Hu, Y. Xu, D. Zhao, S. Jiang, K. Fan, M. Zu, M. Al-Mamun, H. Yin, and S. Chen, "Photocatalytic Hydrogen Production," *Photo-and Electro-Catalytic Processes: Water Splitting, N_2 Fixing, CO_2 Reduction*, pp. 415-483, 2022.

- [101] X. Chen and S. S. Mao, "Titanium dioxide nanomaterials: synthesis, properties, modifications, and applications," *Chemical reviews*, vol. 107, pp. 2891-2959, 2007.
- [102] A. Kudo and Y. Miseki, "Heterogeneous photocatalyst materials for water splitting," *Chemical Society Reviews*, vol. 38, pp. 253-278, 2009.
- [103] M. A. Aziz Aljar, M. Zulqarnain, A. Shah, M. S. Akhter, and F. J. Iftikhar, "A review of renewable energy generation using modified titania for photocatalytic water splitting," *AIP Advances*, vol. 10, p. 070701, 2020.
- [104] M. Solakidou, A. Giannakas, Y. Georgiou, N. Boukos, M. Louloudi, and Y. Deligiannakis, "Efficient photocatalytic water-splitting performance by ternary CdS/Pt-N-TiO₂ and CdS/Pt-N, F-TiO₂: interplay between CdS photo corrosion and TiO₂-dopping," *Applied Catalysis B: Environmental*, vol. 254, pp. 194-205, 2019.
- [105] E. Starodub, N. C. Bartelt, and K. F. McCarty, "Oxidation of graphene on metals," *The Journal of Physical Chemistry C*, vol. 114, pp. 5134-5140, 2010.
- [106] J. Barber and P. D. Tran, "From natural to artificial photosynthesis," *Journal of The Royal Society Interface*, vol. 10, 2013/04/06 2013.
- [107] B. M. Hunter, H. B. Gray, and A. M. Muller, "Earth-abundant heterogeneous water oxidation catalysts," *Chemical reviews*, vol. 116, pp. 14120-14136, 2016.
- [108] W. Wang, M. Tadé, and Z. Shao, "ChemInform Abstract: Research Progress of Perovskite Materials in Photocatalysis- and Photovoltaics-Related Energy Conversion and Environmental Treatment," *Chem. Soc. Rev.*, vol. 44, 2015.
- [109] S. P. Badwal, S. S. Giddey, C. Munnings, A. I. Bhatt, and A. F. Hollenkamp, "Emerging electrochemical energy conversion and storage technologies," *Frontiers in Chemistry*, vol. 2, 2014.
- [110] S. Geiger, O. Kasian, B. R. Shrestha, A. M. Mingers, K. J. Mayrhofer, and S. Cherevko, "Activity and stability of electrochemically and thermally treated iridium for the oxygen evolution reaction," *Journal of The Electrochemical Society*, vol. 163, 2016.
- [111] V. Kumaravel, M. D. Imam, A. Badreldin, R. K. Chava, J. Y. Do, M. Kang, and A. Abdel-Wahab, "Photocatalytic hydrogen production: role of sacrificial reagents on the activity of oxide, carbon, and sulfide catalysts," *Catalysts*, vol. 9, p. 276, 2019.
- [112] A. Steinfeld and A. Meier, "Solar fuels and materials," in *Encyclopedia of energy*. vol. 5, ed: Elsevier Academic Press, 2004, pp. 623-637.
- [113] K. Maeda, "Z-scheme water splitting using two different semiconductor photocatalysts," *ACS Catalysis*, vol. 3, pp. 1486-1503, 2013.
- [114] X. Chen, S. Shen, L. Guo, and S. S. Mao, "Semiconductor-based photocatalytic hydrogen generation," *Chemical reviews*, vol. 110, pp. 6503-6570, 2010.
- [115] J. Zhu, L. Hu, P. Zhao, L. Y. S. Lee, and K.-Y. Wong, "Recent advances in electrocatalytic hydrogen evolution using nanoparticles," *Chemical reviews*, vol. 120, pp. 851-918, 2019.

- [116] N.-T. Suen, S.-F. Hung, Q. Quan, N. Zhang, Y.-J. Xu, and H. M. Chen, "Electrocatalysis for the oxygen evolution reaction: recent development and future perspectives," *Chemical Society Reviews*, vol. 46, pp. 337-365, 2017.
- [117] K. Sardar, E. Petrucco, C. I. Hiley, J. D. Sharman, P. P. Wells, A. E. Russell, R. J. Kashtiban, J. Sloan, and R. I. Walton, "Water-Splitting Electrocatalysis in Acid Conditions Using Ruthenate-Iridate Pyrochlores," *Angewandte Chemie*, vol. 126, pp. 11140-11144, 2014.
- [118] D. Strmcnik, M. Uchimura, C. Wang, R. Subbaraman, N. Danilovic, D. Van Der Vliet, A. P. Paulikas, V. R. Stamenkovic, and N. M. Markovic, "Improving the hydrogen oxidation reaction rate by promotion of hydroxyl adsorption," *Nature chemistry*, vol. 5, pp. 300-306, 2013.
- [119] M. Huynh, T. Ozel, C. Liu, E. C. Lau, and D. G. Nocera, "Design of template-stabilized active and earth-abundant oxygen evolution catalysts in acid," *Chemical science*, vol. 8, pp. 4779-4794, 2017.
- [120] I. Firtina-Ertis, C. Acar, and E. Erturk, "Optimal sizing design of an isolated stand-alone hybrid wind-hydrogen system for a zero-energy house," *Applied Energy*, vol. 274, p. 115244, 2020/09/15/ 2020.
- [121] M. Yu, E. Budiyo, and H. Tüysüz, "Principles of Water Electrolysis and Recent Progress in Cobalt-, Nickel-, and Iron-Based Oxides for the Oxygen Evolution Reaction," *Angewandte Chemie International Edition*, vol. 61, 2022.
- [122] M. Zanfir, "Portable and small-scale stationary hydrogen production from micro-reactor systems," in *Advances in Hydrogen Production, Storage and Distribution*, ed: Elsevier, 2014, pp. 123-155.
- [123] J. Riccardi, M. Schiavetti, I. Fastelli, and M. Smitkova, "Modelling of westinghouse and sulphur-iodine water splitting cycles for hydrogen production," *International Journal of Energy and Environmental Engineering*, vol. 2, 2011.
- [124] S. Anantharaj, S. R. Ede, K. Sakthikumar, K. Karthick, S. Mishra, and S. Kundu, "Recent trends and perspectives in electrochemical water splitting with an emphasis on sulfide, selenide, and phosphide catalysts of Fe, Co, and Ni: a review," *ACS Catalysis*, vol. 6, pp. 8069-8097, 2016.
- [125] J.-H. Kim, K. Shin, K. Kawashima, D. H. Youn, J. Lin, T. E. Hong, Y. Liu, B. R. Wygant, J. Wang, and G. Henkelman, "Enhanced activity promoted by CeO_x on a CoO_x electrocatalyst for the oxygen evolution reaction," *ACS Catalysis*, vol. 8, pp. 4257-4265, 2018.
- [126] J. Masa, S. Piontek, P. Wilde, H. Antoni, T. Eckhard, Y.-T. Chen, M. Muhler, U.-P. Apfel, and W. Schuhmann, "Ni-Metalloid (B, Si, P, As, and Te) Alloys as Water Oxidation Electrocatalysts," *Advanced Energy Materials*, vol. 9, 2019.
- [127] Z. Fang, L. Peng, H. Lv, Y. Zhu, C. Yan, S. Wang, P. Kalyani, X. Wu, and G. Yu, "Metallic transition metal selenide holey nanosheets for efficient oxygen evolution electrocatalysis," *ACS nano*, vol. 11, pp. 9550-9557, 2017.

- [128] X. Wang, X. Huang, W. Gao, Y. Tang, P. Jiang, K. Lan, R. Yang, B. Wang, and R. Li, "Metal–organic framework derived CoTe₂ encapsulated in nitrogen-doped carbon nanotube frameworks: a high-efficiency bifunctional electrocatalyst for overall water splitting," *Journal of Materials Chemistry A*, vol. 6, pp. 3684–3691, 2018.
- [129] Z. W. Seh, J. Kibsgaard, C. F. Dickens, I. Chorkendorff, J. K. Nørskov, and T. F. Jaramillo, "Combining theory and experiment in electrocatalysis: Insights into materials design," *Science*, vol. 355, 2017.
- [130] T. Shinagawa, A. T. Garcia-Esparza, and K. Takanebe, "Insight on Tafel slopes from a microkinetic analysis of aqueous electrocatalysis for energy conversion," *Scientific reports*, vol. 5, pp. 1–21, 2015.
- [131] D. Xu, M. B. Stevens, M. R. Cosby, S. Z. Oener, A. M. Smith, L. J. Enman, K. E. Ayers, C. B. Capuano, J. N. Renner, and N. Danilovic, "Earth-abundant oxygen electrocatalysts for alkaline anion-exchange-membrane water electrolysis: Effects of catalyst conductivity and comparison with performance in three-electrode cells," *ACS Catalysis*, vol. 9, pp. 7–15, 2018.
- [132] S. Wang, A. Lu, and C.-J. Zhong, "Hydrogen production from water electrolysis: role of catalysts," *Nano Convergence*, vol. 8, pp. 1–23, 2021.
- [133] M. Yu, G. h. Moon, R. G. Castillo, S. DeBeer, C. Weidenthaler, and H. Tüysüz, "Dual role of silver moieties coupled with ordered mesoporous cobalt oxide towards electrocatalytic oxygen evolution reaction," *Angewandte Chemie*, vol. 132, pp. 16687–16695, 2020.
- [134] M. S. Reza, N. B. H. Ahmad, S. Afroze, J. Taweekun, M. Sharifpur, and A. K. Azad, "Hydrogen Production from Water Splitting Through Photocatalytic Activity of Carbon-Based Materials, A Review," *Chemical Engineering & Technology*, 2022.
- [135] R. Bhandari, C. A. Trudewind, and P. Zapp, "Life cycle assessment of hydrogen production via electrolysis—a review," *Journal of cleaner production*, vol. 85, pp. 151–163, 2014.
- [136] A. Singhanian and A. N. Bhaskarwar, "Development of catalysts for hydrogen production from hydrogen iodide decomposition in thermo-chemical water-splitting sulfur-iodine cycle: a review," *Catalysis Reviews*, 2017.
- [137] S. V. Mohan and A. Pandey, "Chapter 1 - Biohydrogen Production: An Introduction," in *Biohydrogen*, A. Pandey, J.-S. Chang, P. C. Hallenbecka, and C. Larroche, Eds., ed Amsterdam: Elsevier, 2013, pp. 1–24.
- [138] M. Ni, D. Y. Leung, M. K. Leung, and K. Sumathy, "An overview of hydrogen production from biomass," *Fuel processing technology*, vol. 87, pp. 461–472, 2006.
- [139] O. Yamada, "Generation of hydrogen gas by reforming biomass with superheated steam," *Thin solid films*, vol. 509, pp. 207–211, 2006.
- [140] M. Asadullah, S.-i. Ito, K. Kunimori, M. Yamada, and K. Tomishige, "Energy Efficient Production of Hydrogen and Syngas from Biomass: Development of Low-Temperature

- Catalytic Process for Cellulose Gasification," *Environmental Science & Technology*, vol. 36, pp. 4476-4481, 2002.
- [141] Kopiersperre, "Haupttypen von (Biomasse-)Vergasern," ed: Wikimedia Commons, the free media repository, 2014.
- [142] M. F. Demirbas, "Hydrogen from various biomass species via pyrolysis and steam gasification processes," *Energy Sources, Part A*, vol. 28, pp. 245-252, 2006.
- [143] A. Flamos, P. Georgallis, H. Doukas, and J. Psarras, "Using biomass to achieve European Union Energy Targets—A review of biomass status, potential, and supporting policies," *International Journal of Green Energy*, vol. 8, pp. 411-428, 2011.
- [144] T. Y. Ahmed, M. M. Ahmad, S. Yusup, A. Inayat, and Z. Khan, "Mathematical and computational approaches for design of biomass gasification for hydrogen production: A review," *Renewable and Sustainable Energy Reviews*, vol. 16, pp. 2304-2315, 2012.
- [145] S. Sarma and S. Chakma, "Advancements in Bio-hydrogen Production from Waste Biomass," *Biotechnology for Zero Waste: Emerging Waste Management Techniques*, pp. 283-302, 2022.
- [146] T. Gaj, C. A. Gersbach, and C. F. Barbas, "ZFN, TALEN, and CRISPR/Cas-based methods for genome engineering," *Trends in Biotechnology*, vol. 31, pp. 397-405, 2013/07/01/ 2013.
- [147] P. Sinha and A. Pandey, "An evaluative report and challenges for fermentative biohydrogen production," *International Journal of Hydrogen Energy*, vol. 36, pp. 7460-7478, 2011.
- [148] R. Łukajtis, I. Hołowacz, K. Kucharska, M. Glinka, P. Rybarczyk, A. Przyjazny, and M. Kamiński, "Hydrogen production from biomass using dark fermentation," *Renewable and Sustainable Energy Reviews*, vol. 91, pp. 665-694, 2018.
- [149] A. Melis, L. Zhang, M. Forestier, M. L. Ghirardi, and M. Seibert, "Sustained photobiological hydrogen gas production upon reversible inactivation of oxygen evolution in the green alga *Chlamydomonas reinhardtii*," *Plant physiology*, vol. 122, pp. 127-136, 2000.
- [150] P. Hallenbeck, C. Lazaro, and E. Sagir, "CHAPTER 1. Photosynthesis and Hydrogen from Photosynthetic Microorganisms," ed, 2018, pp. 1-30.
- [151] D. B. Levin, L. Pitt, and M. Love, "Biohydrogen production: prospects and limitations to practical application," *International Journal of Hydrogen Energy*, vol. 29, pp. 173-185, 2004.
- [152] F. R. Hawkes, I. Hussy, G. Kyazze, R. Dinsdale, and D. L. Hawkes, "Continuous dark fermentative hydrogen production by mesophilic microflora: principles and progress," *International Journal of Hydrogen Energy*, vol. 32, pp. 172-184, 2007.
- [153] I. K. Kapdan and F. Kargi, "Bio-hydrogen production from waste materials," *Enzyme and microbial technology*, vol. 38, pp. 569-582, 2006.

- [154] A. Guwy, R. Dinsdale, J. Kim, J. Massanet-Nicolau, and G. Premier, "Fermentative biohydrogen production systems integration," *Bioresource technology*, vol. 102, pp. 8534-8542, 2011.
- [155] S. Satyapal, & Thomas, G. , "Targets for Onboard Hydrogen Storage " in *Hydrogen Fuel: Production, Transport, and Storage* ed, 2009, pp. 327-340.
- [156] K. Pant and R. B. Gupta, "Hydrogen storage in carbon materials," in *Hydrogen fuel: production, transport and storage*, ed: CRC Press, Taylor and Francis Group Boca Raton, Florida, USA, 2009, pp. 381-436.
- [157] M. Conte, P. P. Prosini, and S. Passerini, "Overview of energy/hydrogen storage: state-of-the-art of the technologies and prospects for nanomaterials," *Materials Science and Engineering: B*, vol. 108, pp. 2-8, 2004.
- [158] M. Hirscher, V. A. Yartys, M. Baricco, J. B. von Colbe, D. Blanchard, R. C. Bowman Jr, D. P. Broom, C. E. Buckley, F. Chang, and P. Chen, "Materials for hydrogen-based energy storage—past, recent progress and future outlook," *Journal of Alloys and Compounds*, vol. 827, p. 153548, 2020.
- [159] L. Ouyang, K. Chen, J. Jiang, X.-S. Yang, and M. Zhu, "Hydrogen storage in light-metal based systems: a review," *Journal of Alloys and Compounds*, vol. 829, p. 154597, 2020.
- [160] M. U. Niemann, S. S. Srinivasan, A. R. Phani, A. Kumar, D. Y. Goswami, and E. K. Stefanakos, "Nanomaterials for hydrogen storage applications: a review," *Journal of Nanomaterials*, vol. 2008, 2008.
- [161] K. Pant and R. B. Gupta, "Hydrogen storage in metal hydrides," in *Hydrogen fuel: production, transport and storage*, ed: CRC Press Boca Raton, 2008, pp. 381-408.
- [162] R. Schulz, J. Strom-Olsen, L. Zaluski, and A. Zaluska, "Nanocrystalline Mg or Be-based materials and use thereof for the transportation and storage of hydrogen," ed: Google Patents, 1999.
- [163] B. Sakintuna, F. Lamari-Darkrim, and M. Hirscher, "Metal hydride materials for solid hydrogen storage: a review," *International Journal of Hydrogen Energy*, vol. 32, pp. 1121-1140, 2007.
- [164] D.-L. Zhao and Y.-H. Zhang, "Research progress in Mg-based hydrogen storage alloys," *Rare Metals*, vol. 33, pp. 499-510, 2014.
- [165] J.-J. Li, C.-C. Wang, J. Guo, J.-R. Cui, P. Wang, and C. Zhao, "Three coordination compounds based on tris (1-imidazolyl) benzene: Hydrothermal synthesis, crystal structure and adsorption performances toward organic dyes," *Polyhedron*, vol. 139, pp. 89-97, 2018.
- [166] L. Ouyang, F. Liu, H. Wang, J. Liu, X.-S. Yang, L. Sun, and M. Zhu, "Magnesium-based hydrogen storage compounds: a review," *Journal of Alloys and Compounds*, vol. 832, p. 154865, 2020.

- [167] G.-x. Liang, J. Huot, S. Boily, A. Van Neste, and R. Schulz, "Catalytic effect of transition metals on hydrogen sorption in nanocrystalline ball milled MgH₂-Tm (Tm= Ti, V, Mn, Fe and Ni) systems," *Journal of Alloys and Compounds*, vol. 292, pp. 247-252, 1999.
- [168] D. Fruchart, P. De Rango, J. Charbonnier, N. Skryabina, and M. Jehan, "Nanocrystalline composite for storage of hydrogen," *Patent US*, vol. 278086, p. 12, 2009.
- [169] M. Dornheim, "Hydrogen Storage: Metal Hydrides in Comparison to Alternative Solutions for Emission-Free Vehicles," ed: GKSS-Forschungszentrum, 2006.
- [170] B. D. Adams and A. Chen, "The role of palladium in a hydrogen economy," *Materials Today*, vol. 14, pp. 282-289, 2011.
- [171] P. Chen and M. Zhu, "Recent progress in hydrogen storage," *Materials Today*, vol. 11, pp. 36-43, 2008.
- [172] X. Yu, Z. Tang, D. Sun, L. Ouyang, and M. Zhu, "Recent advances and remaining challenges of nanostructured materials for hydrogen storage applications," *Progress in Materials Science*, vol. 88, pp. 1-48, 2017.
- [173] M. A. Rahmaninasab, S. Raygan, H. Abdizadeh, M. Pourabdoli, and S. H. Mirghaderi, "Properties of activated MgH₂+ mischmetal nanostructured composite produced by ball-milling," *Materials for Renewable and Sustainable Energy*, vol. 7, pp. 1-11, 2018.
- [174] B. Bogdanović, U. Eberle, M. Felderhoff, and F. Schüth, "Complex aluminum hydrides," *Scripta Materialia*, vol. 56, pp. 813-816, 2007.
- [175] A. Zaluska, L. Zaluski, and J. Ström-Olsen, "Lithium-beryllium hydrides: the lightest reversible metal hydrides," *Journal of Alloys and Compounds*, vol. 307, pp. 157-166, 2000.
- [176] A. Maddalena, M. Petris, P. Palade, S. Sartori, G. Principi, E. Settimo, B. Molinas, and S. L. Russo, "Study of Mg-based materials to be used in a functional solid state hydrogen reservoir for vehicular applications," *International Journal of Hydrogen Energy*, vol. 31, pp. 2097-2103, 2006.
- [177] F. Schüth, B. Bogdanović, and M. Felderhoff, "Light metal hydrides and complex hydrides for hydrogen storage," *Chemical Communications*, pp. 2249-2258, 2004.
- [178] L. Heung, "Using Metal Hydride to Store Hydrogen," ed. Springfield, VA: US Department of Commerce, National Technical Information Service, 2003.
- [179] B. Bogdanović and M. Schwickardi, "Ti-doped alkali metal aluminium hydrides as potential novel reversible hydrogen storage materials," *Journal of Alloys and Compounds*, vol. 253, pp. 1-9, 1997.
- [180] P. Chen, Z. Xiong, J. Luo, J. Lin, and K. L. Tan, "Interaction of hydrogen with metal nitrides and imides," *Nature*, vol. 420, pp. 302-304, 2002.
- [181] A. Züttel, S. Rentsch, P. Fischer, P. Wenger, P. Sudan, P. Mauron, and C. Emmenegger, "Hydrogen storage properties of LiBH₄," *Journal of Alloys and Compounds*, vol. 356, pp. 515-520, 2003.

- [182] Y. Kojima, "Hydrogen storage materials for hydrogen and energy carriers," *International Journal of Hydrogen Energy*, vol. 44, pp. 18179-18192, 2019.
- [183] J. Wang, T. Wang, A. D. Ebner, and J. A. Ritter, "Synthesis of Complex Hydride Reversible Hydrogen Storage Materials," in *The 2006 Annual Meeting*, 2006.
- [184] L. Schlapbach and A. Züttel, "Hydrogen-storage materials for mobile applications," in *Materials for sustainable energy: a collection of peer-reviewed research and review articles from nature publishing group*, ed: World Scientific, 2011, pp. 265-270.
- [185] S.-i. Orimo, Y. Nakamori, J. R. Eliseo, A. Züttel, and C. M. Jensen, "Complex hydrides for hydrogen storage," *Chemical reviews*, vol. 107, pp. 4111-4132, 2007.
- [186] Y. Guo, W. Sun, Z. Guo, H.-K. Liu, D. Sun, and X. Yu, "Dehydrogenation promotion of LiBH₄·NH₃ through heating in ammonia or mixing with metal hydrides," *The Journal of Physical Chemistry C*, vol. 114, pp. 12823-12827, 2010.
- [187] Y. Guo, X. Yu, W. Sun, D. Sun, and W. Yang, "The hydrogen-enriched Al–B–N system as an advanced solid hydrogen-storage candidate," *Angewandte Chemie*, vol. 123, pp. 1119-1123, 2011.
- [188] Y. Guo, Y. Jiang, G. Xia, and X. Yu, "Ammine aluminium borohydrides: an appealing system releasing over 12 wt% pure H₂ under moderate temperature," *Chemical Communications*, vol. 48, pp. 4408-4410, 2012.
- [189] Z. Tang, Y. Tan, H. Wu, Q. Gu, W. Zhou, C. M. Jensen, and X. Yu, "Metal cation-promoted hydrogen generation in activated aluminium borohydride ammoniates," *Acta materialia*, vol. 61, pp. 4787-4796, 2013.
- [190] S. Akbayrak and S. Özkar, "Ammonia borane as hydrogen storage materials," *International Journal of Hydrogen Energy*, vol. 43, pp. 18592-18606, 2018.
- [191] M. Mohan, V. K. Sharma, E. A. Kumar, and V. Gayathri, "Hydrogen storage in carbon materials—A review," *Energy Storage*, vol. 1, 2019.
- [192] S. J. Yang, H. Jung, T. Kim, and C. R. Park, "Recent advances in hydrogen storage technologies based on nanoporous carbon materials," *Progress in Natural Science: Materials International*, vol. 22, pp. 631-638, 2012.
- [193] M. Inagaki and T. Suwa, "Pore structure analysis of exfoliated graphite using image processing of scanning electron micrographs," *Carbon*, vol. 39, pp. 915-920, 2001.
- [194] L. Schlapbach, "Hydrogen in Intermetallic Compounds II Surface and Dynamic Properties, Applications," *Topics in Applied Physics*, 1992.
- [195] R. Ströbel, J. Garche, P. Moseley, L. Jörissen, and G. Wolf, "Hydrogen storage by carbon materials," *Journal of Power Sources*, vol. 159, pp. 781-801, 2006.
- [196] G. Balkourani, A. Brouzgou, M. Archonti, N. Papandrianos, S. Song, and P. Tsiakaras, "Emerging materials for the electrochemical detection of COVID-19," *Journal of Electroanalytical Chemistry*, vol. 893, p. 115289, 2021/07/15/ 2021.

- [197] G. Balkourani, T. Damartzis, A. Brouzgou, and P. Tsiakaras, "Cost Effective Synthesis of Graphene Nanomaterials for Non-Enzymatic Electrochemical Sensors for Glucose: A Comprehensive Review," *Sensors*, vol. 22, p. 355, 2022.
- [198] G. Balkourani, A. Brouzgou, C. L. Vecchio, A. S. Aricò, V. Baglio, and P. Tsiakaras, "Selective electro-oxidation of dopamine on Co or Fe supported onto N-doped ketjenblack," *Electrochimica Acta*, vol. 409, p. 139943, 2022/03/20/ 2022.
- [199] G. Ning, F. Wei, G. Luo, Q. Wang, Y. Wu, and H. Yu, "Hydrogen storage in multi-wall carbon nanotubes using samples up to 85 g," *Applied Physics A*, vol. 78, pp. 955-959, 2004.
- [200] A. Dillon and M. Heben, "Hydrogen storage using carbon adsorbents: past, present and future," *Applied Physics A*, vol. 72, pp. 133-142, 2001.
- [201] P. Bénard and R. Chahine, "Storage of hydrogen by physisorption on carbon and nanostructured materials," *Scripta Materialia*, vol. 56, pp. 803-808, 2007/05/01/ 2007.
- [202] A. Züttel, P. Wenger, P. Sudan, P. Mauron, and S.-i. Orimo, "Hydrogen density in nanostructured carbon, metals and complex materials," *Materials Science and Engineering: B*, vol. 108, pp. 9-18, 2004.
- [203] T. Guo, P. Nikolaev, A. Thess, D. T. Colbert, and R. E. Smalley, "Catalytic growth of single-walled nanotubes by laser vaporization," *Chemical physics letters*, vol. 243, pp. 49-54, 1995.
- [204] S. Satyapal, J. Petrovic, C. Read, G. Thomas, and G. Ordaz, "The US Department of Energy's National Hydrogen Storage Project: Progress towards meeting hydrogen-powered vehicle requirements," *Catalysis today*, vol. 120, pp. 246-256, 2007.
- [205] A. D. Lueking, R. T. Yang, N. M. Rodriguez, and R. T. K. Baker, "Hydrogen storage in graphite nanofibers: effect of synthesis catalyst and pretreatment conditions," *Langmuir*, vol. 20, pp. 714-721, 2004.
- [206] S. Iijima, "Helical microtubules of graphitic carbon," *Nature*, vol. 354, pp. 56-58, 1991.
- [207] V. Ivanov, J. Nagy, P. Lambin, A. Lucas, X. Zhang, X. Zhang, D. Bernaerts, G. Van Tendeloo, S. Amelinckx, and J. Van Landuyt, "The study of carbon nanotubes produced by catalytic method," *Chemical physics letters*, vol. 223, pp. 329-335, 1994.
- [208] A. Dillon, P. Parilla, Y. Zhao, Y. Kim, T. Gennett, C. Curtis, J. Blackburn, K. Gilbert, J. Alleman, and K. Jones, "NREL activities in DOE Carbon-based Materials Center of Excellence," *Proc. of US DOE, Hydrogen Program Review*, p. 35, 2005.
- [209] H. W. Kroto, J. R. Heath, S. C. O'Brien, R. F. Curl, and R. E. Smalley, "C₆₀: Buckminsterfullerene," *Nature*, vol. 318, pp. 162-163, 1985.
- [210] A. Peera, L. Alemany, and W. Billups, "Hydrogen storage in hydrofullerides," *Applied Physics A*, vol. 78, pp. 995-1000, 2004.
- [211] J. G. Lavin, S. Subramoney, R. S. Ruoff, S. Berber, and D. Tomanek, "Scrolls and nested tubes in multiwall carbon nanotubes," *Carbon*, vol. 40, pp. 1123-1130, 2002.

- [212] D. Quinn and J. MacDonald, "Natural gas storage," *Carbon*, vol. 30, pp. 1097-1103, 1992.
- [213] W.-C. Xu, K. Takahashi, Y. Matsuo, Y. Hattori, M. Kumagai, S. Ishiyama, K. Kaneko, and S. Iijima, "Investigation of hydrogen storage capacity of various carbon materials," *International Journal of Hydrogen Energy*, vol. 32, pp. 2504-2512, 2007.
- [214] A. Chambers, C. Park, R. T. K. Baker, and N. M. Rodriguez, "Hydrogen storage in graphite nanofibers," *The journal of physical chemistry B*, vol. 102, pp. 4253-4256, 1998.
- [215] H. Jin, Y. S. Lee, and I. Hong, "Hydrogen adsorption characteristics of activated carbon," *Catalysis today*, vol. 120, pp. 399-406, 2007.
- [216] X. Zhao, B. Xiao, A. J. Fletcher, K. M. Thomas, D. Bradshaw, and M. J. Rosseinsky, "Hysteretic adsorption and desorption of hydrogen by nanoporous metal-organic frameworks," *Science*, vol. 306, pp. 1012-1015, 2004.
- [217] N. Alam and R. Mokaya, "Evolution of optimal porosity for improved hydrogen storage in templated zeolite-like carbons," *Energy & Environmental Science*, vol. 3, pp. 1773-1781, 2010.
- [218] H. Itoi, H. Nishihara, T. Kogure, and T. Kyotani, "Three-Dimensionally Arrayed and Mutually Connected 1.2-nm Nanopores for High-Performance Electric Double Layer Capacitor," *Journal of the American Chemical Society*, vol. 133, pp. 1165-1167, 2011.
- [219] G. J. Kubas, "Molecular hydrogen complexes: coordination of a sigma. bond to transition metals," *Accounts of Chemical Research*, vol. 21, pp. 120-128, 1988.
- [220] Y. Gogotsi, A. Nikitin, H. Ye, W. Zhou, J. E. Fischer, B. Yi, H. C. Foley, and M. W. Barsoum, "Nanoporous carbide-derived carbon with tunable pore size," *Nature materials*, vol. 2, pp. 591-594, 2003.
- [221] S. Orimo, A. Züttel, L. Schlapbach, G. Majer, T. Fukunaga, and H. Fujii, "Hydrogen interaction with carbon nanostructures: current situation and future prospects," *Journal of Alloys and Compounds*, vol. 356-357, pp. 716-719, 2003.
- [222] J. Chen and F. Wu, "Review of hydrogen storage in inorganic fullerene-like nanotubes," *Applied Physics A*, vol. 78, pp. 989-994, 2004.
- [223] P. Guay, B. L. Stansfield, and A. Rochefort, "On the control of carbon nanostructures for hydrogen storage applications," *Carbon*, vol. 42, pp. 2187-2193, 2004.
- [224] F. Mulder, T. Dingemans, M. Wagemaker, and G. Kearley, "Modelling of hydrogen adsorption in the metal organic framework MOF5," *Chemical Physics*, vol. 317, pp. 113-118, 2005.
- [225] D. Warheit, B. Laurence, K. Reed, D. Roach, G. Reynolds, and T. Webb, "Lung toxicity bioassay study in rats with single-wall carbon nanotubes," ed: ACS Publications, 2004.
- [226] J. Muller, F. Huaux, N. Moreau, P. Misson, J.-F. Heilier, M. Delos, M. Arras, A. Fonseca, J. B. Nagy, and D. Lison, "Respiratory toxicity of multi-wall carbon nanotubes," *Toxicology and applied pharmacology*, vol. 207, pp. 221-231, 2005.

- [227] A. Eftekhari and B. Fang, "Electrochemical hydrogen storage: opportunities for fuel storage, batteries, fuel cells, and supercapacitors," *International Journal of Hydrogen Energy*, vol. 42, pp. 25143-25165, 2017.
- [228] T. Gholami and M. Pirsaeheb, "Review on effective parameters in electrochemical hydrogen storage," *International Journal of Hydrogen Energy*, vol. 46, 2020.
- [229] M. Kaur and K. Pal, "Review on hydrogen storage materials and methods from an electrochemical viewpoint," *Journal of Energy Storage*, vol. 23, pp. 234-249, 2019.
- [230] M. Ghodrati, M. Mousavi-Kamazani, and S. Zinatloo-Ajabshir, "Zn₃V₃O₈ nanostructures: facile hydrothermal/solvothermal synthesis, characterization, and electrochemical hydrogen storage," *Ceramics International*, vol. 46, pp. 28894-28902, 2020.
- [231] E. Gorbova, F. Tzorbatzoglou, C. Molochas, D. Chloros, A. Demin, and P. Tsiakaras, "Fundamentals and Principles of Solid-State Electrochemical Sensors for High Temperature Gas Detection," *Catalysts*, vol. 12, 2022.
- [232] H. Cheng, F. Li, G. Su, H. Pan, L. He, X. Sun, and M. Dresselhaus, "Large-scale and low-cost synthesis of single-walled carbon nanotubes by the catalytic pyrolysis of hydrocarbons," *Applied physics letters*, vol. 72, pp. 3282-3284, 1998.